The Manual Control of Vehicles Undergoing Slow Transition in Dynamic Characteristics

THOMAS E. MORIARTY

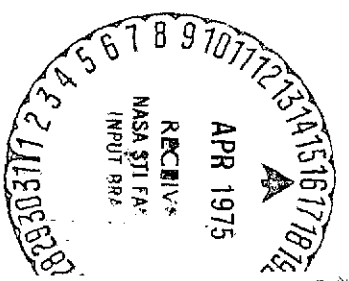

National Aeronautics and Space Administration
Contract No. NSR 23-005-364 by

Department of Aerospace Engineering

NASA CR-132442

THE MANUAL CONTROL OF VEHICLES UNDERGOING SLOW TRANSITION IN DYNAMIC CHARACTERISTICS

By Thomas E. Moriarty

Prepared under Contract No. NSR 23-005-364 by
the Department of Aerospace Engineering
THE UNIVERSITY OF MICHIGAN
Ann Arbor, Mich.

for

NATIONAL AERONAUTICS AND SPACE ADMINISTRATION

ABSTRACT

THE MANUAL CONTROL OF VEHICLES UNDERGOING SLOW TRANSITIONS IN DYNAMIC CHARACTERISTICS

by

Thomas E. Moriarty

The objective of this research is to study the manual control of a vehicle with slowly time-varying dynamics. Implicit in this objective are the development of analytic techniques and computer implementation necessary for the study of time-varying systems. Previous analyses of the behavior of human operators when controlling vehicles or plants have generally dealt with time-invariant plants or plants which undergo an abrupt change in dynamic characteristics. For manual control of time-invariant plants stationary statistics can be assumed, so that a frequency-domain representation of the human operator can be computed in the form of a describing function plus a remnant term. Probabilistic mode-switching models of the human operator have been generated for the case of plants undergoing abrupt changes. This research deals with the human operator as he controls atime-varying plant in which the changes are neither abrupt nor so slow that the time variations are unimportant.

An experiment in which human pilots controlled the longitudinal mode of a simulated time-varying aircraft is described. The vehicle changed from a pure double integrator to a damped second order

system, either instantaneously or smoothly over time intervals of 30, 75, or 120 seconds. The regulator task consisted of trying to null the error term resulting from injected random disturbances with bandwidths of 0.8, 1.4, and 2.0 radians per second. Each of the twelve experimental conditions was replicated ten times.

Ensemble averages across the ten replicates were taken at 0.1 second intervals to compute the time-varying signal variances and autocovariance functions. Further smoothing was obtained by time averaging the resulting variances and autocovariances over respective intervals of 1.5 and 1.1 seconds, based on the assumption of quasi-stationarity over such short intervals. A new means of estimating the bandwidth of a quasi-stationary signal is developed, based on the positions of relative minima observed in the signal's autocovariance function. This estimate, called the bandwidth parameter, is the cutoff frequency of a rectangular low-pass spectrum whose autocorrelation exhibits a first relative minimum at the same distance from the origin as the autocovariance of the unknown spectrum. A power parameter, which estimates the average power in a quasi-stationary signal based upon the variance of the signal, is also developed. The variability of these estimates is analyzed for the discrete data resulting from the experiment.

A Pilot-Vehicle-Regulator system whose input is the disturbance and whose output is the resulting error is defined. It is found that the time-varying power parameter for the error signal is independent of the speed of vehicle variation for the three finite variation speeds;

and that it is only a function of the input bandwidth and the vehicle's configuration at any point during the changes. The bandwidth parameter is shown to be, to a first approximation, only a function of the vehicle's configuration, independent of transition speed and input cutoff frequency.

For the tasks encompassed by this experiment, it is shown that the pilot's performance in the time-varying task is essentially equivalent to his performance in stationary tasks which correspond to various points in the transition. A rudimentary model for the Pilot-Vehicle-Regulator is presented along with a comparison of these experimental results with D. T. McRuer's Crossover Model for the compensatory tracking task.

ACKNOWLEDGMENTS

The author wishes to express his gratitude for the suggestions and inspiration offered by each committee member. Dr. R. M. Howe and Dr. R. W. Pew have provided valuable assistance on all aspects of this research. Dr. W. L. Root was of considerable assistance in some of the more theoretical aspects of the research, and Dr. L. E. Fogarty and Dr. W. F. Powers provided constructive criticism and suggestions throughout the investigation.

The author is indebted to Miss Caroline Rehberg and Miss Jane Weyher for their excellent work in typing the manuscript.

Finally, the author wishes to express his deep appreciation to his wife, Beatrice, for her patience, understanding and encouragement, without which this effort would not have been possible.

This research was sponsored in part by the National Aeronautics and Space Administration under Contract NSR-23-005-364.

TABLE OF CONTENTS

LIST OF TABLES

LIST OF ILLUSTRATIONS

LIST OF APPENDICES

LIST OF SYMBOLS

db	Decibels
f_c	Spectrum cutoff frequency in hertz
k_θ	Control stick spring constant
n	Input disturbance, noise signal
n(t)	Input disturbance, a time function
s	Laplace transform operator
t	Absolute time
t_o	Absolute midpoint time for autocorrelation and autocovariance functions
t_1	Absolute running time for autocorrelation and autocovariance functions
x_p	Pilot's stick deflection
$x_p(t)$	Pilot's stick deflection, a time function
y(t)	Arbitrary function of time
$\bar{y}$	Time-invarient mean of y(t)
$\bar{y}(t)$	Time-varying mean of y(t)
$C_y(t_1, t_o)$	Autocovariance function of y(t), t_o = midpoint, t_1 = running time
EXP	Exponentiation to the base e
FaaTbb	Notation for experimental condition, aa denotes input filter cutoff frequency, bb denotes variation time
P_y	Average Power in y(t)
$P_y(t)$	Average Power in y(t), a time function
$R_y(t_1, t_o)$	Autocorrelation of y(t), t_o = midpoint, t_1 = running time
$R_y(\tau)$	Autocorrelation of y(t), $\tau = t_1 - t_o$

$S_y(\omega)$	Power spectral density of y(t)
T_o	Absolute midpoint time for autocorrelation and autocovariance functions
T_1	Absolute running time for autocorrelation and autocovariance functions
Y_c	Vehicle transfer function
Y_p	Pilot describing function
α	Vehicle output
$\alpha(t)$	Vehicle output, a time function
α_i	Desired vehicle output
$\alpha_i(t)$	Desired vehicle output, a time function
ϵ	Vehicle error
$\epsilon(t)$	Vehicle error, a time function
ζ	Damping ratio of the control stick
σ	Standard deviation
σ_y	Time-invariant standard deviation of y(t)
$\sigma_y(t)$	Time-varying standard deviation of y(t)
τ	Time variable, $= t_1 - t_o$
$\hat{\tau}$	Time value at first relative minimum of autcorrelation or autocovariance function
$\hat{\tau}_L$	Time value at first relative minimum of autocovariance function to left of origin
$\hat{\tau}_R$	Time value at first relative minimum of autocovariance function to right of origin
ϕ	Time-varying parameter in vehicle transfer function

ω	Frequency, radians per second
ω_f	Input filter cutoff frequency
ω_{MS}	Mean Square bandwidth
ω_n	Undamped natural frequency of the control stick
$\bar{\omega}_c$	Spectrum cutoff frequency
$\hat{\omega}_c$	Bandwidth parameter
$\bar{\omega}_{c_1}$	Equivalent rectangular bandwidth
$\bar{\omega}_{c_2}$	-3db bandwidth

1. INTRODUCTION

Background

In recent years there has been an increasing interest in analyzing the behavior of human operators as controllers. In particular, vehicle control has been important, since by designing the vehicle in light of man's capabilities, a better man-machine system can result. Frequency domain specifications of human pilot dynamics for stationary tasks were first presented in the late 1950's (10). Refinement of the describing functions plus a remnant term to account for nonlinearities and non-stationary terms were developed in the 1964-1966 time period (11). Further refinement of these techniques followed in subsequent years, but this approach is still directed toward a description of the pilot's behavior as he controls a time-invariant vehicle.

Most physical vehicles, however, do change with time, at least to some extent. For example, the dynamic characteristics of a motorcycle change significantly as it slows down and enters a curve. An aircraft has different handling qualities when it changes altitude, and certainly in the event of a hardware failure, any vehicle may exhibit either abrupt or slow or perhaps both types of variations in its dynamic characteristics. Within the set of all possible types of vehicle changes that can occur with time, there are certain subsets that can be identified. Certainly one class of changes is that of variations whose effects are so minor that they are not noticed, and thus need little attention. On the other hand, one can consider those changes which

are so great that they produce an impossible task for the human controller. Between these two extremes, there exist a great many possible vehicle changes during which the human operator can and must control. Another dimension that needs to be considered concerns the speed with which these changes take place. At one end of the spectrum are the abrupt or instantaneous changes; and this has been an area of research since the mid-1960's. Young et al (19) studied the effects of abrupt gain changes and polarity reversals within the controlled element. Elkind and Miller (6) extended the research and included controlled elements whose dynamics changed abruptly between a pure gain, a single integration and a double integration. Common to these and similar efforts to describe the effects of abrupt changes are the assertions of multiple modes of control such as detection, identification, modification and optimization; and probabilistic models to account for the controller's actions. The interested reader can obtain further information about these effects from the excellent summary by Young (20). These effects have only dealt, however, with abrupt changes and are not readily extendable to smooth changes. At the other end of the spectrum lie those changes which may be of large magnitude but which occur so slowly as to allow good prediction of performance on a point-by-point basis. An example of this would be the dynamic changes that occur in an aircraft as it flies straight and level, and burns off fuel. This sort of change can be analyzed by existing methodology for time-invariant systems.

The midrange of vehicle time-variations is certainly vast and yet, prior to 1969 as is pointed out by Young (20), little effort had been expended to describe the action of the human in controlling a moderately time-varying plant, i.e., one in which the changes are neither abrupt, nor so slow that the variation is unimportant.

In 1972, Ince and Williges (9) studied the ability of a pilot to detect slow changes in system dynamics. The experimenters studied system dynamics that changed from a pure rate control to a pure acceleration control with the variations occurring in 11, 16, and 33 seconds. They also analyzed a pure rate control system with a time varying gain which changed at rates of 3, 6 and 9 percent of the initial level per second. This effort showed that the times necessary to detect changes in both control dynamics and control sensitivity were functions of the rates of those changes. In the cases where the system dynamics changed from a pure rate control to a pure acceleration control, the authors also stated that tracking error increased as the speed of the variations increased.

One reason for the relatively small amount of research into slowly time-varying man-vehicle systems is that the more traditional frequency domain techniques are not in general applicable when the system is time varying. Even assumptions of stationarity within a region must be carefully tested since if time averaging is used in the analysis, any time variations present will be smoothed over by the analysis. On the other hand, certain methods of time domain analysis,

while valid in application, yield results that are not easily generalized to wider applications. Research efforts in this area such as that of Baron et al (1) are, in general, applications of optimal control theory using recursive filtering. They require careful choice of cost function and weighting matrices in order to get convergence to the solution for a given problem. A change in the structure of the problem, even though slight, generally requires a complete new solution using digital computer algorithms.

Goal

The goal of this research effort is to study the manual control of a vehicle which slowly varies with time. Implicit in this goal are the development of both analytic techniques and computer implementation that are needed to study time-varying systems.

Research Description and Scope

A time-varying vehicle was simulated on the Applied Dynamics 64-PB hybrid computer. The simulation initially represented a large orbital vehicle. The dynamics then slowly changed until they represented those of a large jet transport aircraft. Trained human pilots were used as subjects for an experiment in which the speeds of variation and the input disturbances were varied.

The task chosen for the pilot was one of regulation, i.e., that of maintaining a constant angle of attack in the presence of disturbances. This task can be related easily to the more usual compensatory

tracking task, and it results in a simplified analysis problem that has wide practical application.

Ensemble averaging methods were utilized for analysis in order to generate statistical descriptors for the recorded data. This approach does not require or assume the signals to be stationary.

Organization

The contents of this thesis are divided as follows: The definitions and fundamental concepts associated with the analysis of time-varying systems are discussed in Chapter 2. Chapters 3 and 4 present a description of the experiment and the experimental procedure, respectively. Chapter 3 also summarizes a preliminary experiment that was performed. The form of the experimental data, along with the numerical methods to be used in data analysis, are given in Chapter 5. In Chapter 6, the development and validation of time-varying system descriptors are given, and Chapter 7 contains the results of the data analysis using those descriptors. Chapter 8 contains the conclusions and recommendations for further study. Four Appendices are included which present details of the simulation, procedure, subject data and some of the intermediate results of the data analysis.

2. BASIC CONCEPTS

In order to present a firm foundation for the reader, this chapter will present fundamental definitions and concepts that are important to this thesis. Also presented are some of the statistical considerations which dictate the particular methodology utilized.

Stationarity

A signal or system whose first and second order statistics are independent of the absolute value of observation time is defined to be wide-sense stationary; during the remainder of this thesis, the use of the term "stationary" will mean stationary in the wide-sense as opposed to the strict-sense which requires the statistics of all orders to be time independent. A non-stationary system can be statistically described but its statistics will depend upon the point in time of description. At some other time point, its characteristics would be different.

The terms "time-varying" and "time-invariant" are equivalent to "non-stationary" and "stationary" respectively.

Quasi-Stationarity

A quasi-stationary signal or system is one for which the describing statistics do not vary appreciably during some short period of time, and thus a slowly time-varying system could be described as a quasi-stationary system. The motivation for utilizing the concept of quasi-stationarity comes from the theory of the Fourier Transform.

The spectral representation of a signal is only defined when that signal is stationary. However, a quasi-stationary signal can be thought of as being equivalent, during any short period of time, to some stationary signal, and the latter stationary signal does, in fact, have a well defined spectral representation.

Quasi-stationarity then provides a link between a slowly time-varying signal and a series of different spectral representations. In the remainder of this work, this series of spectral representations will be called the pseudo-spectral representation of the quasi-stationary signal, and the pseudo-spectra are in general time-varying quantities.

Subject Stationarity

A third kind of stationarity is important whenever lengthy experiments are performed with human subjects. This subject stationarity is his day-to-day or his session-to-session consistency. Care must be taken when planning an experiment to minimize the influence of possible fatigue or other factors which can change a subject's characteristics when data are being collected on different days, or even at different times during one day.

Ensemble Averaging

Statistical measurement of a stationary random process in terms of such quantities as mean, standard deviation or autocorrelation, is usually accomplished by means of time averaging over a long observation of the process. When the process is non-stationary, time

averaging would mask or confound any time variations present and thus a different way of generating the desired statistics must be utilized.

By repeatedly observing and recording a non-stationary process, one can record a set or ensemble of replicates for that process such that each replicate is an exact duplicate (in the statistical sense) of every other replicate in the ensemble. With this ensemble available it is possible to generate time-varying statistics in the following manner: Suppose it is desired to generate the mean value of the non-stationary random process at 10 seconds after the process has begun. This quantity can be calculated by adding the values of each replicate at the 10 second point and then by dividing by the number of replicates.

The method of generating process statistics by means of averaging across replicates within an ensemble is called Ensemble Averaging and the mathematical forms for the various statistics used in this thesis are presented in Chapter 5. When using ensemble averaging, it is a priori assumed that the ensemble does represent only one condition in the experiment. Careful attention must be paid to the possibility of subject non-stationarity between replicates, since this would invalidate the above assumption and result in an inhomogeneous sample of the condition.

Statistical Variability

It should be obvious that the variability associated with ensemble averages becomes smaller as the number of replicates gets larger. Unfortunately, the variability is inversely proportional to the square root of the number of replicates, thus requiring a very large number

of replicates in order to get narrow regions of high confidence for ensemble average statistics. Often, as is the case in this study, there are too many different factors to be considered in an experiment to allow the experimenter to generate a very large number of replicates for each condition.

It is possible to utilize the concepts of stationarity and quasi-stationarity in conjunction with ensemble averaging in order to decrease the statistical variation. This is accomplished by taking ensemble-averaged statistics and time averaging them within regions of stationarity or quasi-stationarity. The effect of this process is to increase the effective number of replicates, the amount of increase depending upon the correlation between the values being averaged. A possible disadvantage of this technique, or at least phenomenon to be aware of, is that any time variations which do occur within the region of assumed stationarity or quasi-stationarity will by washed out or masked by this technique.

3. EXPERIMENT DESCRIPTION

This chapter presents the design and justification of an experiment to study the effects of a slowly varying plant on operator performance. It also includes a summary of a preliminary experiment.

Experimental Task

The task chosen in order to study the effects of a slowly varying plant upon operator performance was, in concept, that of piloting a large vehicle which is initially in orbit outside the earth's atmosphere and then enters the atmosphere on some nominal trajectory. A simplified version of this task, which was suitable for simulation was the longitudinal control of a linearized vehicle, represented by the transfer function in Figure 3.1, where ϕ varies linearly from 0.0 to 1.0 during the experiment.

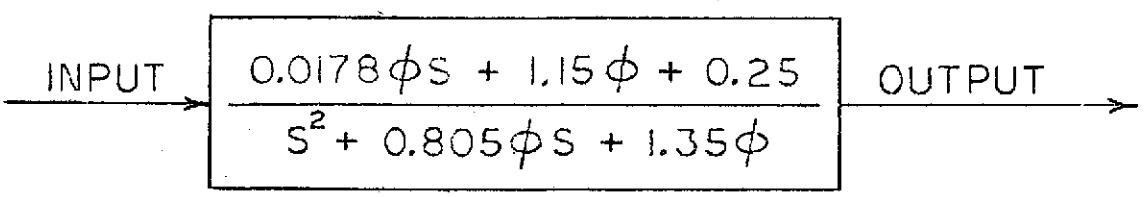

Figure 3.1 Time-Varying Vehicle Transfer Function

It can be noted that with $\phi = 0.0$, the vehicle is a pure inertia with acceleration control, and that as ϕ approaches 1.0, the vehicle resembles the short period approximation for attack angle in a large transport aircraft. Figure 3.2 shows the Bode magnitude plot for the

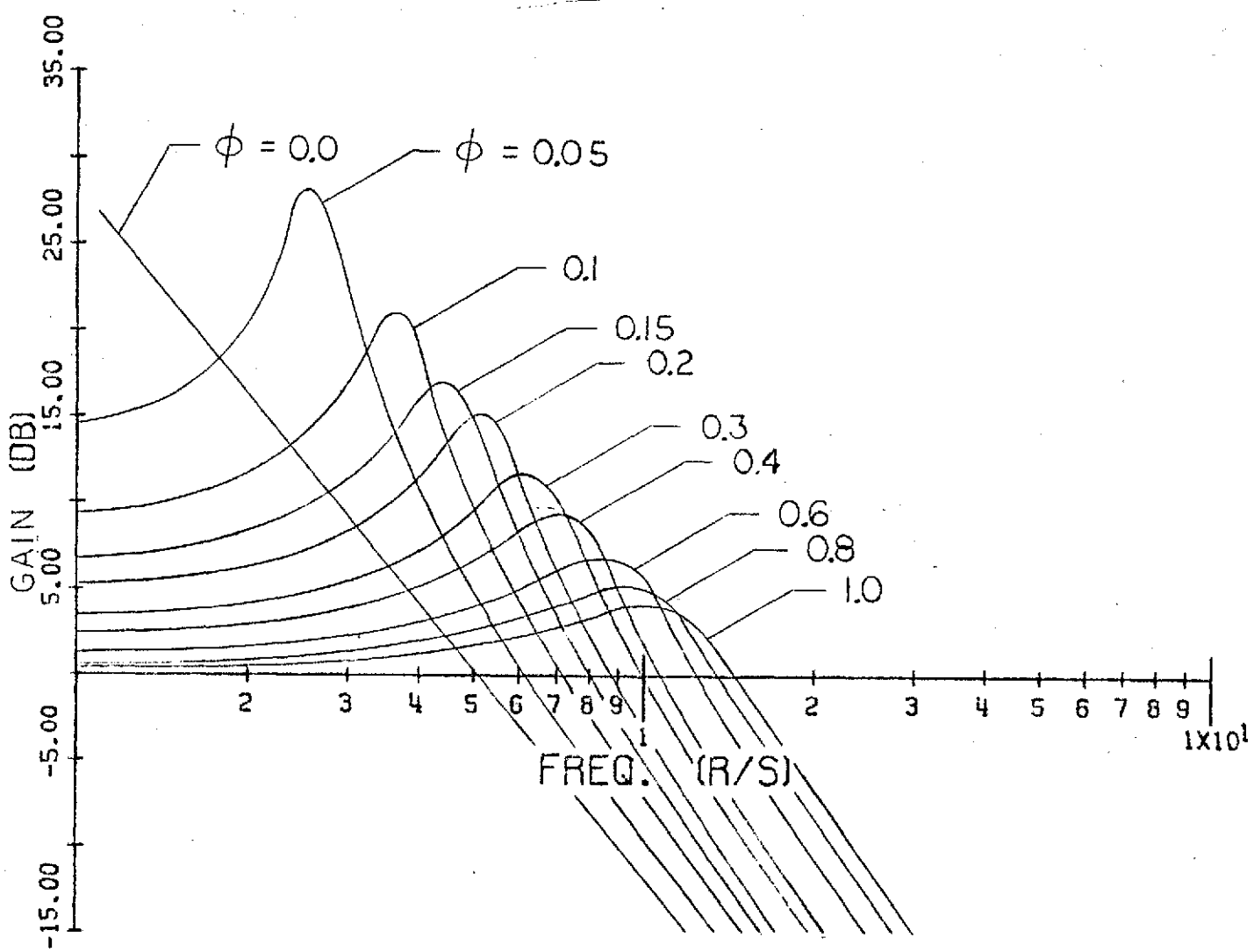

Figure 3.2 Bode Magnitude Plot for Vehicle

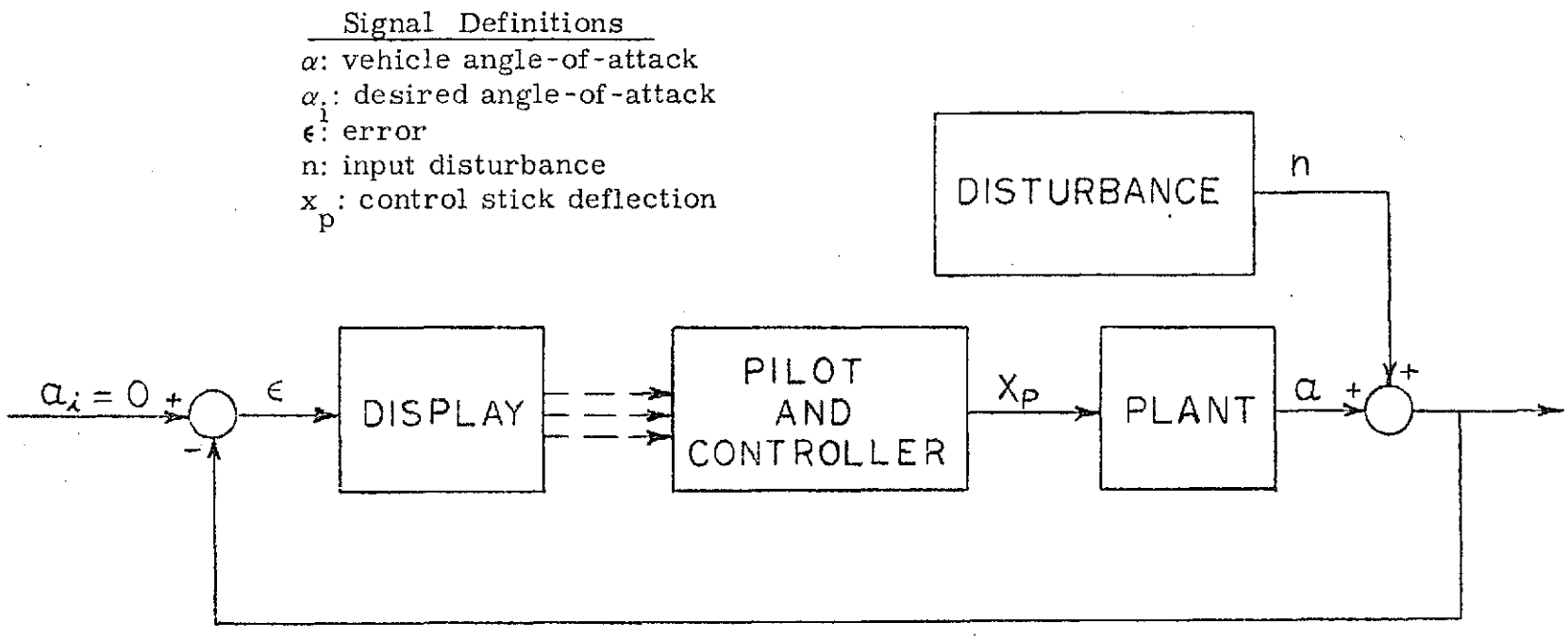

Figure 3.3 Simulation Block Diagram

vehicle. Thus the task can be considered to be that of controlling a vehicle's angle of attack during reentry.

Figure 3.3 presents the block diagram for the simulation as mechanized for the experiment. The input signal $\alpha_i(t)$ was held at zero to make the task that of regulation; i.e., that of holding the vehicle angle of attack to zero in the face of disturbances. While the addition of the disturbance to the vehicle output does not correspond to the true physical situation, it does provide good correspondence between the compensatory tracking task and this experiment. There is some linear transfer operator which could act upon the noise in such a way that its output could then be added to the vehicle's output to give a linear approximation of the physical situation; however, this would then correspond to a time varying input when the system is compared to the compensatory tracking task. Two main factors influenced this particular choice of experiment. To see them most easily, it is convenient to consider the closed loop regulator task as a single system with the disturbance as the input and the vehicle's deviation from the reference condition as the output, as shown in Figure 3.4.

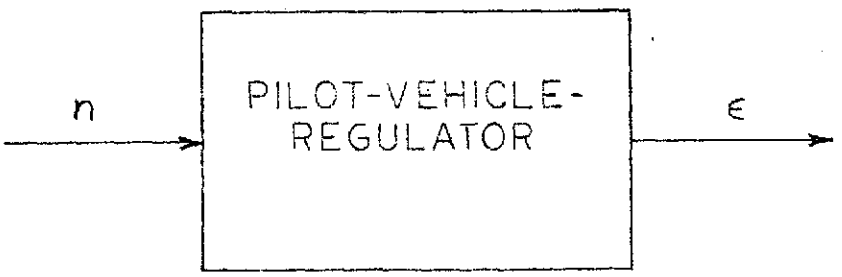

Figure 3.4 Pilot - Vehicle - Regulator

With the formulation of the Pilot-Vehicle-Regulator, it is possible to address directly the question: "what is the capability of

the combined pilot vehicle system to reject disturbing inputs?" Another reason for using this combination is that the resulting configuration is simple, it is mathematically tractable, and it is structurally amenable to the methods of system identification. As Root (16) points out, when trying to identify the characteristics of the pilot within the closed loop, the experimenter is constrained by the fact that he cannot choose the input signals to the pilot, i.e., $\epsilon(t)$. In using the combined Pilot-Vehicle-Regulator representation, the experimenter knows exactly the input to the system. This approach also makes maximum use of the fact that the pilot will, within certain limits, adjust his characteristics to complement those of the vehicle. Thus, this single input, single output system will exhibit a change in output characteristics only when the pilot cannot or does not change his characteristics to account for a change in the vehicle or the input.

Equipment and Facilities

A 22-bit Pseudo-Random Binary Noise generator with a variable register length, which could produce a zero-mean, approximately-Gaussian, band-limited white noise with bandwidth up to 7.2 radians per second was used. A pulse generator was used to signal the digital computer to sample and record the data channels. It was designed to be unusually stable as indicated in Appendix A. This appendix also

contains further explanations of the functions and specifications of these devices.

A small room in The University of Michigan Simulation Center was set up for conducting the experiment. The windows were shielded and doors blocked to isolate the experiment from peripheral disturbances. Two trunklines from the 64-PB Hybrid Computer were permanently wired into the experiment room to provide connections for the display and control units.

One trunkline from the 64-PB Hybrid Computer was wired to provide permanent connections to the CDC 160-A Digital Computer and the A-D Conversion Unit.

A control unit for the 160-A Digital Computer was fabricated and installed in the control panel of the AD 64-PB Hybrid Computer. This unit allowed the experimenter to control the 160-A from the 64-PB console, thus enabling on-line digital conversion of the data during the experiment, and the storage of this data directly on magnetic tape at the same time. The actual data conversion technique is discussed in Appendix A.

Simulation Philosophy

The simulation equipment consists of the 64-PB Hybrid Computer, a display unit, a control stick, and a noise generator. The hybrid computer was used to represent the time varying vehicle dynamics as well as to generate the analog filters for the noise, and the switching and signal processing for the display signals.

The simulation was designed to provide a very closely controlled experiment. When the experimenter started the trial, the hybrid computer then performed all subsequent sequencing to begin taking data, to provide the start of the time variation, and finally to stop the trial and stop taking data. In effect, then, the entire trial was run by the hybrid computer, once the experimenter initiated it. This provided maximum repeatability of the trial.

The display unit was a CRT x-y plotter and the display signals were generated within the hybrid computer. The 6 1/2" by 8 1/2" face was as shown below, with a short, non-moving reference line (2 1/8" in length) and a long moving line, generally corresponding to the artificial horizon in an aircraft cockpit.

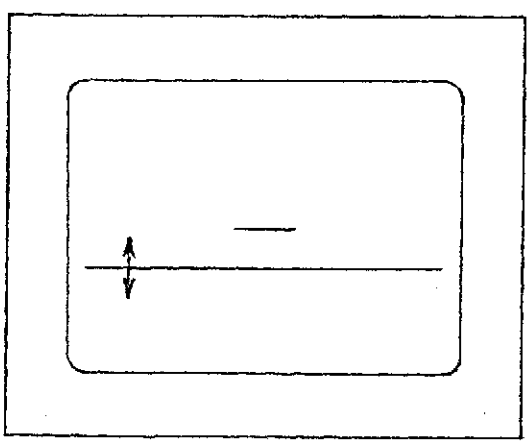

Figure 3.5 Display Unit Face

In order to work with data signal magnitudes that were reasonable, the angle-of-attack, error and noise signals were converted from recorded voltages to their magnitudes in units of millimeters

(mm) deflection on the display face. The reference value for scaling purposes was a full deflection of ± 24° in attack angle which was equivalent to ± 82.55 mm full screen deflection on the display.

The control stick was mounted on an arm rest of a chair, and the stick was connected to a potentiometer to provide a voltage proportional to stick deflection in degrees. The recorded stick deflection signals were converted back to degrees deflection for computation purposes during the data analysis.

Between the control stick and the display, there was a sensitivity coefficient which varied as the vehicle varied. When the vehicle was a pure inertia, a constant stick deflection produced an acceleration

Figure 3.6 Experiment Room

and the sensitivity was 1.56 [mm/sec^2] /^{o} def. After the transition was completed, the steady-state sensitivity related a constant stick deflection to a constant display deflection and the coefficient was 6.5 mm/^{o}def.

The arrangement of control stick, chair and display within the experiment room is shown in Figure 3.6.

A more detailed specification of the components of the simulation and the physical dimensions of the various devices are presented in Appendix A.

Preliminary Experiment

A preliminary experiment was conducted to study the feasibility of the entire simulation and procedure, and is fully documented in Supplement I of Reference 8. The preliminary experiment was performed at the Simulation Center with essentially the same equipment discussed in this documentation. The first portion consisted of recording the data from twenty-one replicates of one condition, that of input disturbance filter bandwidth (ω_f) = 1.0 radians per second, and a vehicle transition from a pure inertia to a damped second order system in 200 seconds. The subject for this experiment was a trained pilot but he was not naive with respect to the purpose of the experiment.

The results of the first phase indicated that the subject was encountering the control limits during the trials, so the second phase was a set of trials with various values of control gain or sensitivity. The gain value used in the main experiment is about 25% over the minimum level such that the subject did not encounter the controller limits.

A third phase of the preliminary experiment was that of determining the sources and magnitudes of the inaccuracies present in the data conversion and recording process. The preliminary experiment was also used to verify that the magnitude of the noise injected didn't have a significant effect upon pilot characteristics providing it was not so large as to cause limiting nor so small as to not be discernable. Between these limits, the pilot compensated for magnitude changes by relatively linear magnitude changes in his own output.

Finally, the preliminary experiment served to test the experimental procedure which is described in the next chapter.

Conversion Noise. - Inaccuracies in the recorded data came from three sources: (1) actual voltage errors within the analog unit, (2) roundoff errors resulting from the fact that the least significant conversion bit corresponded to 0.05 volts, (3) errors in the conversion process over and above the roundoff. The first two sources were an order of magnitude smaller than the last, and thus, for this experiment, all inaccuracies in the recorded data were lumped under the classification of conversion noise.

An analysis of the conversion noise, as documented in Reference (8), yielded the following results: The mean of the conversion noise was always less than 0.04 volts in magnitude and the standard deviation was always less than or equal to 0.4 volts. Spectral analysis indicated that the noise was essentially low-frequency band-limited

white noise with a cutoff frequency at about 0.7 rad/sec. The maximum voltage levels for the 64-PB hybrid computer were ± 100 volts, full scale. The simulation was scaled so that the expected maximum values of the various data signals would be at 75% of the full scale voltages. If that had been the case, the standard deviations of the data signals would have been about 53 volts. The ratio of signal standard deviation to noise standard deviation in that situation would have been 132.5 and the signal to noise power ratio would have been 17556 (44.2 db). To provide another reference point, consider the case where a signal's standard deviation was on the order of 10 volts, which was representative of the lowest observed data value. Then the standard deviation ratio was 25.0 and the signal to noise power ratio was 625 (27.95 db). Based on these figures, it was decided to neglect the effects of conversion noise upon the data. It should be noted at this point that the value of $\sigma = 0.4$ volts for conversion noise is quite high compared with the present state of the art in analog to digital signal conversion. More modern converters exhibit considerably higher accuracy.

Ensemble Size

The question of the number of replicates for the main experiment was answered by taking the preliminary experimental data (twenty-one replicates) and reducing the number of replicates utilized for the data calculations. It was found that when the number of replicates fell below nine, the smoothness of the autocovariance functions deteriorated

markedly. For this reason and to insure accuracy in the calculation of mean and standard deviation, a sample size of ten replicates was chosen.

4. EXPERIMENTAL PROCEDURE

This chapter presents the experimental conditions and the procedures for performing the experiment.

Conditions

The parameter ϕ is a coefficient in the vehicle's dynamic equations (see Figure 3.1), and thus time variations of ϕ determined the manner in which the vehicle characteristics varied with time. As was stated in Chapter 3, ϕ varied linearly with time and the speed of variation assumed one of four values, corresponding to a total variation occurring in 0, 30, 75 or 120 seconds. The input noise filter cutoff frequency (ω_f) took on values of 0.8, 1.4 and 2.0 radians per second with the mean standard deviation held constant at 6.25 mm deflection on the display. Thus, each of the two subjects experienced twelve experimental conditions, with 10 replicates of each condition, as shown in Table 4.1.

Input Noise Frequency	Length of Time Variation			
	0 sec	30 sec	75 sec	120 sec
$\omega_f = 2.0$ (rad/sec)	F20T0	F20T30	F20T75	F20T120
$\omega_f = 1.4$ (rad/sec)	F14T0	F14T30	F14T75	F14T120
$\omega_f = 0.8$ (rad/sec)	F8T0	F8T30	F8T75	F8T120

Table 4.1 Experimental Conditions

Table 4.1 also serves to introduce the shorthand representations for the twelve conditions. For example: Condition F14T0 is the condition where the input noise filter cutoff frequency is 1.4 radians per second and time variation occurs instantaneously (0 seconds). Similarly, condition F8T120 indicates that the input noise filter frequency is 0.8 radians per second and the time variation takes 120 seconds.

In order to provide a measure of the effect of choosing ten replicates for ensemble averaging, the condition F14T75 with Subject B was also studied with forty replicates. An additional set of experiments was performed with ϕ fixed at 0.0, 0.05, 0.15, 0.4, 0.7 and 1.0. This was to allow comparison of the time-varying pilot performance with performance on a time-invariant vehicle with similar characteristics.

Subject Briefing

Each of the two subjects was briefed informally but extensively before beginning the experiment. The only restriction employed was that of not telling the subject that his actual control characteristics would be under analysis. The subject was told that the vehicle would vary with time and the endpoint conditions were explained. Since the subjects had had little experience with piloting a vehicle without damping or spring forces, special attention was given to the dynamic characteristics of the initial configuration. Other than explicitly explaining what would be done with the collected data, all questions were answered as well as possible. The subject was allowed to "fly"

the two endpoint conditions for 10-15 minutes, with and without external disturbances, as part of his initial briefing. Appendix C contains pertinent subject data.

Procedure

The experiment was conducted in the following manner. Each subject experienced one session on seven different days and each session consisted of taking ten replicates of two different conditions. The seven sessions were required in order to duplicate the first session with the last session. This was done in order to eliminate the learning effects which were present in the first few trials of the first session. It was felt that the inclusion of these trials would have introduced a good deal of subject non-stationarity into the two ensembles being generated. Subsequent data analysis thus dealt with the results of only the last six sessions, where it was felt that subjects were well enough "into the learning curve" so that they were stationary within sessions and that the tendency to improve performance with time would be balanced by the idle days between sessions. Within a session the two different conditions were presented in a random order with a constraint applied on the probabilistic selection of the order.

A particular random trials order for a session could have been obtained merely by taking any arbitrary sequence of 20 trials chosen at random from a group containing 10 trials for one condition and 10 trials for the other condition. This would, however, allow the possibility of obtaining an order which does not appear to be random at all, such as 10 trials of one condition followed by 10 trials of the other

condition. Thus, it was decided a priori to accept only random orders which have a probability of occurance by chance that is equal to or greater than some value, and in this case $P \geq 0.022$ was chosen. Each occasion within a session that the experimenter changed the variation time from one value to the other represented as a system change; and when the order selection was made as outlined above, the number of system changes was a random variable with a binomial distribution. The chosen probability then required that for this experiment, only random orders which contained at least 5 and not more than 14 system changes were accepted as "appropriately random". Appendix B presents the sessions and the variable values for each.

Each of the 20 experimental trials in a session began with a 60 second initial phase, followed by one of the four transition times and then a final phase of at least 60 seconds so that each trial lasted 240 seconds. The subject was given a random length (30 seconds or less) of time initially to acclimate himself to the task prior to beginning the actual recorded 240 second section. The subjects were not aware of the length of this initial phase and thus could not develop a sense of timing to determine the start of the variation.

Between each trial the subject was asked to leave the experiment room and walk into the next room where he read the digital computer output consisting of the file number and the number of records recorded on magnetic tape. He then gave this information to the experimenter and returned to the experiment room. Not only did

this serve to provide a check on the data bookkeeping methods, but it broke the monotony of the subject's task. As the subject walked by the computer console, he was able to see the mean-square integral error level for each run. Although he was briefed as to the statistical variation of this measure, it did provide considerable personal motivation to keep him alert at the task. The time between each trial was approximately one minute.

Because of the length of each run, the fatigue of the subject was an important consideration. In order to reduce the fatigue, a complete change of pace was made after each group of five runs, and the subject was encouraged to get some refreshments and actively change his behavior for 10 to 15 minutes.

Data Recording

During the run, $\alpha(t)$ - the vehicle output, $x_p(t)$ - the stick deflection, $n(t)$ - the disturbance noise, and $\epsilon(t)$ - the error signal were recorded along with a timing signal. The data signals are indicated in Figure 3.2 and the timing signal is a voltage which takes on values of plus or minus ten volts depending upon what phase the simulation is in. This timing signal also provided an on-line calibration capability within the data, although it was not necessary to use it, since a full-scale ± 100 volt calibration signal and sinusoidal calibration signal were recorded before and after every session.

5. DATA REDUCTION AND ANALYSIS

Data Reduction

After the data had been recorded on the CDC-160A computer and then converted to IBM 360 compatible form, one further step was required to put the data in its most useful form. This step consisted of a final editing and alignment of the data runs.

The technique used in the hybrid computer to time the various intervals within a trial was that of generating a ramp voltage and switching modes when the ramp reached various preset voltage levels. A more accurate method would have been to actually count the data recording pulses, but the necessary equipment was not available. Thus, when all ten replicates of a condition were compared by means of their timing tracks, it was not uncommon to find that some of the individual interval lengths differed by a few tenths of a second. When this occurred on the initial or final static intervals, the remedy was to drop the last few entries of the longer initial intervals or to drop the last few entries of the longer final intervals so that they were equal in length to those of the shortest replicate. When a difference occurred in the time-varying intervals, a different procedure was employed. A sequence of random numbers within the nominal range of time points for the interval was generated. Using this sequence, entries were removed from the larger time-varying intervals until all the intervals were of the same length. As a rule of thumb, it was decided that any interval which required removal of more than one percent of its

nominal entries was not reliable for frequency information. Thus the most that could be removed from a 1200 point interval was 12 points, and the 750 point and 300 point intervals would allow the removal of 7 and 3 entries respectively.

When the timing editing was completed, all the data runs for each experimental condition had exactly the same timing, and these runs were stored on magnetic tape on the IBM 360 computer. The data consisted of over 4 million words that were well arranged and readily available for analysis without further editing.

Ensemble Analysis

This section presents the ensemble methods used to analyze the experimental data, as well as a comparison with the more conventional time-invariant form and some general results of applying these methods to the data.

Mean - The mean of a time-varying signal y(t) is also a time-varying quantity. For n replicates of the signal, the mean at time t_o is computed by

$$\bar{y}(t_o) = \frac{1}{n} \sum_{i=1}^{n} y_i(t_o). \tag{5.1}$$

The time-invariant form is a constant and is given by

$$\bar{y} = \frac{1}{2T} \int_{-T}^{T} y(t)\, dt, \tag{5.2}$$

which will equal (as the number of replicates get large) the time average of time-varying mean.

For the signals $\alpha(t)$, $x_p(t)$, $n(t)$ and $\epsilon(t)$, the expected values of the sampling distributions of the ensemble means were essentially zero, and they provided unbiased estimates of the population means for those signals. The standard errors of the replicate means were on the order of 10% of the maximum signal levels, and while the population means could be assumed zero, it was felt that sample variations in the signal means would have to be accounted for.

Standard Deviation - The standard deviation of the time-varying signal is time-varying and at t_o is given by

$$\sigma_y(t_o) = \sqrt{\frac{1}{n} \sum_{i=1}^{n} [y_i(t_o) - \bar{y}(t_o)]^2} \quad . \tag{5.3}$$

In this case too, applying the time-invariant form

$$\sigma_y = \sqrt{\frac{1}{2T} \int_{-T}^{T} (y(t) - \bar{y})^2 \, dt} \tag{5.4}$$

will yield the average value of $\sigma_y(t)$ over the time period 2T.

The variation of $\sigma_y(t)$ evaluated at individual points of time for the data was fairly large. By using quasi-stationarity and taking the time average of the standard deviation over 1.5 seconds, an improvement was made; but, as Figure 5.1 indicates, there was still a significant variation present. This result was important since it influenced some subsequent analyses. In Chapter 6, the decrease in variation associated with increasing the number of replicates from 10 to 40 will be shown.

Figure 5.1 presents the 10-replicate ensemble standard deviation as a function of time for 3 signals: stick deflection, $x_p(t)$;

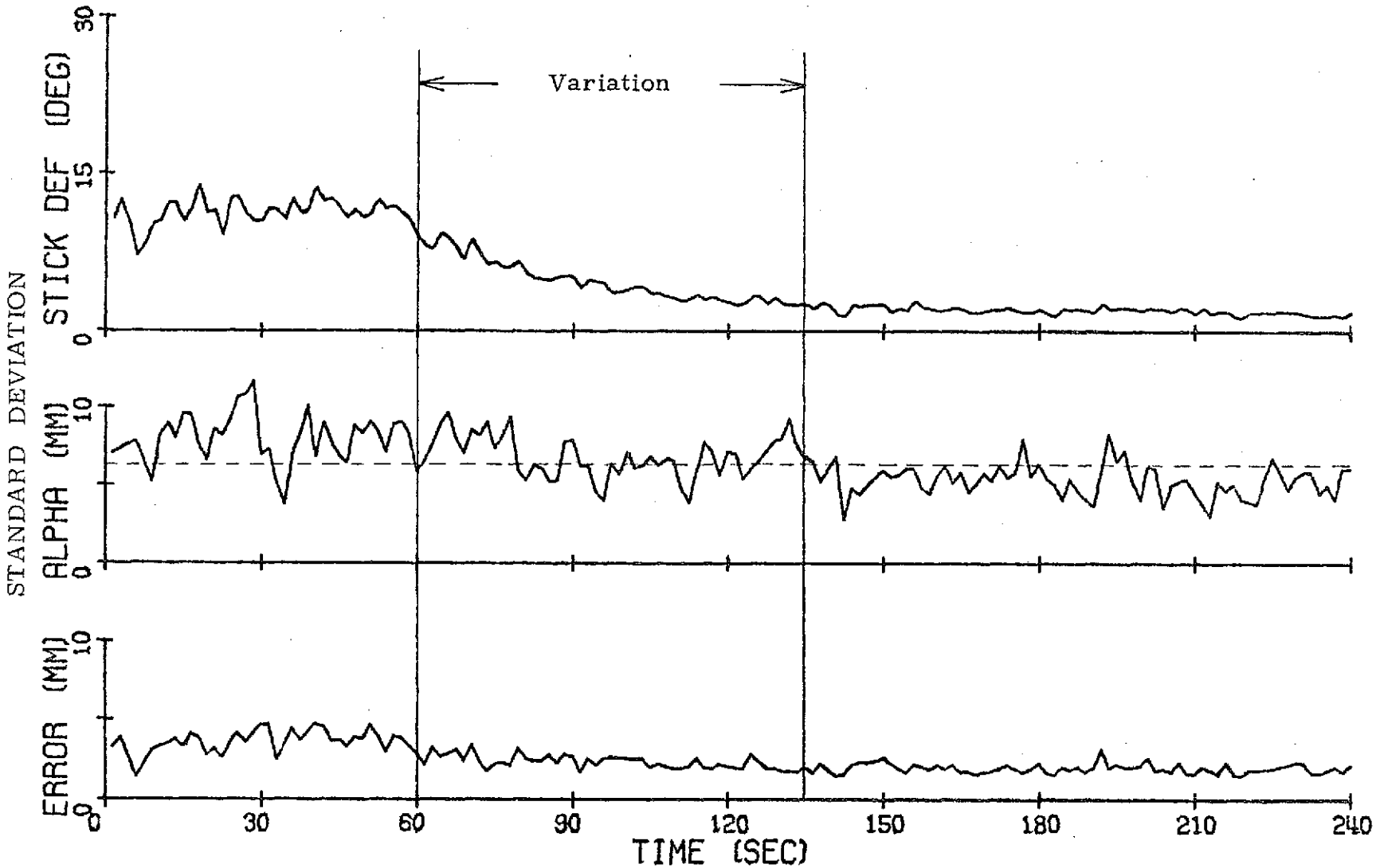

Figure 5.1 Standard Deviation of Recorded Data for Condition F14T75, Subject B

vehicle output, $\alpha(t)$; and error, $\epsilon(t)$. The mean standard deviation of the input noise was equal to 6.25 mm as indicated by the straight line superimposed on the vehicle output plot. The starting point and ending point of the time variation are also shown. Each plot consists of 159 to 160 points separated by 1.5 seconds, and each point represents the numerical average of 15 ensemble standard deviations taken at 0.1 second intervals up to and including the point shown. Assuming quasi-stationarity over a 1.5 second interval represents a trade-off between the desire for accurate time varying statistics and the desire to decrease the effect of sample variation. When the time variation of the vehicle is at its highest rate (30 seconds for the total transition), the 1.5 second assumption is equivalent to assuming the system is essentially stationary during 5% of the vehicle's transition. As the speed of vehicle transition decreases, the validity of this assumed quasi-stationary interval gets better. Figure 5.1 represents the particular condition F14T75 with Subject B. Appendix D contains a similar plot for each subject and each point of the twelve conditions.

Autocorrelation - The autocorrelation function (and there is a natural extension to the cross correlation function) for a time-varying signal is a function of two time points t_o and t_1. It is most easily treated by thinking of t_o being fixed (called the midpoint) and t_1 varying on both sides of the midpoint. Its ensemble form is

$$R_y(t_1, t_o) = \frac{1}{n} \sum_{i=1}^{n} y_i(t_o)\, y_i(t_1) \qquad (5.5)$$

as compared with the time-invariant form of

$$R_y(t_1 - t_o) = \frac{1}{2T} \int_{-T}^{T} y(t_o)\, y(t_1)\, dt_o \ . \qquad (5.6)$$

Autocovariance - In this study the autocovariance function of a time-varying signal y(t) is defined in its ensemble form by

$$C_y(t_1, t_o) = \frac{\frac{1}{n} \sum_{i=1}^{n} [y_i(t_o) - \bar{y}(t_o)]\, [y_i(t_1) - \bar{y}(t_1)]}{\sigma_y(t_1)\, \sigma_y(t_o)} \qquad (5.7)$$

This function doesn't really have a well known time-invariant form, but in the following paragraphs it is shown to be similar to the autocorrelation function.

Consider that the autocovariance function is taken on an ensemble whose mean is zero and whose standard deviation is a constant σ_y. Then

$$C_y(t_o, t_1) = \frac{R_y(t_o, t_1)}{\sigma_y^{\,2}} = \frac{R_y(t_o, t_1)}{R_y(t_o, t_o)} \qquad (5.8)$$

and the autocovariance is just a normalized autocorrelation. Since it is the purpose of this study to look at signals which are quasi-stationary, or essentially stationary over small periods of time, it is reasonable to assume that the mean of the signal population is zero and to account for sample variation of the mean by subtracting it in the manner done by the autocovariance function. By similar reasoning, one accounts for the sample variation in standard deviation between two points in time by using the two values of σ as normalizing factors. The validity of the latter practice is inversely proportional to the value of $|t_1 - t_o|$, since as $|t_1 - t_o|$ gets larger, it becomes less likely that

the observed variations in σ are due to sample variation rather than system non-stationarity.

The result of using the autocovariance function as opposed to the autocorrelation function on the experimental data is striking. It improves the symmetry of the resulting plot considerably. It also reduces peaks that occur away from the origin to an extent where they become physically believable. This difference is illustrated in Figures 5.2 and 5.3 of autocorrelation and autocovariance respectively for the same data. In the remainder of this study, it will be assumed that the autocovariance function is very closely related to the autocorrelation function and that the properties of the autocovariance function reflect those of a hypothetical autocorrelation function generated for the same process but with a better sample.

Figure 5.4 is a plot of $C(t_1, t_o)$ of $\epsilon(t)$, the average of 40 autocovariance functions taken at one second intervals during the first 60 seconds of condition F14T75 with subject B. This average spans the entire 60 second time-invariant first phase of the condition and thus the average over such large time intervals is allowable. Using such an average provides maximum smoothness and symmetry and generally yields an autocovariance function that is quite well behaved.

Figures 5.5, 5.6, 5.7 and 5.8 show the averages of 11 autocovariance functions taken at 0.1 second intervals symmetrically about the stated midpoint for each figure. They are all taken from condition F14T75,

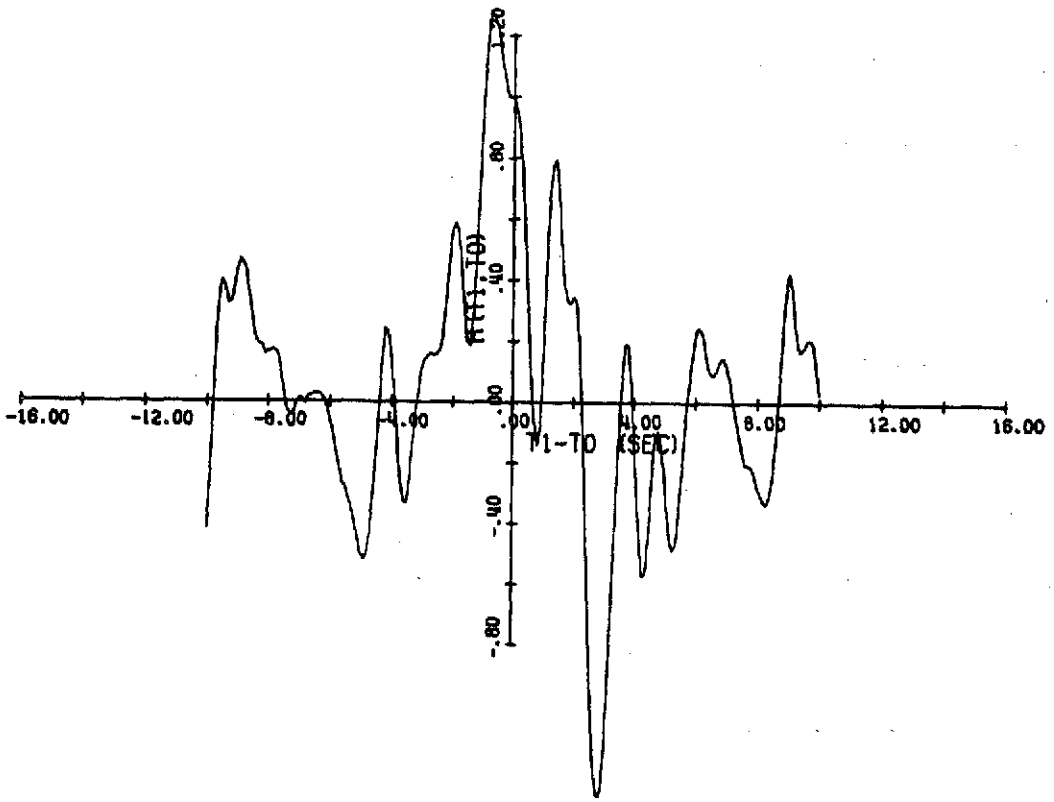

Figure 5.2 Example Autocorrelation Function

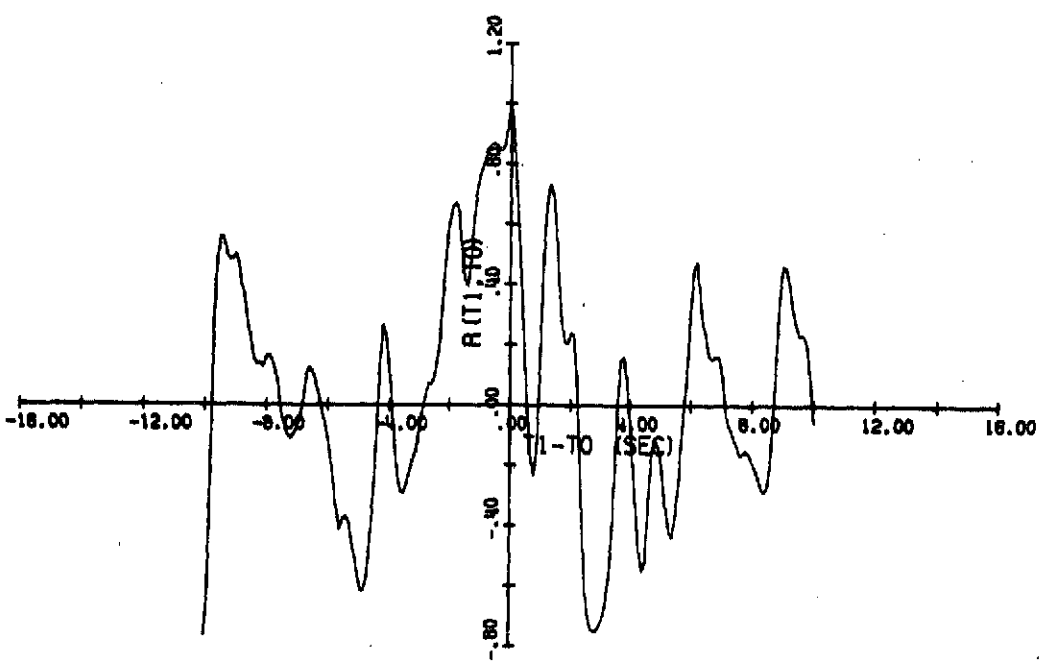

Figure 5.3 Example Autocovariance Function

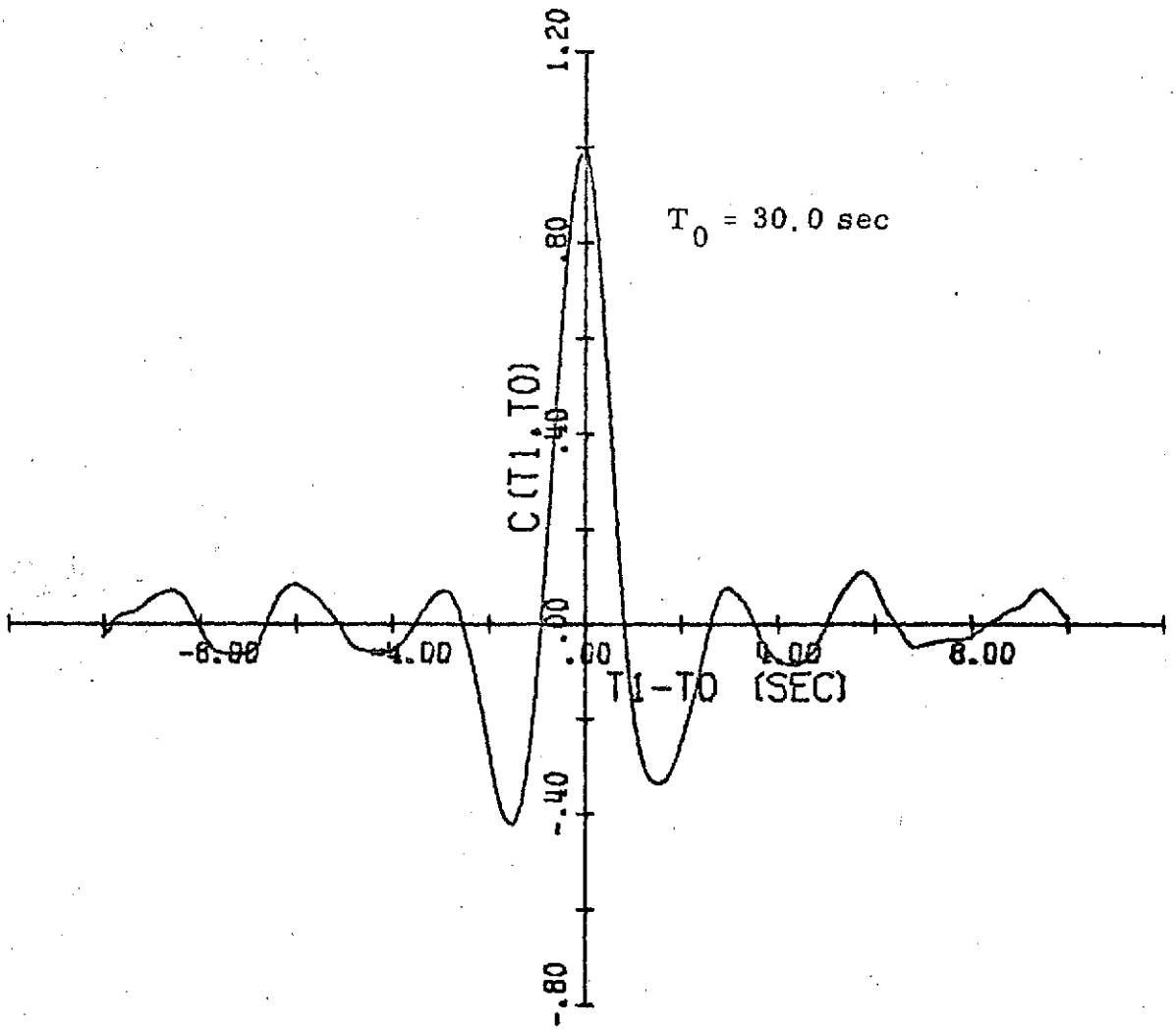

Figure 5.4 Error Signal Average Autocovariance Function over Initial Static Interval for F14T75, Subject B

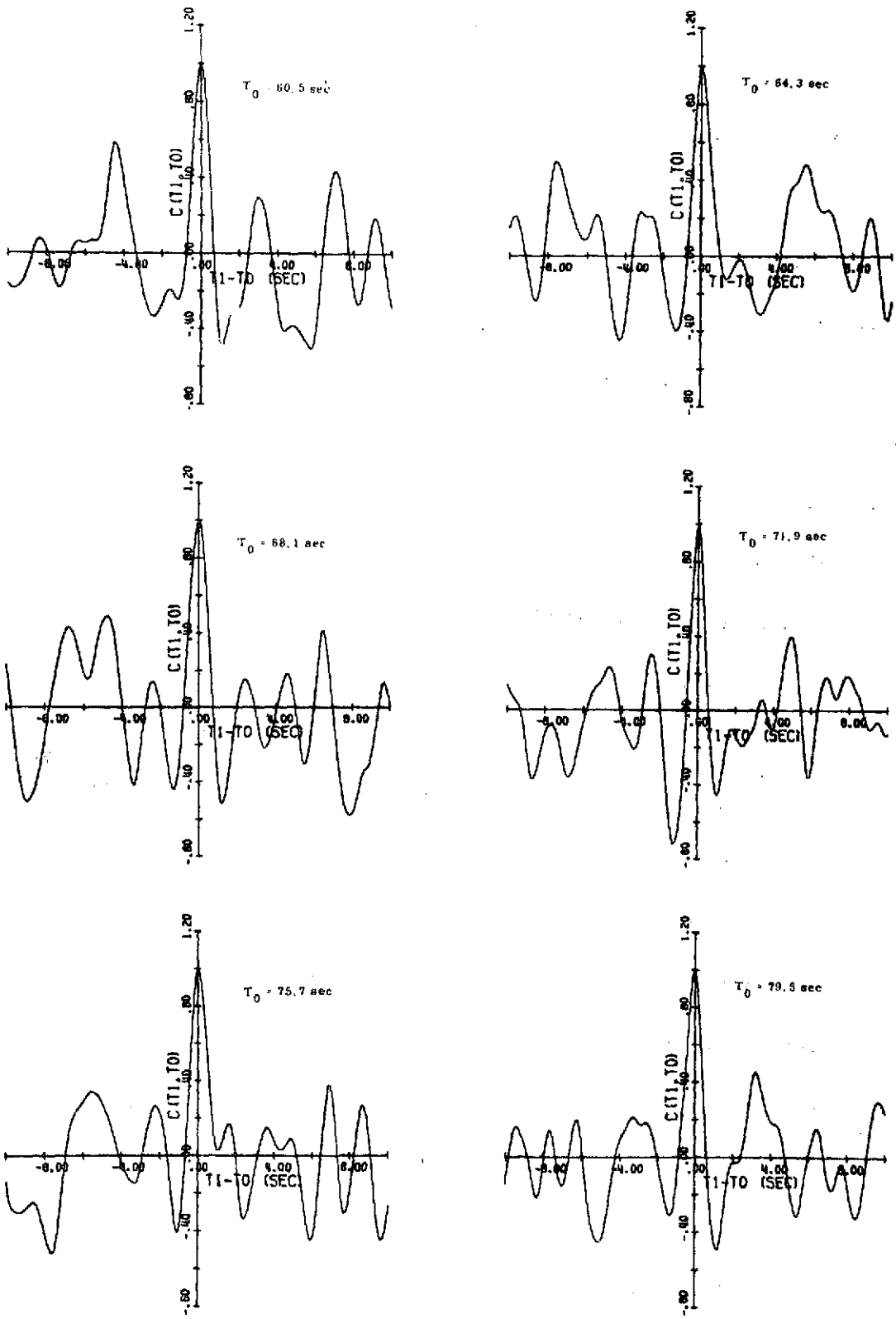

Figure 5.5 Error Signal Average Autocovariance Functions for F14T75, Subject B, Midpoints as Indicated by T_0

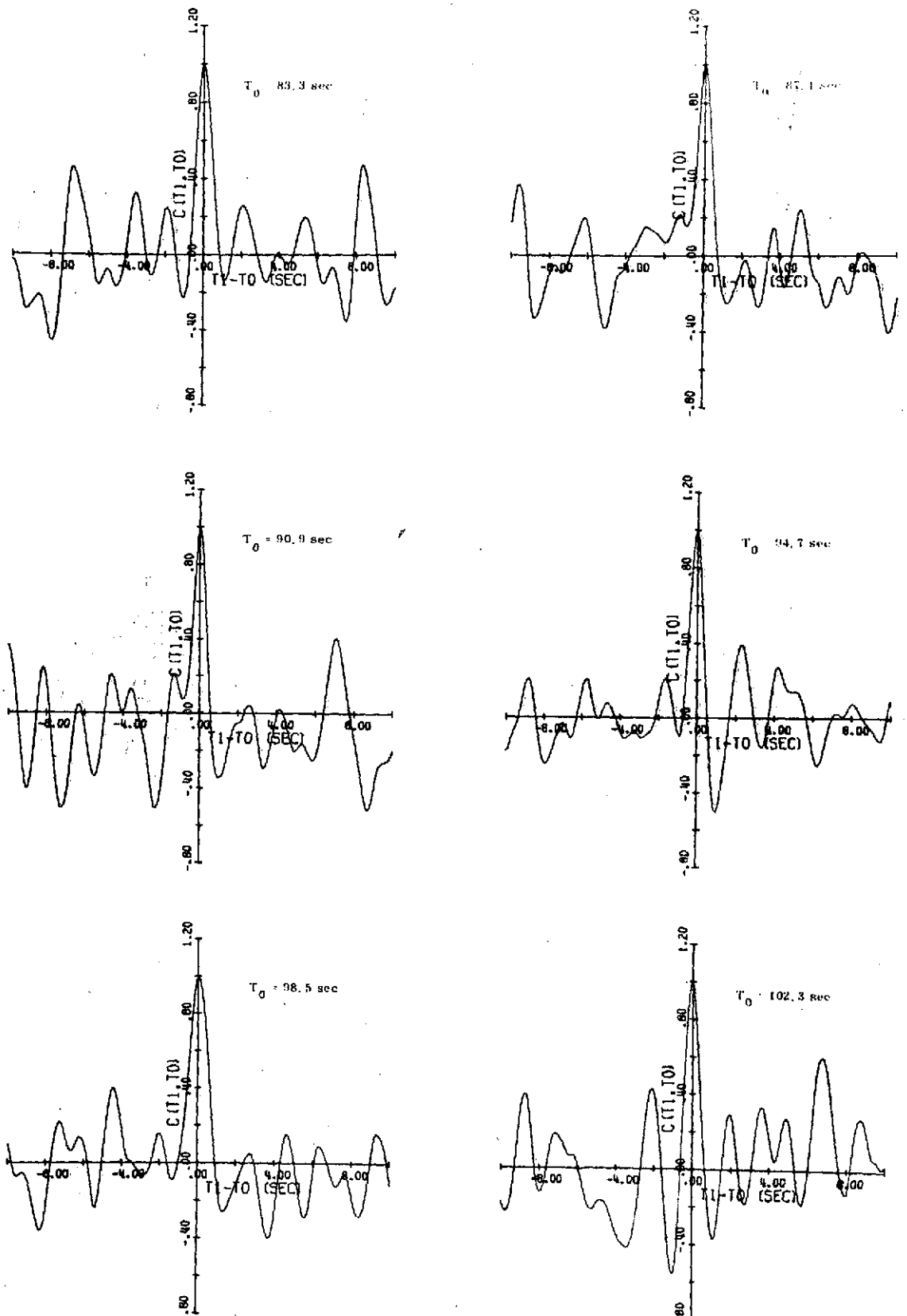

Figure 5.6 Error Signal Average Autocovariance Functions for F14T75, Subject B, Midpoints as Indicated by T_0

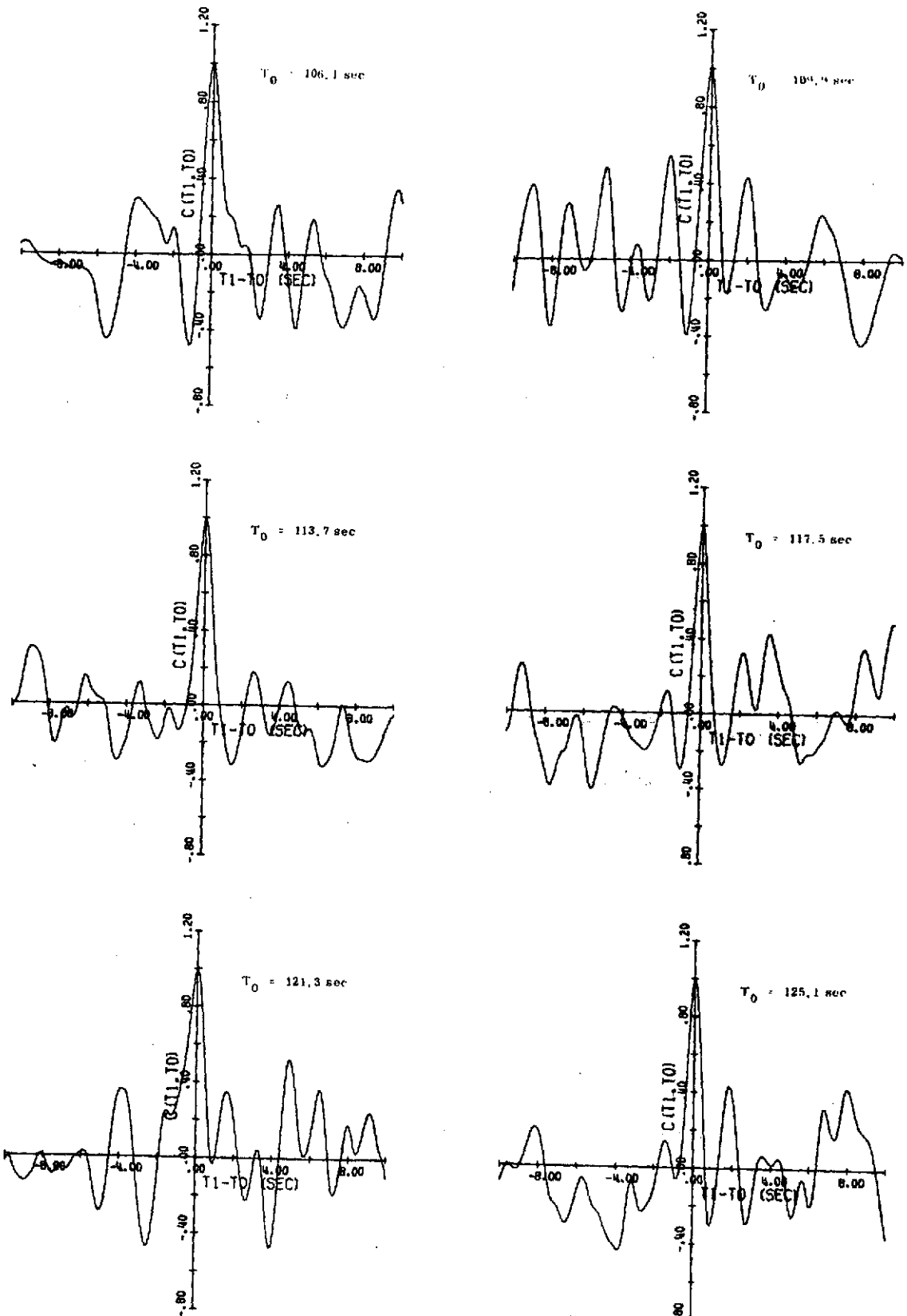

Figure 5.7 Error Signal Average Autocovariance Functions for F14T75, Subject B, Midpoints as Indicated by T_0

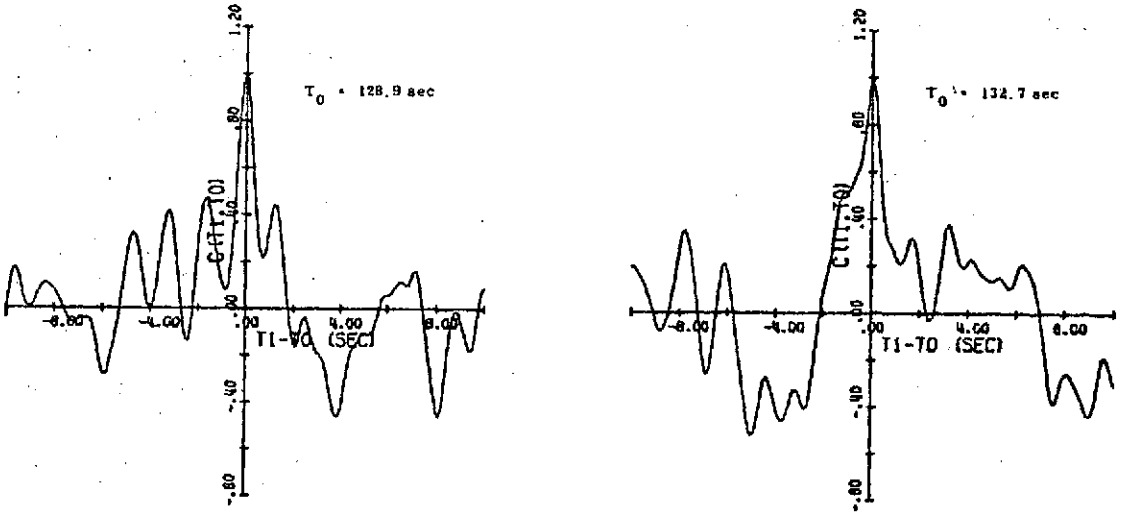

Figure 5.8 Error Signal Average Autocovariance Function for F14T75, Subject B, Midpoints as Indicated by T_0

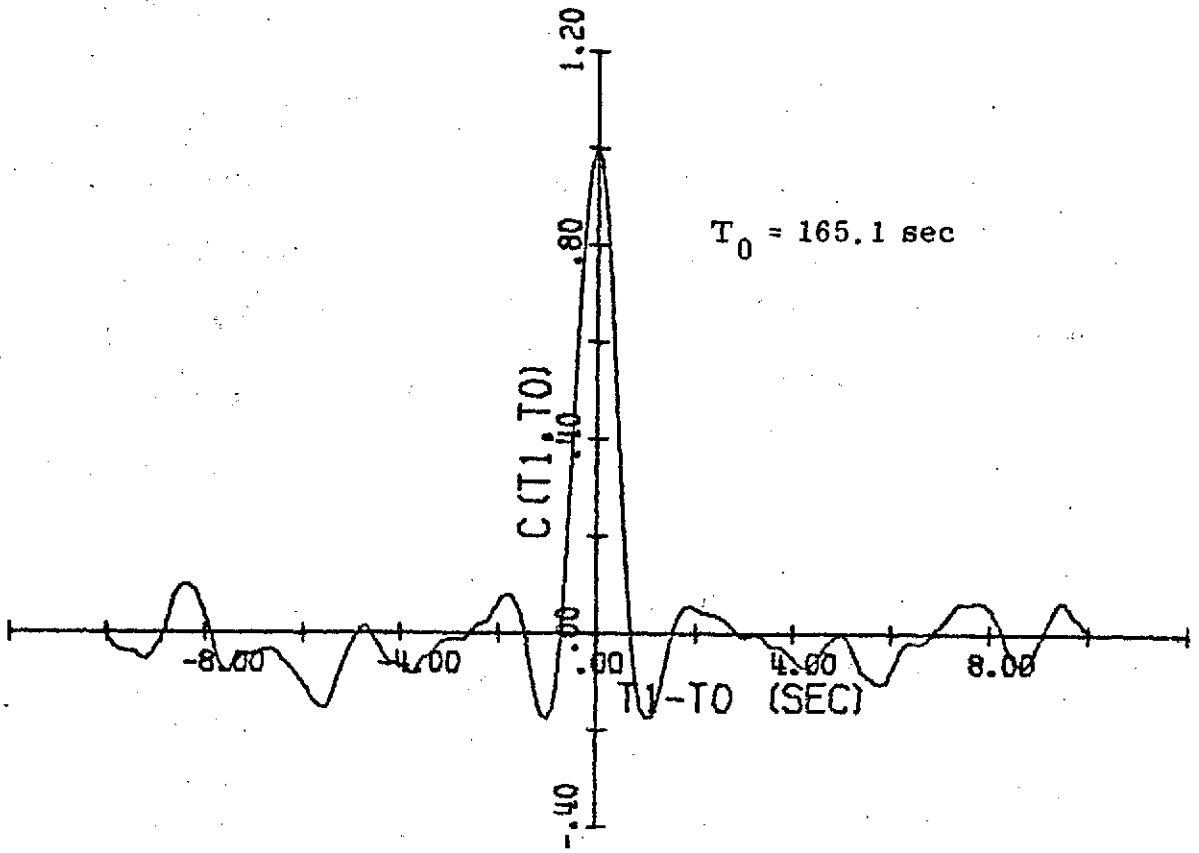

Figure 5.9 Error Signal Average Autocovariance Function over Final Static Interval for F14T75, Subject B

subject B; and they are evenly spaced at 5% intervals through the vehicle's transition period. Using the 11 adjacent autocovariance functions for an average serves to smooth out the data by washing out any sample or time variations which occur in less than one second. This provides a lower bound on the assumed region of quasi-stationarity, since these midpoints all lie within the time interval where the vehicle varies with time.

A plot of the average autocovariance function for the time-invariant final phase of the experiment, is presented in Figure 5.9. It is the average of (40) autocovariance functions taken at one second intervals during the last 60 seconds of the run, and is similar in character to the plot of Figure 5.4.

A similar set of average autocovariance functions can be developed for each point in the experimental matrix for each subject. In theory, at least, the time-varying autocovariance function provides a complete description of the magnitude characteristics of $\epsilon(t)$, and thus implies a time domain description of the Pilot-Vehicle-Regulator's gain characteristics (phase information is not present) for the given class of inputs. On the other hand, this type of information, doesn't provide a very meaningful description of the system; that is to say, time domain descriptions of this sort do not provide much insight into the character of the Pilot-Vehicle-Regulator.

The next section presents some techniques which can be employed to obtain more useful descriptive information from the time-varying standard deviation and autocovariance function.

6. DEVELOPMENT AND EVALUATION OF PSEUDO-SPECTRUM PARAMETERS

The purpose of this section is to show the development and evaluation of the parameters used to describe the pseudo-spectra. The method followed is to apply the Fourier Transform to a power spectral density and get a time-invariant autocorrelation function. Some of the properties of this autocorrelation function can then be applied to the autocovariance functions to give useful information about the pseudo-spectra.

Given an autocorrelation function for a stationary signal, the Fourier Transform provides a unique power spectral density for that signal, at least in the theoretical sense. Practically speaking, the transform is often difficult to perform when the autocorrelation is given in numerical form. For functions like those plotted in Figures 5.5 through 5.8, the results of numerically integrating the Fourier Transform would introduce great uncertainty. The functions are not symmetrical, which results in imaginary components in the power spectral density. They are not defined outside a rectangular window, which destroys the uniqueness properties of the transform and requires the introduction of digital filtering to smooth the resulting spectrum. It was thus felt that an attempt to actually transform these autocovariance functions would yield spectra which would not be meaningful. On the other hand, since there is a theoretical relationship between each autocovariance function and a corresponding pseudo-spectrum, it

should be possible to estimate some spectral information from the autocovariance functions. One of the most important characteristics of a spectrum is its bandwidth, and the following development shows how this characteristic can be estimated.

Bandwidth Parameter Development

In 1944, Rice (15) showed that one could estimate the bandwidth of a spectrum by counting the number of times the related signal crossed the zero value. Specifically, he demonstrated that, for a normally distributed random signal with mean zero and an ideal rectangular spectrum, the expected number of zero crossings per second is related to the cutoff frequency in hertz by the following equation:

$$E[\#\ \text{zeros/second}] = 1.155\ f_c \qquad (6.1)$$

This is a good indicator for a rectangular spectrum when the signal is stationary since then the expected number of zero crossing per second can be obtained by time averaging. When the signal is non-stationary the expected number of zero crossings per second can be estimated by ensemble averaging over a quasi-stationary period of time. In either case, however, Rice's technique is limited by the assumption that the signal has an ideal rectangular spectrum.

There are definitions of bandwidth which do not identify cutoff frequencies, but instead provide information about the concentration of signal power. For example, the Mean Square bandwidth is defined for any signal, regardless of its spectral shape. This bandwidth

definition can be used to indicate the region on the autocovariance functions where one might expect to find information about the bandwidth of the related unknown spectra. For a stationary, zero-mean signal y(t), the Mean Square bandwidth, given by Equation 6.2,

$$\omega_{MS} = \frac{\int_{-\infty}^{\infty} \omega^2 S_y(\omega)d\omega}{\int_{-\infty}^{\infty} S_y(\omega)d\omega} \tag{6.2}$$

can be interpreted in the time domain using the Fourier Transform pair

$$F(\omega) = \int_{-\infty}^{\infty} f(\tau)e^{-j\omega\tau}\, d\tau \tag{6.3}$$

and

$$f(\tau) = \frac{1}{2\pi} \int_{-\infty}^{\infty} F(\omega)e^{j\omega\tau}\, d\omega \tag{6.4}$$

The time differentiation theorem (13) of the Fourier Transform yields

$$\omega^2 S_y(\omega) \iff -\frac{d^2 R_y(\tau)}{d\tau^2} \tag{6.5}$$

The inverse Fourier Transform, Equation 6.4, with $\tau = 0$ is

$$f(0) = \frac{1}{2\pi} \int_{-\infty}^{\infty} F(\omega)\, d\omega, \tag{6.6}$$

and finally, combining Equations 6.5 and 6.6 yields

$$\left.\frac{-d^2 R_y(\tau)}{d\tau^2}\right|_{\tau = 0} = \frac{1}{2\pi} \int_{-\infty}^{\infty} \omega^2 S_y(\omega)d\omega \tag{6.7}$$

Similarly,

$$R_y(0) = \frac{1}{2\pi} \int_{-\infty}^{\infty} S_y(\omega)\, d\omega \tag{6.8}$$

but the autocorrelation for $\tau = 0$ is also defined as

$$R_y(0) = \sigma_y^2. \tag{6.9}$$

Thus, using time-domain quantities, Equation 6.2 becomes

$$\omega_{MS} = \frac{-\left.\frac{d^2 R_y(\tau)}{d\tau^2}\right|_{\tau=0}}{\sigma_y^2} \tag{6.10}$$

Unfortunately, when dealing with digitized signals it is very difficult to get accurate second derivative information as is required by Equation 6.10. The relationship does, however, serve to indicate the sort of information that the autocovariance functions should contain in regions close to the origin.

The technique utilized in this thesis consists of observing the lowest value of $|t_1 - t_o|$ in the plotted autocovariance functions for which the function has a relative minimum. This value is then used to estimate the bandwidth of the unknown pseudo-spectrum. The estimate is actually the bandwidth of a low-pass rectangular spectrum whose transform or autocorrelation exhibits a first relative minimum at the same distance from the origin as that of the autocovariance for the unknown spectrum.

At this point it is necessary to develop the relationship between the bandwidth of a rectangular spectrum and the value τ of its first relative minimum. Consider the rectangular spectrum and its corresponding transform as shown in Figure 6.1. The general form for this sort of spectrum is given by

$$S(\omega) = \begin{cases} a & , \quad |\omega| \leq \bar{\omega}_c \\ 0 & , \quad \text{elsewhere} \end{cases} \tag{6.11}$$

where $\bar{\omega}_c$ is the cutoff frequency of the spectrum. The transform of Equation 6.11, using Equation 6.4 is

$$R(\tau) = \frac{a\,\bar{\omega}_c}{2\pi} \cdot \frac{\sin \bar{\omega}_c \tau}{\bar{\omega}_c \tau} \,. \tag{6.12}$$

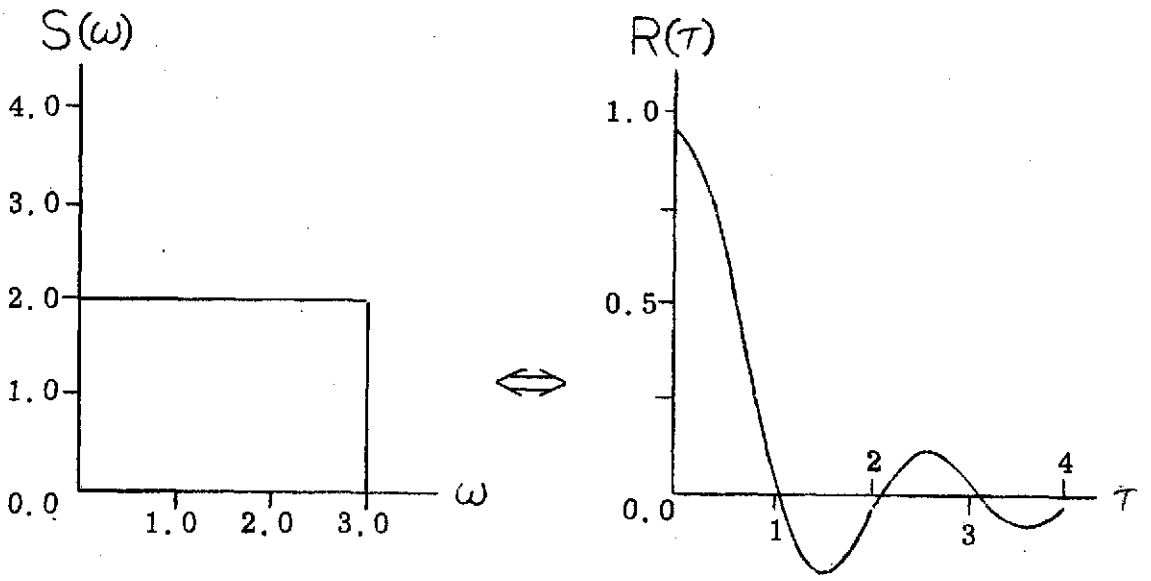

Figure 6.1 Low-Pass Rectangular Spectrum and Corresponding Autocorrelation Function

For the point of the first relative minimum of $R(\tau)$, it is necessary to look at

$$\frac{dR(\tau)}{d\tau} = 0 = \frac{a\,\bar{\omega}_c}{2\pi} \cdot \left[\frac{\bar{\omega}_c \cos \bar{\omega}_c \tau}{\bar{\omega}_c \tau} - \frac{\bar{\omega}_c \sin \bar{\omega}_c \tau}{(\bar{\omega}_c \tau)^2} \right] \tag{6.13}$$

or

$$0 = \cos \bar{\omega}_c \tau - \frac{\sin \bar{\omega}_c \tau}{\bar{\omega}_c \tau} \tag{6.14}$$

This equation can be solved numerically to obtain

$$\overline{\omega}_c \tau = 1.43 \pi \quad . \tag{6.15}$$

Thus, the relationship between the first observed relative minimum of the autocorrelation function $\hat{\tau}$ and the cutoff frequency of the corresponding low-pass rectangular spectrum is given by

$$\overline{\omega}_c = \frac{1.43\pi}{\hat{\tau}} \tag{6.16}$$

Equation 6.16 provides the means for estimating the bandwidth of the arbitrary spectrum; this estimate will hereafter be called the Bandwidth Parameter $\hat{\omega}_c$. To make the estimate, one plots the autocovariance for the signal in question, observes the value $\hat{\tau}$ of the first relative minimum, and then uses Equation 6.17 to obtain the bandwidth parameter $\hat{\omega}_c$.

$$\hat{\omega}_c = \frac{1.43\pi}{\hat{\tau}} \tag{6.17}$$

In order to give the reader a better understanding of how the bandwidth parameter relates to the bandwidth of an arbitrary spectrum, the following example is given: Consider the arbitrary bandlimited spectrum shown in Figure, 6.2, along with a reasonable approximation of its autocorrelation function. The first relative minimum occurs at $\hat{\tau} = 1.03$ seconds and using Equation 6.17 results in a bandwidth parameter value of $\hat{\omega}_c = 4.36$ radians per second. Figure 6.3 shows a rectangular low-pass spectrum with cutoff frequency of 4.36 radians per second superimposed on the original spectrum. The average power in the rectangular spectrum was taken to be that of the original

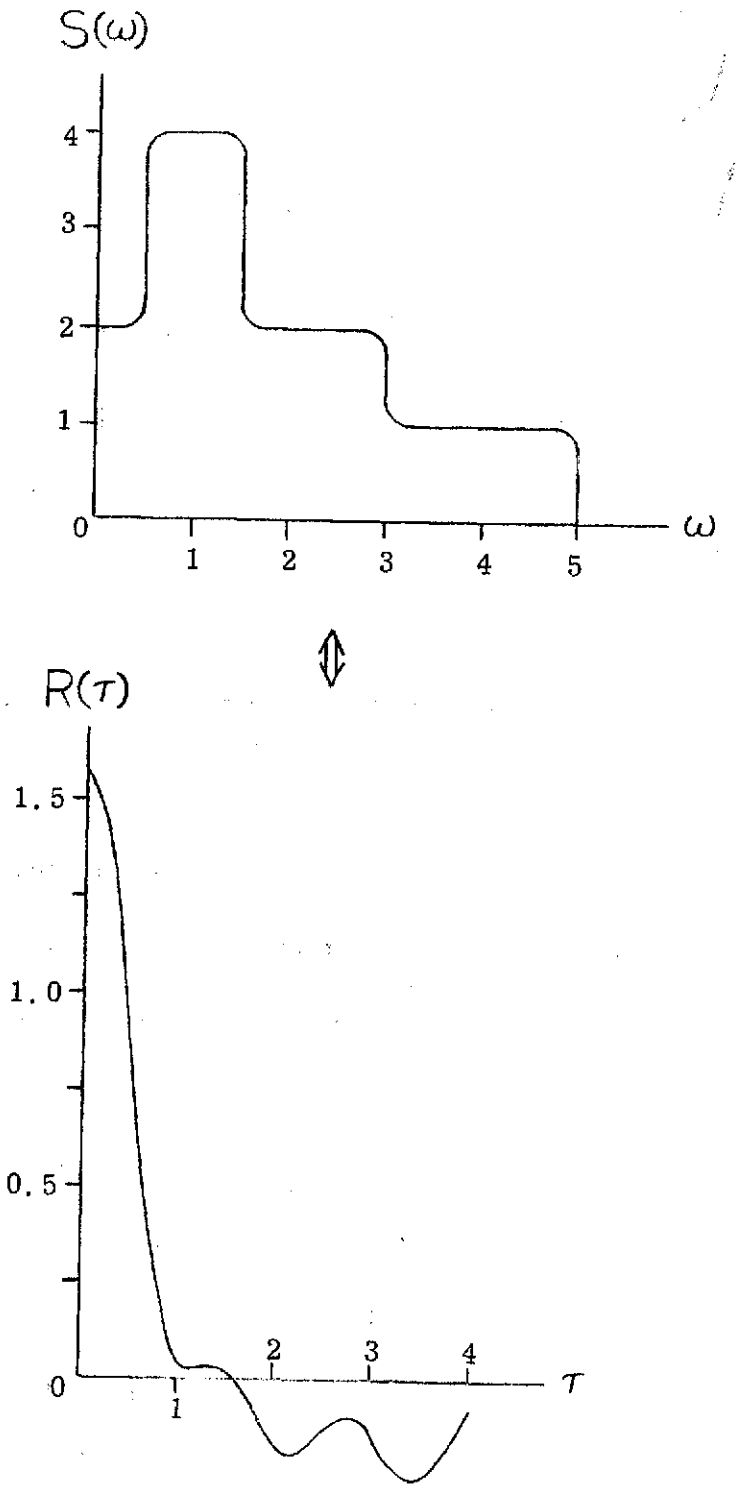

Figure 6.2 Example Spectrum and Autocorrelation Function

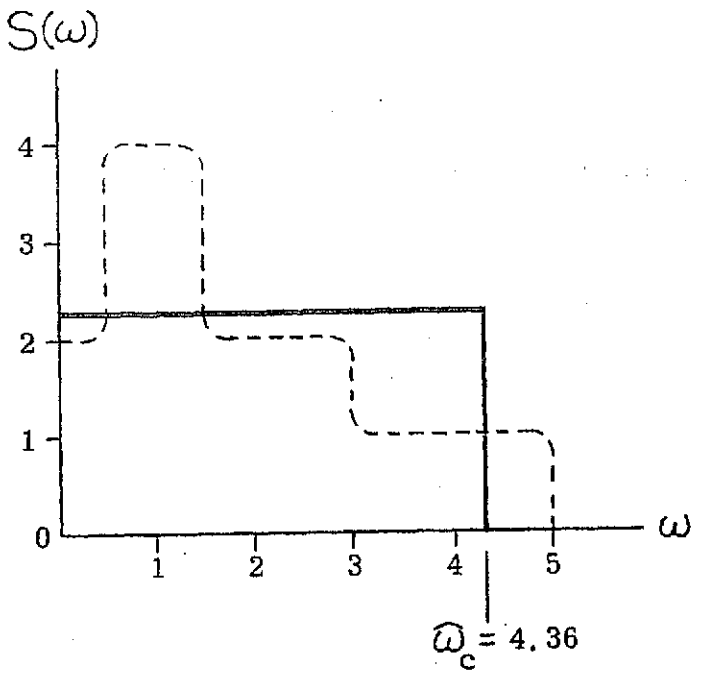

Figure 6.3 Comparison of Bandwidth Parameter Results and Original Example Spectrum

spectrum. Clearly, the estimate $\hat{\omega}_c = 4.36$ radians per second is quite reasonable for this situation. Further validation of this technique, using experimental data signals, will be presented in the next section of this chapter.

Further Considerations of the Bandwidth Parameter Approach - A study of the autocovariance function plots such as Figures 5.4 through 5.8 yields some important facts when one assumes that they represent autocorrelations, as discussed in the previous chapter. The plot of the autocovariance function doesn't, in itself, give a unique indication of the signal's frequency content since the function's behavior is unknown as $|t_1 - t_o|$ goes toward infinity. Thus, the Fourier

transform of the given plot would have no particular relevance to a power spectral density. Efforts to work around this problem such as defining the autocovariance function to be zero beyond the indicated window and/or the use of filter windows in the Fourier Transform, all have the property of influencing the frequency content of the resultant power spectral density.

On the other hand, if one assumes that the spectrum or pseudo spectrum (although unknown) of the observed signal is bandlimited, then immediately the mathematical structure of the problem is more solid and it follows that the bandwidth is indicated by the behavior of the autocovariance relatively close to the origin, without further consideration of the behavior of the autocovariance function as $|t_1 - t_o|$ gets large.

Another consideration is that as the signal bandwidth gets larger, the necessary autocovariance window width gets smaller. An a priori selection of window width doesn't affect the indicated value of bandwidth in any way, so long as a first relative minimum is, in fact, observed. Thus, one can estimate bandwidth with relatively short segments of data, the length depending inversely upon the signal bandwidth.

Application Methods - It is useful to note that when asymmetry does occur in the autocovariance functions, the time corresponding to the first relative minimum to the left of the origin has a different magnitude than that corresponding to the first relative minimum to the right of the origin. Further, when the times of the relative minima

are compared with those which result from other autocovariances generated for the same stationary signal, it is generally found that when one time increases relative to its expected value, the other decreases. Thus, it was decided to use

$$\hat{\tau} = \frac{\hat{\tau}_L + \hat{\tau}_R}{2} \tag{6.18}$$

to calculate $\hat{\omega}_c$, where $\hat{\tau}_L$ and $\hat{\tau}_R$ are the time magnitudes of the first relative minima to the left and right of the origin respectively. This also serves to include information about signals in both the past and future, relative to the midpoint. Occasionally, one of the two relative minima occurs at such a large value that it is inconsistent with the other minimum for that function and with the minima observed in other similar functions. When this occurs, judicious reason dictates that value of $\hat{\tau}_L$ or $\hat{\tau}_R$ not be used to generate $\hat{\omega}_c$. In every instance in which this problem arose, the value of τ that was in error was much too large. Thus the rule applied was that when one value of τ_L or τ_R was greater than 2.5 times the other value, the smaller of the two values was adopted as $\hat{\tau}$.

Power Parameter Development

The arbitrary spectrum $S_y(\omega)$ is related to the autocorrelation function $R_y(\tau)$ by

$$R_y(\tau) = \frac{1}{2\pi} \int_{-\infty}^{\infty} S_y(\omega)\, e^{j\omega\tau}\, d\omega \ . \tag{6.19}$$

Letting τ go to zero, the relationship becomes

$$R_y(0) = \frac{1}{2\pi} \int_{-\infty}^{\infty} S_y(\omega)\, d\omega \tag{6.20}$$

or

$$\int_{-\infty}^{\infty} S_y(\omega)\, d\omega = 2\pi R_y(0) . \tag{6.21}$$

$R_y(0)$ equals the variance of y under the mean-zero assumption. Thus

$$\int_{-\infty}^{\infty} S_y(\omega)\, d\omega = 2\pi \sigma_y^2 \tag{6.22}$$

and by defining the area under the curve of $S_y(\omega)$ as the average power, P_y, of y, the result is

$$P_y = 2\pi \sigma_y^2 \tag{6.23}$$

In the case of time-varying signals, the pseudo spectrum can have a time-varying average power or power parameter given by

$$P_y(t) = 2\pi \sigma_y^2(t) \tag{6.24}$$

Parameter Variability

In the development of any descriptive parameters for stochastic processes, it is important to obtain some sort of estimate of the variability of the parameter. In this particular situation, it is also desirable to include the effects of the human subject's variability since this will cause variation in the thing which is being described. When dealing with the variability of the bandwidth parameter, one must also be concerned with the various definitions of bandwidth. Rather than make an a priori selection of one single definition, two useful definitions will be used and data analyzed for both. The two definitions are: $\overline{\omega}_{c_1}$, the bandwidth of the rectangular spectrum whose area and midband density value are equal to those of the spectrum in question; and $\overline{\omega}_{c_2}$, the

frequency at which the power density level has dropped by 3 decibels from that at the midband. The latter bandwidth is also called the half-power frequency.

Data Analysis - The first step in determining the precision of the bandwidth parameter $\hat{\omega}_c$ is to apply the methodology to a signal which is stationary in the wide-sense and whose bandwidth is known. A suitable test signal in this instance is the input disturbance or noise which was recorded during each trial, thus providing 10 replicates of a stationary signal. Utilizing a statistical analysis program available in The University of Michigan Computing Center (7), the power spectral density is computed by time-averaging methods for one of the noise signals from condition F14T0, Subject A. The spectrum is shown in Figure 6.4, along with the 99% confidence intervals for the density levels. The -3db break point (half-power point) occurs at $\omega = 1.05$ rad/sec, and the equivalent square cutoff frequency is $\omega = 1.36$ rad/sec. The filter break frequency is at 1.4 rad/sec, as indicated.

The bandwidth parameter methodology is now applied to the noise signals in the same condition, i.e, condition F14T0, Subject A. Using ensemble techniques, autocovariance functions were generated and in Figure 6.5, the results of averaging 41 autocovariance functions with midpoints taken one second apart is shown. The value of the first relative minima are $\hat{\tau}_L = 4.2$ seconds and $\hat{\tau}_R = 4.6$ seconds which yield the estimate $\hat{\omega}_c = 1.02$ rad/sec from Equation 6.17. Using

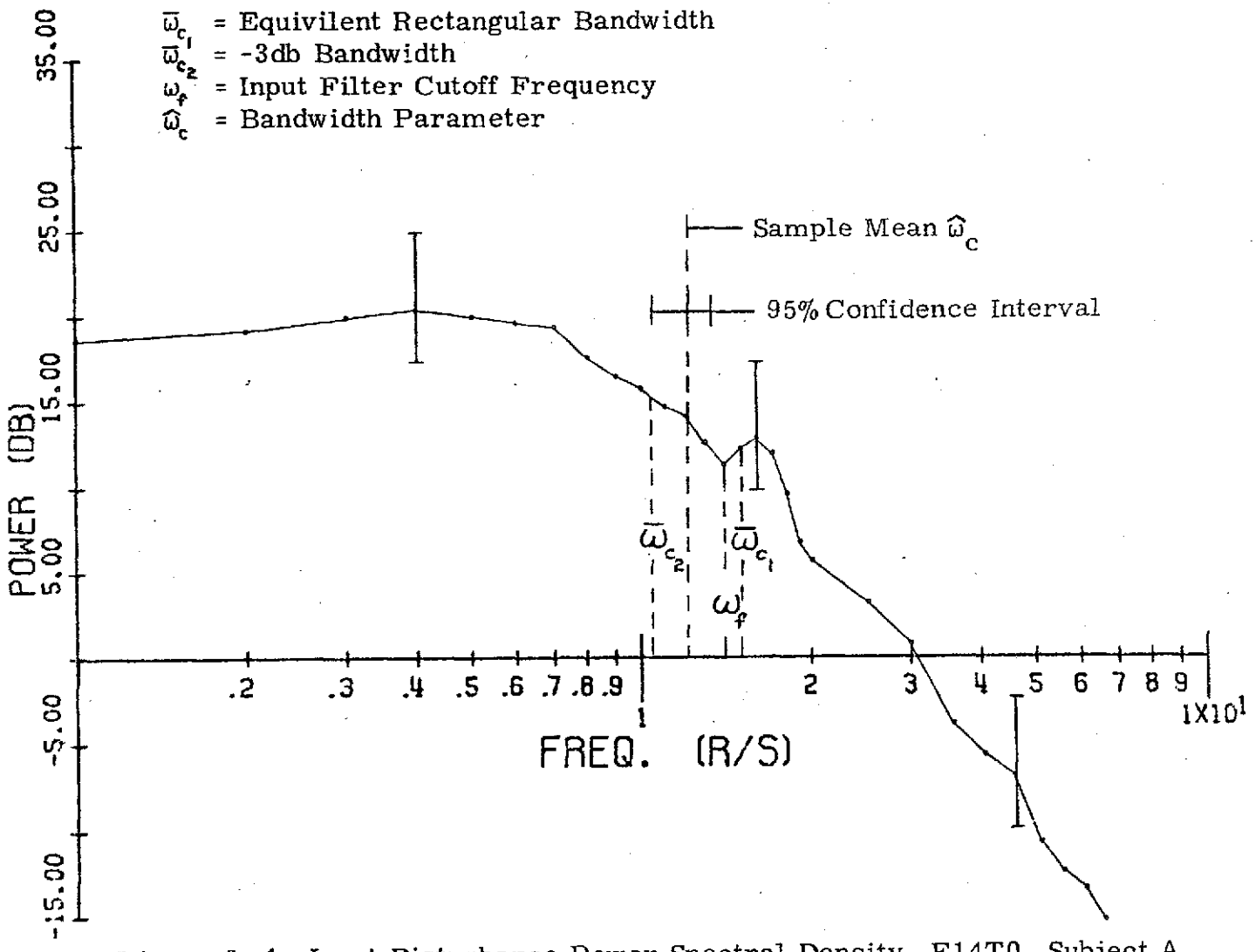

Figure 6. 4 Input Disturbance Power Spectral Density, F14T0, Subject A

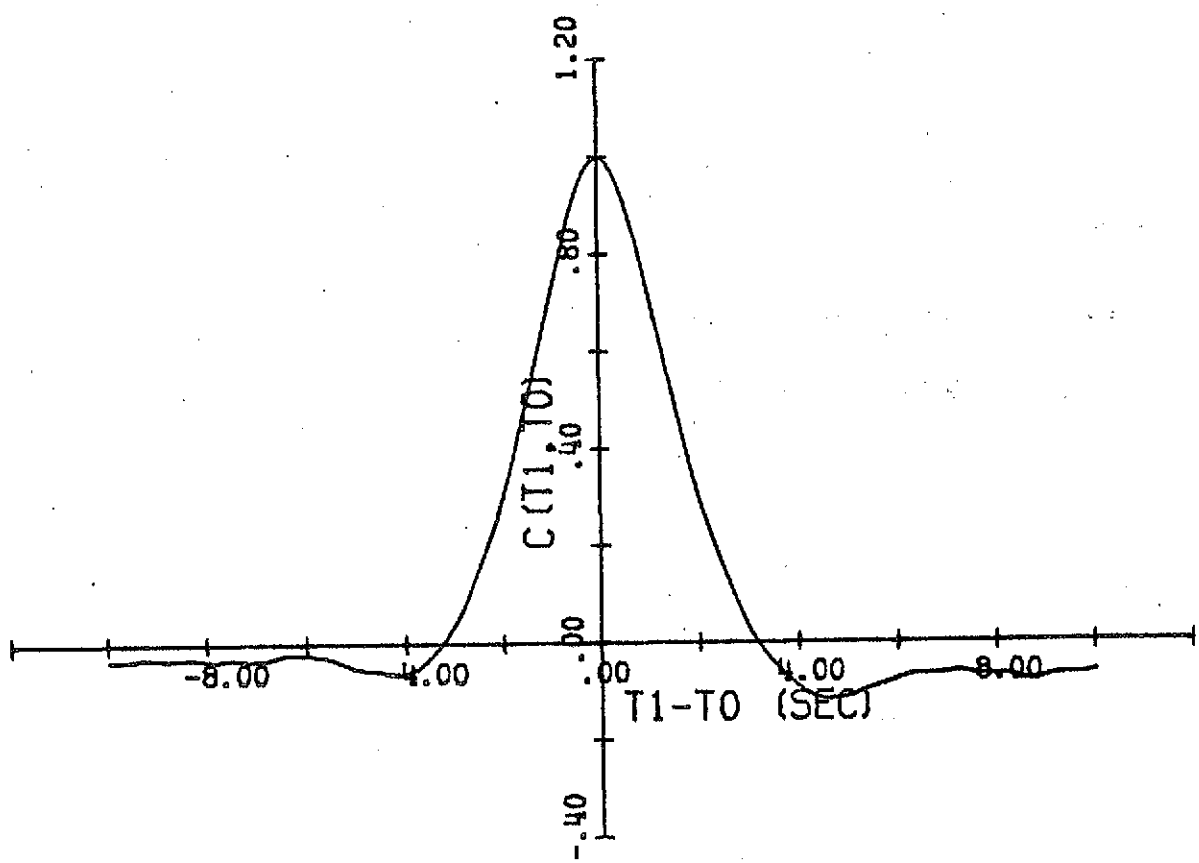

Figure 6.5 41-Point Average Autocovariance Function for Noise Signal, F14T0, Subject A

the value of the covariance function for this signal at one second intervals, it can be estimated that this average is equivalent to taking one ensemble autocovariance over about 90 replicates. This estimation is done as follows: The actual equation for the variation of the sample mean of error signal is developed for the case where the variance is determined by doing ensemble averaging at time intervals of one second and averaging the 41 resulting values. This formula is then equated to the formula for the variation of the sample mean computed at one point in time from N replicates, where N is an unknown integer. Using the empirically determined correlation for the error signal, one can then solve the equation for N, which is the number of replicates necessary for one ensemble average, in order that it have equivalent precision to the combined ensemble-time average. Thus, whenever autocovariance functions are averaged in this manner, i.e., a large number taken one second apart in a portion of the signal that is time-stationary by definition, then the accuracy associated with each average is relatively high.

Figure 6.6 shows an autocovariance function that is the average of 11 autocovariances with midpoints separated by 0.1 seconds in the 10.1 to 11.1 second range of the condition. This average is approximately equivalent to one ensemble autocovariance taken over 13 replicates when the covariance at these separations is considered. For the function shown in Figure 6.6, the bandwidth parameter $\hat{\omega}_c$ is 1.219 rad/sec. Table 6.1 below shows $\hat{\omega}_c$ for 15 different midpoints on the same ensemble of noise signals.

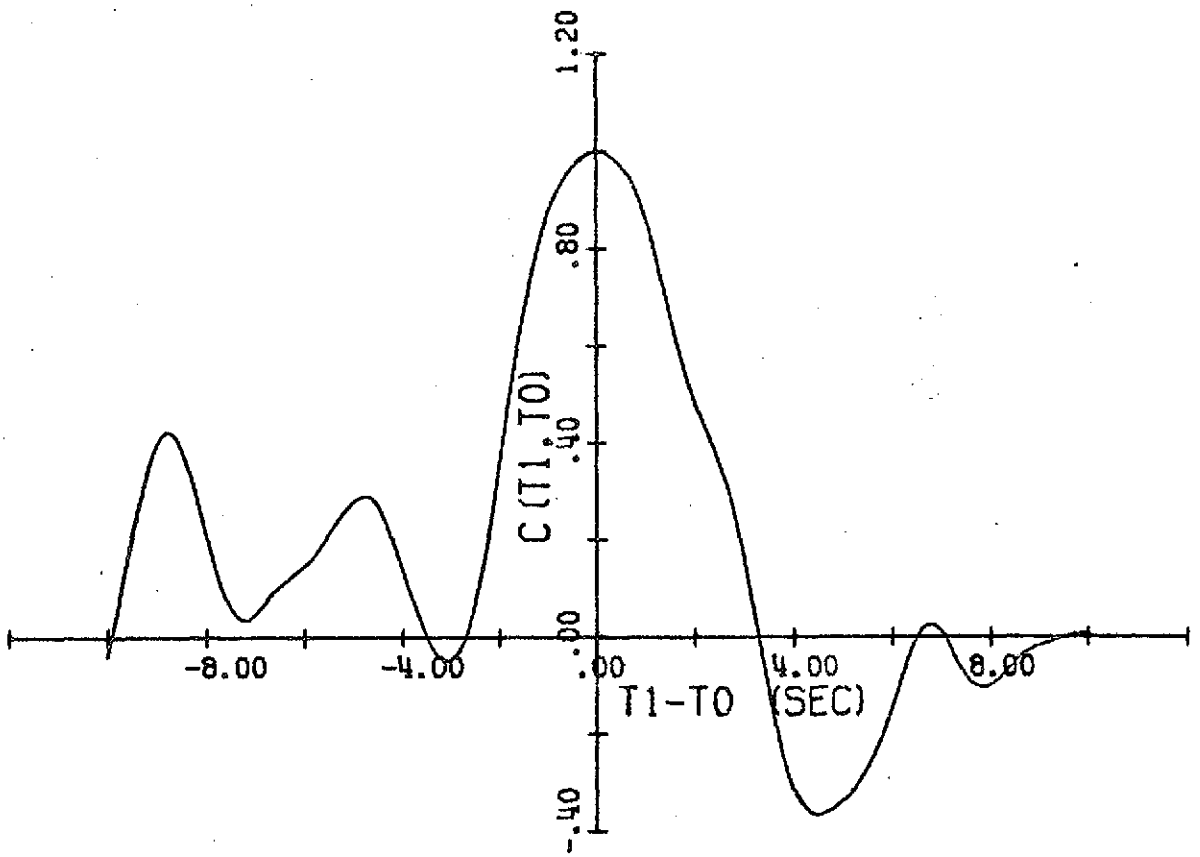

Figure 6.6 11-Adjacent-Point Average Autocovariance Function for Noise Signal, F14T0, Subject A

Midpoint (sec)	$\hat{\tau}$ (sec)	$\hat{\omega}_c$ (rad/sec)
10.6	3.85	1.16
16.6	4.0	1.12
22.6	3.85	1.16
28.6	2.45	1.83
34.6	4.05	1.10
40.6	4.1	1.09
46.6	4.95	.90
52.6	3.4	1.32
58.6	3.65	1.23
64.6	3.1	1.44
70.6	2.95	1.52
76.6	4.25	1.05
82.6	4.8	0.93
88.6	4.2	1.06
44.6	4.55	0.98

Table 6.1 Bandwidth Parameter Values using Midpoints in One Ensemble

Computing the sample mean and standard deviation gives 1.19 radians per second and 0.256 radians per second respectively. The 95% confidence limits on the population mean are 1.337 and 1.043 rad/sec and in Figure 6.4, the same mean is shown along with the 95% confidence interval.

Identical analyses were performed on the noise signals for conditions F20T0 and F8T0, Subject A; and the results of this effort are presented in Table 6.2.

Another source of test signals to determine the variability of the bandwidth parameter is the last 170 seconds of data for the situations where the plant changes instantaneously, as is the case for conditions F20T0, F14T0 and F8T0. The error signals after the switch transients have died out are by definition, stationary in the wide sense and long enough for time averaging techniques. Since the human in the system can provide some time variance, this analysis may allow the estimation of that portion of the parameter variation which is due to the pilot. When calculated for a particular signal in the ensemble for F14T0, Subject A, the power spectral density is as shown in Figure 6.7. Ten values of $\hat{\omega}_c$ were computed from this ensemble in the manner previously presented. The results of this analysis are shown on Figure 6.7 and are also included in Table 6.2.

Table 6.2 summarizes the analysis of the variability of the bandwidth parameter. Both the equivalent square bandwidth and the -3db bandwidth definitions are provided as reference points for the reader. The variability of the samples is quite low since the 95% confidence interval is between ± 8% and ±12% of the sample mean for each different set of samples. In two of the cases shown on Table 6.2, both the mean $\hat{\omega}_c$ and its 95% confidence interval lie in between the values of cutoff frequency for the Equivalent Square and -3db definitions. In the other two cases, the mean $\hat{\omega}_c$ is above the two reference points. For the samples taken from generated noise signals (the first three sample sources), the mean $\hat{\omega}_c$ is reasonably close to the input filter

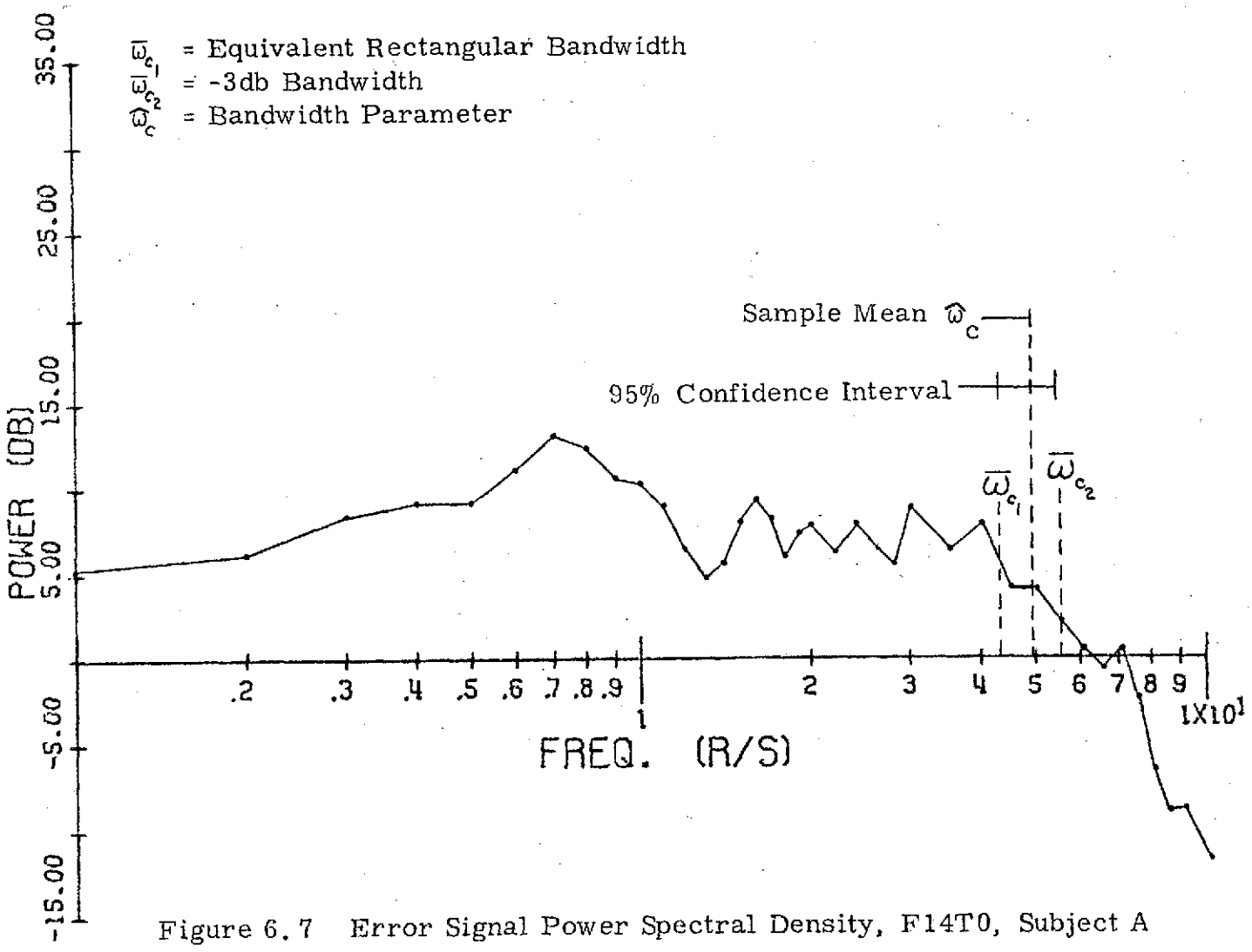

Figure 6.7 Error Signal Power Spectral Density, F14T0, Subject A

Sample Source	Equiv. Square Cutoff Frequency	-3db Cutoff Frequency	Sample Mean of $\hat{\omega}_c$	Sample Standard Deviation of $\hat{\omega}_c$	$\hat{\omega}_c$ Sample Size	95% Confidence Interval on Mean $\hat{\omega}_c$
F8T0 Subject A Noise	0.46 r/s	0.4 r/s	0.86 r/s	0.17 r/s	15	0.76 r/s to 0.96 r/s
F14T0 Subject A Noise	1.36 r/s	1.05 r/s	1.19 r/s	0.25 r/s	15	1.09 r/s to 1.33 r/s
F20T0 Subject A Noise	1.56 r/s	1.3 r/s	2.33 r/s	0.33 r/s	15	2.14 r/s to 2.52 r/s
F14T0 Subject A Error	4.31 r/s	5.5 r/s	4.87 r/s	0.73 r/s	10	4.31 r/s to 5.43 r/s

Table 6.2 Summary of Bandwidth Parameter Variability Analyses

frequency $\hat{\omega}_c$. However, there appears to be no clear relationship between the mean value of $\hat{\omega}_c$ and either the equivalent squre cutoff frequency or the -3db cutoff frequency. This is not surprising when the relative arbitrariness of the two definitions is considered.

The analysis performed on the error signal for condition F14T0, Subject A, is the only one of the four entries in Table 6.2 that can show any effects due to pilot's variability. Since for this case, the 95% confidence interval is ±11% of the mean $\hat{\omega}_c$, it seems safe to say that the introduction of the subject's variability does not significantly affect the precision of the bandwidth parameter. The precision associated with the power parameter is directly related to the variability of the standard deviation σ. To get a measure of the variation of the points on the plots of standard deviation, the following technique was used:

The last 173.5 seconds of one of the replicates of the error signal from F14T0, Subject A, were analyzed to get the time invariant standard deviation $\sigma_\epsilon = 1.814$ mm and mean $m_\epsilon = 0.0817$.

The 1.5 second average values of $\sigma_\epsilon(t)$ computed by ensemble methods were obtained for the same time period, resulting in 115 samples. The mean of these samples was 1.903 mm and the sample standard deviation was 0.633. Computing the 95% confidence interval on the population mean yields the limits of 1.785 mm and 2.021 mm; and this is ± 6% of the sample mean. The resulting power parameter precision is ± 12% of the average power parameter value.

7. RESULTS

This chapter presents the results of the data reduction and analysis. The emphasis is upon obtaining a description of the Pilot-Vehicle-Regulator as previously discussed. Thus, the results concentrate upon analysis of the error signal, $\epsilon(t)$. There are two main areas of experimental description, one using the standard deviation which reflects the power parameter; and one using the autocovariance function to generate the bandwidth parameter. This chapter also includes a comparison of the time-varying results with the results of time-stationary analysis of the tracking task at several different values of ϕ. The effect of increasing the number of replicates from 10 to 40 is also given. Finally, an attempt to utilize the crossover model to represent the performance of the pilot in this task is outlined, and the results of this analytical effort are presented.

Power Parameter Results

In Figures 7.1 and 7.2, the standard deviation of $\epsilon(t)$ is presented for each subject and each point in the experimental matrix. From these plots it can be seen that, in general the standard deviation, and thus the power parameter, since it is proportional to σ^2, stays at one value during the first 60 second portion of the run and then reduces to a lower level during the variation, where it remains throughout the remainder of the run. This phenomenon is least evident in the case where the input filter cutoff frequency is 0.8 radians per second, and for some of these cases doesn't seem to occur at all. Subject

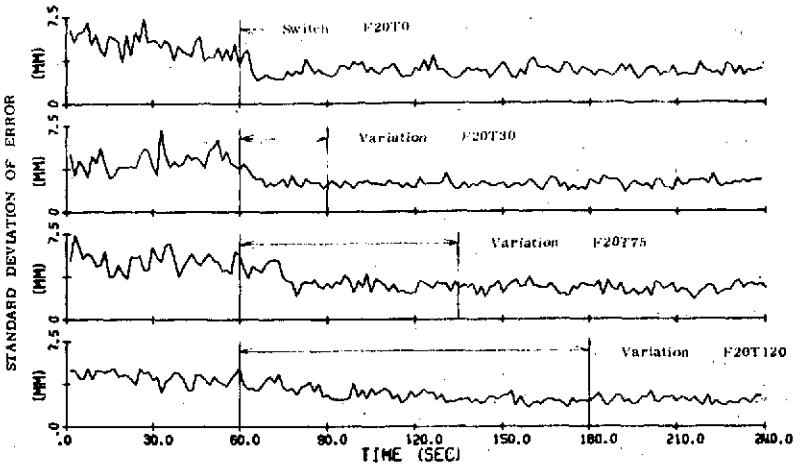

(a) Input Filter Frequency = 2.0 radians per second

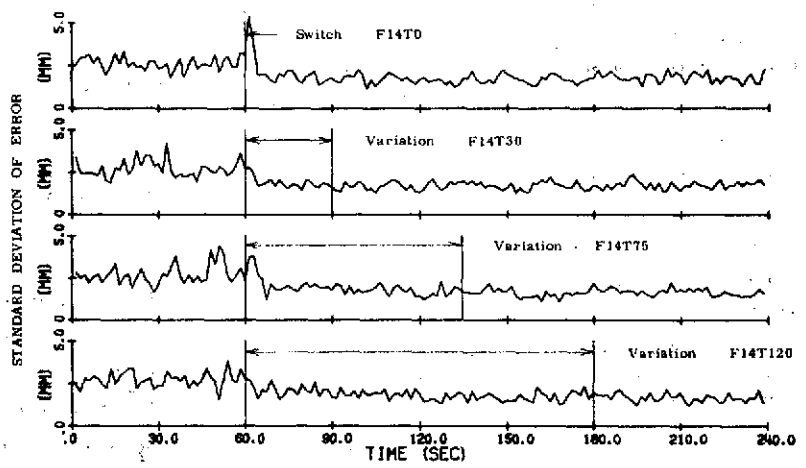

(b) Input Filter Frequency = 1.4 radians per second

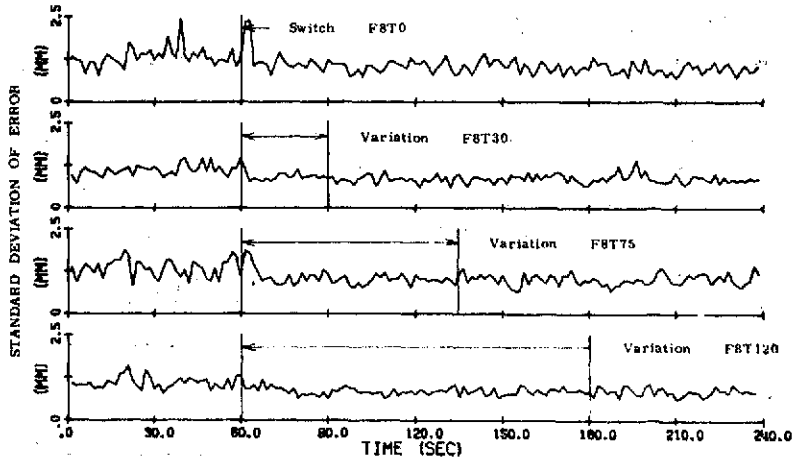

(c) Input Filter Frequency = 0.8 radians per second

Figure 7.1 Standard Deviation of Error Signal, Subject A

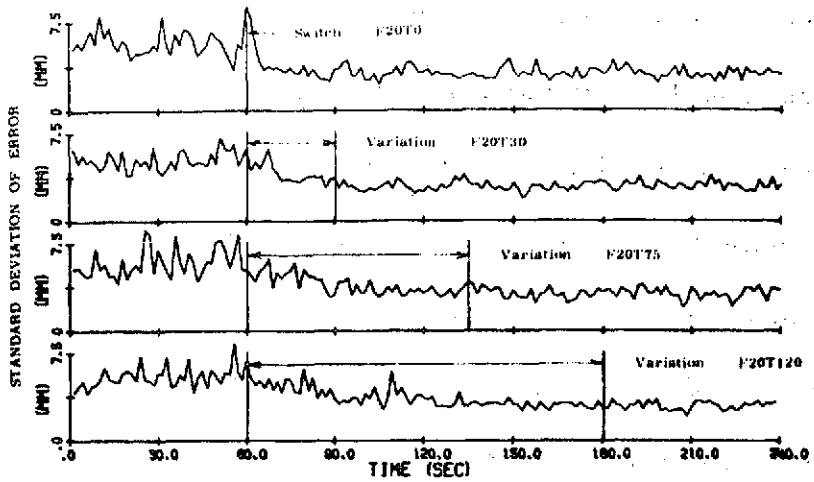

(a) Input Filter Frequency = 2.0 radians per second

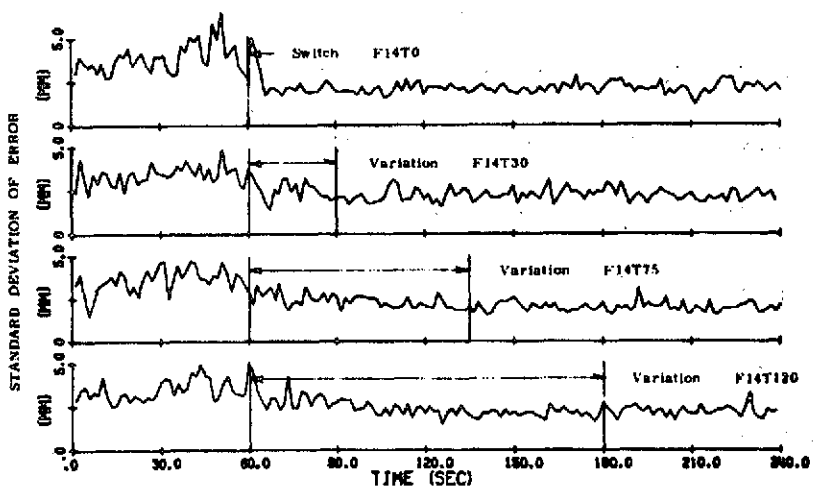

(b) Input Filter Frequency = 1.4 radians per second

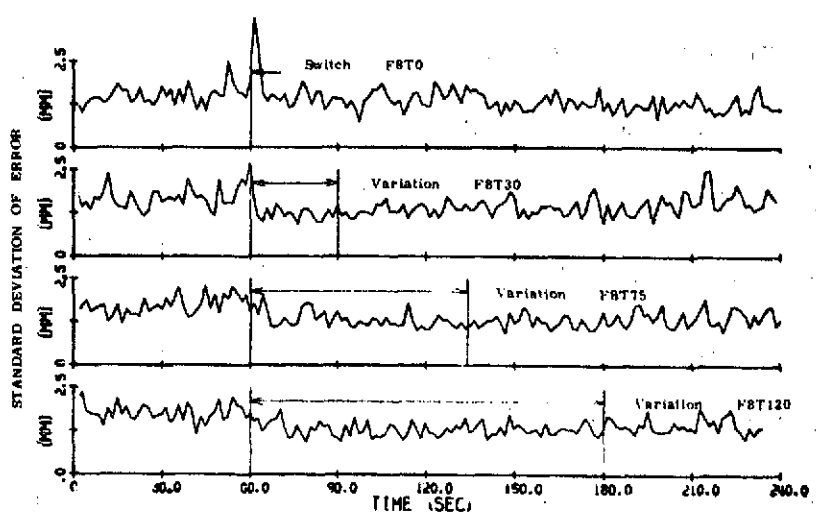

(c) Input Filter Frequency = 0.8 radians per second

Figure 7.2 Standard Deviation of Error Signal, Subject B

comments to the effect that these runs were very frustrating because he wasn't able to do any better regardless of what he tried, lead to the conclusion that the indicated levels for input bandwidth of 0.8 r/s are a lower bound, and a further reduction in input bandwidth would probably not show significant reduction in output power levels. This frustration is further indicated by the tendency for the power levels to increase slightly near the end of the run, which indicates a high fatigue factor.

From these curves it can also be seen that the transition to the final power level is smooth, except for those cases where an instantaneous transition occurs. In those latter cases, the error levels are higher, as indicated by a rise in the standard deviation value, during a 4-5 second period just after the switch occurs. This phenomenon agrees qualitatively with other research efforts such as Young, et al (19) where sudden changes in controlled dynamics were investigated.

For those situations where the transition takes place over 30, 75, or 120 seconds, the change in power level occurs during the early portion of the transition and is completed after 30 to 50 percent of the transition time. When the plots of the standard deviation of the error signal are regrouped and rescaled, as is shown in Figures 7.3 and 7.4, it can be seen that the standard deviation and hence the power levels of the output of the Pilot-Vehicle-Regulator are heavily dependent upon the input disturbance bandwidth, since the input power was held constant. A comparison between subjects yields the fact that the output power levels of Subject B are somewhat higher than those of Subject A,

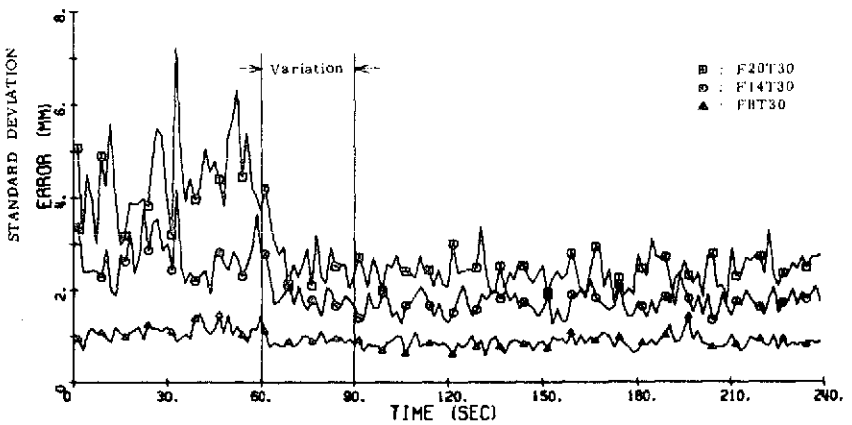

(a) 30 Second Variation

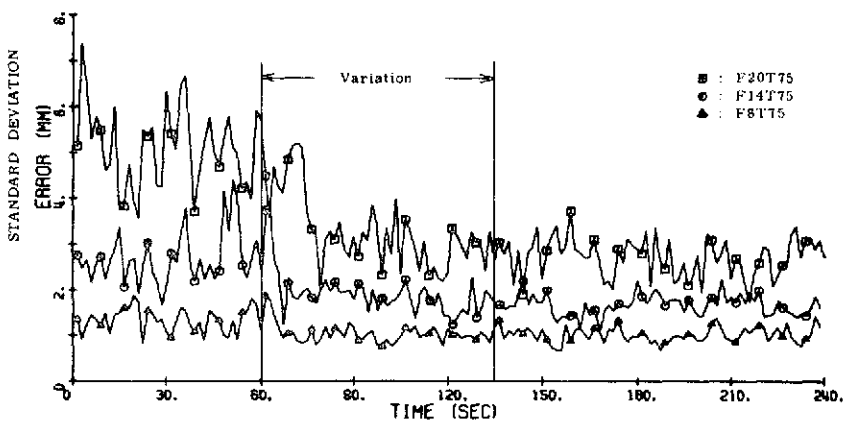

(b) 75 Second Variation

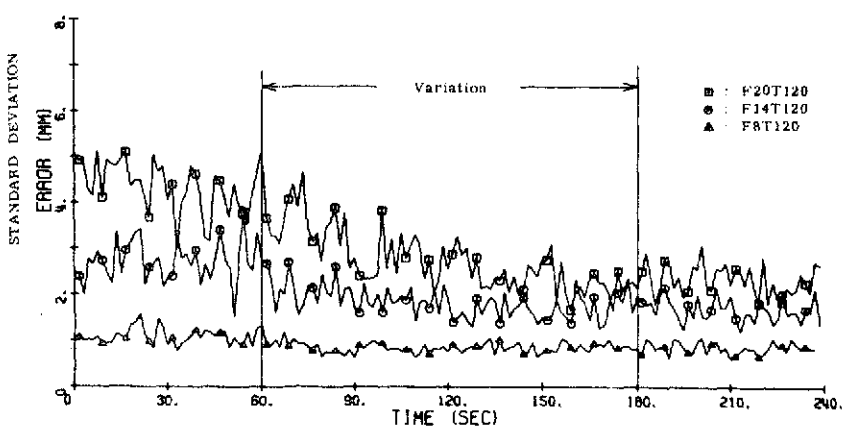

(c) 120 Second Variation

Figure 7.3 Standard Deviation of Error Signal, Subject A

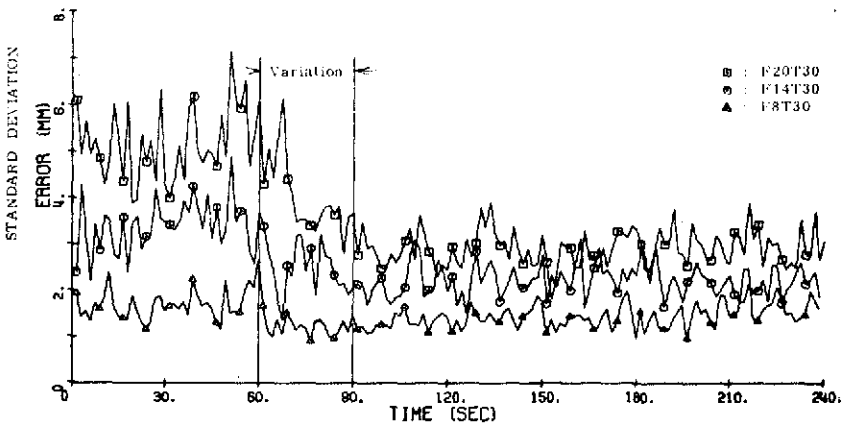

(a) 30 Second Variation

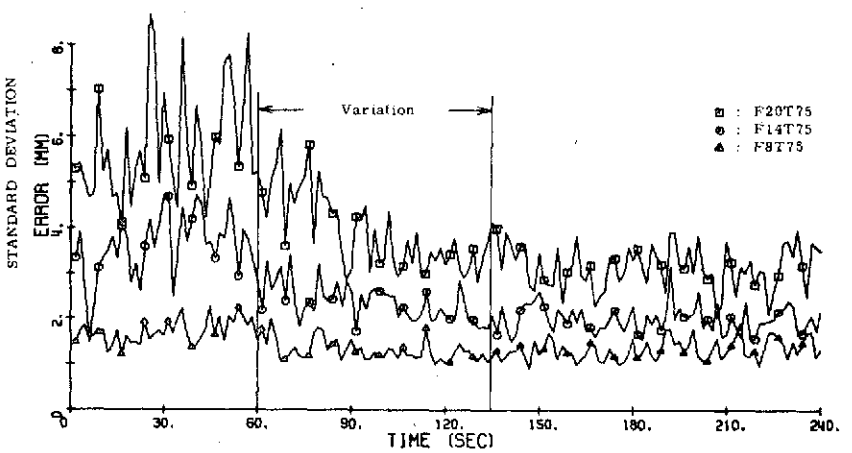

(b) 75 Second Variation

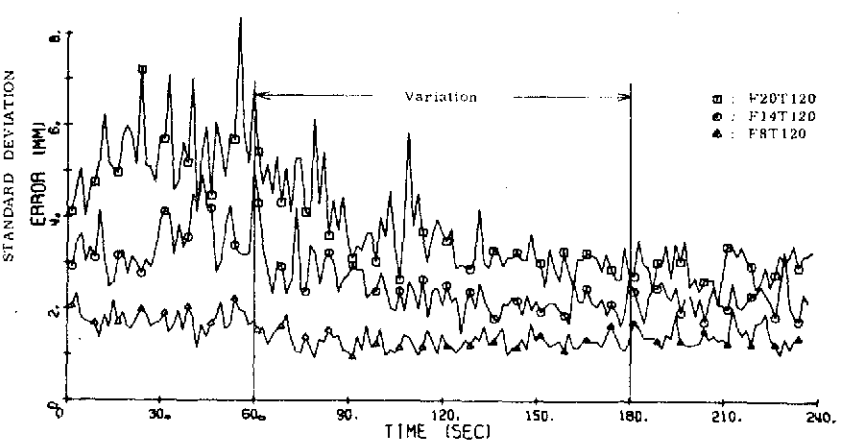

(c) 120 Second Variation

Figure 7.4 Standard Deviation of Error Signal, Subject B

yet the shapes of the respective subject curves are quite similar during the transitions.

In an effort to understand further the changes that occur in the standard deviation of the error signal during the variations, a separate three-way Analysis of Variance was performed on the standard deviation data for each subject. The three data classifications were: (1) by the input noise filter cutoff frequency, hereafter called the Filter Frequency; (2) the speed, in real time, at which the transition occurred, called Speed; and (3) the percent of the variation through which the vehicle has passed, called Percent. This is equivalent to 100 ϕ where ϕ is varying from 0 to 1 as previously discussed. Tables 7.1 and 7.2 show the results of the 3-way Analysis of Variance for Subject A and B, respectively. The Filter Frequency has 3 possible values; 0.8, 1.4 and 2.0 radians per second. The speed has 3 possible values: high, 30 second transition; middle, 75 second transition; and low, 120 second transition. The samples were taken at intervals of 10% of the variation yielding 11 values for the Percent Classification since both 0% and 100% points were included. Each cell in the Analysis of Variance contained one observation.

Table 7.2 shows that Speed is not a significant factor for Subject B, whereas, from Table 7.1, Speed is significant for Subject A. In an effort to further understand this phenomenon, the means for the Speed factor from the Analysis of Variance data for Subject B were analyzed using the Newman-Keuls Test as outlined in Reference 18.

Source	Degrees of Freedom	Mean Square	F Value
Filter Frequency	2	32.565	306.55 *
Speed	2	1.131	10.64 *
Percent	10	1.149	10.81 *
Filter Frequency - Speed	4	0.131	1.24
Filter Frequency - Percent	20	0.317	2.98 **
Speed - Percent	20	0.119	1.12
Filter Frequency - Speed - Percent	40	0.106	

*denotes significance @ $\underline{P} < .001$
**denotes significance @ $\underline{P} < .005$

Table 7.1 3-Way Analysis of Variance for Standard Deviation, Subject A

Source	Degrees of Freedom	Mean Square	F Value
Filter Frequency	2	57.274	198.45 *
Speed	2	0.172	0.59
Percent	10	1.195	4.142 *
Filter Frequency - Speed	4	0.258	0.296
Filter Frequency - Percent	20	0.657	2.276 ****
Speed - Percent	20	0.273	0.967
Filter Frequency - Speed - Percent	40	0.288	

*denotes significance @ $\underline{P} < .001$
****denotes significance @ $\underline{P} < .025$

Table 7.2 3-Way Analysis of Variance for Standard Deviation, Subject B

Analysis of Variance Data

Speed	Mean
Low	1.81515
Middle	2.13151
High	1.80666

Speed Mean Test

	T_1 High	T_2 Low	T_3 Middle	r	$q_{.99}(r,40)\sqrt{MS_{error}/33}$
High	---	0.00349	0.32485***	3	0.2473
Low		---	0.31636***	2	0.2162

***denotes significance @ $P < .01$

Table 7.3 Newman-Keuls Test on Speed Means, σ_ϵ, Subject A.

Table 7.3 shows the results of this test. Since the Newman-Kuels Test shows that there is no significant difference between the high and low speed, logic dictates that the significance of the middle speed relative to the other two must be the result of some other confounding effect. In Appendix B, the experimental sessions are outlined and it can be noted that in every case, the middle speed trials were performed on one day and both the high and low speed trials were performed on a different day. By randomizing the order of high and low speed trials within a session, the subject non-stationarity within a session was balanced; however, subject non-stationarity between sessions could, and in the author's opinion it does, account for the significant difference between the middle speed mean and both the high and low speed means. The subject non-stationarity is thus assumed to be the cause of the significance of the speed variable in the Analysis of Variance and this assumption allows the assertion that the speed variable is not important for either subject.

Figures 7.5 and 7.6 show the standard deviation versus percent of variation for each input filter frequency and each subject. In each case the data has been averaged over the three values of speed. These figures are a further indication that the transition from one level to another does not take place over the entire vehicle variation, but rather it occurs during a portion of it. Further, the point at which the transition is essentially completed appears to be a function of input bandwidth, as is indicated by the significant interaction

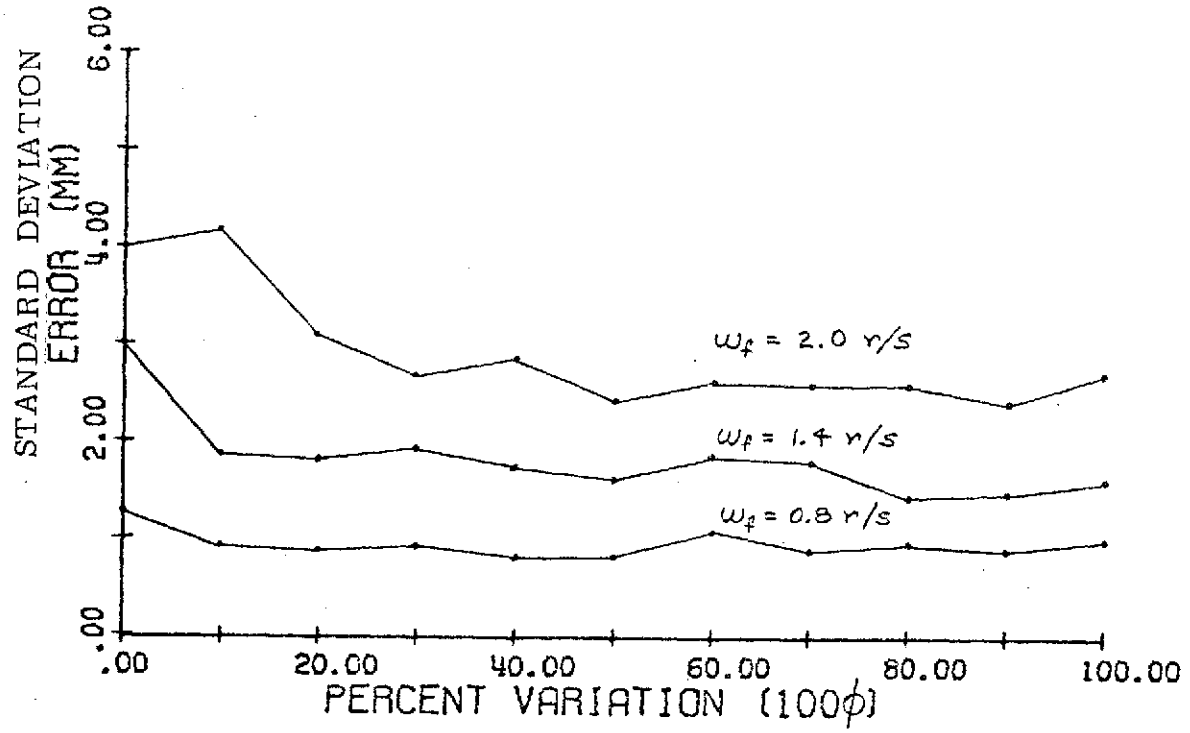

Figure 7.5 σ_ϵ Versus Percent Variation for 3 Input Filter Frequencies, Subject A

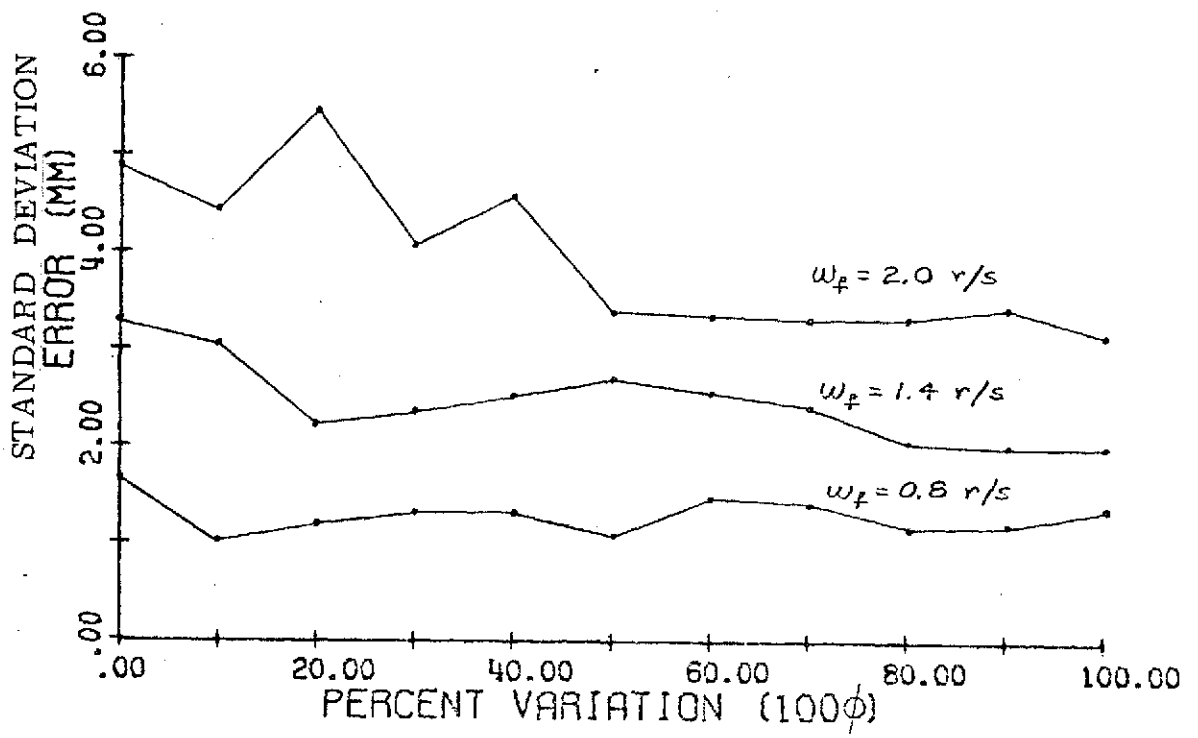

Figure 7.6 σ_ϵ Versus Percent Variation for 3 Input Filter Frequencies, Subject B

between Filter Frequency and Percent in the Analysis of Variance tables for each subject. Note that where the input filter frequency is 0.8 rad/sec, there seems to be little or no transition for either subject.

The actual manner in which the power level changes during the transition is not entirely clear from the data considered thus far. However, it appears that the trend, based upon 10 replicates, is that of a smooth reduction which begins at some point after the start of the transition. It was noted in informal conversations with the subjects, that they were not consciously able to detect the system changes until well into the variation, i.e., around the 30-40% point, and yet they are changing their characteristics almost immediately.

Bandwidth Parameter Results

The bandwidth parameter was evaluated at ten equally spaced intervals during the vehicle transition for each condition. The method of evaluating the bandwidth parameter was as shown in Chapter 6. Tables 7.4, 7.5 and 7.6 summarize 3-way analyses of variance that were performed on the bandwidth parameter (ω_c) data. A 3 x 3 x 10 Analysis of Variance was planned, using the three factors (1) Filter Frequency, 3 values; (2) Speed, 3 values; and (3) Percent, 10 values (10% intervals, 0 through 90% inclusive). Table 7.4 is for Subject A. Unfortunately, the data for condition F8T120, Subject B was not suitable for frequency analysis after the final editing and thus, instead of doing a 3 x 3 x 10 Analysis of Variance, it was necessary to do a

Source	Degrees of Freedom	Mean Square	F Value
Filter Frequency	2	4.031	6.01 ***
Speed	2	11.540	17.22 *
Percent	9	7.810	11.66 *
Filter Frequency - Speed	4	4.230	6.31 *
Filter Frequency - Percent	18	0.782	1.16
Speed - Percent	18	0.448	0.67
Filter Frequency - Speed - Percent	36	0.669	

*denotes significance @ $\underline{P} < .001$
***denotes significance @ $\underline{P} < .01$

Table 7.4 3-Way Analysis of Variance for Bandwidth Parameter, Subject A

Source	Degrees of Freedom	Mean Square	F Value
Filter Frequency	2	3.753	18.41 *
Speed	2	5.928	29.09 *
Percent	9	0.901	4.42 **
Filter Frequency - Speed	2	0.505	2.47
Filter Frequency - Percent	18	0.232	1.14
Speed - Percent	9	0.241	1.18
Filter Frequency - Speed - Percent	18	0.203	

*denotes significance @ $\underline{P} < .001$
**denotes significance @ $\underline{P} < .005$

Table 7.5 3 x 2 x 10 3-Way Analysis of Variance for Bandwidth Parameter, Subject B, High and Middle Speeds.

Source	Degrees of Freedom	Mean Square	F Value
Filter Frequency	1	0.336	0.14
Speed	2	3.386	14.88 *
Percent	9	1.516	6.66 *
Filter Frequency - Speed	2	0.358	1.57
Filter Frequency - Percent	9	0.258	1.13
Speed - Percent	18	0.249	1.09
Filter Frequency - Speed - Percent	18	0.227	

*denotes significance @ $\underline{P} < .001$

Table 7.6 2 x 3 x 10 3-Way Analysis of Variance for Bandwidth Parameter, Subject B, ω_f = 2.0, 1.4 rad/sec.

3 x 2 x 10 (Table 7.5) and a 2 x 3 x 10 (Table 7.6) so as to work around the missing cell.

The Analysis tables provide some insight into the relationships present in the data, but they are rather complex; thus the data is plotted out in Figures 7.7 though 7.12. Figures 7.7 and 7.8 show the data when the three different noise values are averaged together for Subjects A and B, respectively. Figures 7.9 and 7.10 are plots of the data when the three speed levels are averaged. Finally, Figures 7.11 and 7.12 show the data when the 10 values of percent variation are averaged for each condition.

The information contained in the Analysis of Variance tables for Subject B indicates, by the lack of any significant two factor interactions that the shapes of the curves for this subject are essentially the same. Figure 7.12 also indicates this fact. Subject A, on the other hand, shows a significant interaction between Filter Frequency and Speed in Table 7.4. Figure 7.11 also shows this phenomenon, where the curve for Filter Frequency = 1.4 radians per second is significantly different from the other two.

The Newman-Keuls test applied to the Speed Means for Subject A (Table 7.7) shows that all the Speed me ans are significantly different from each other. The same test applied to the Filter Frequency means indicates that the values for 2.0 and 1.4 radians per second are not significantly different. The 0.8 radians per second data are significantly different from the data for the 2.0 or 1.4 radian

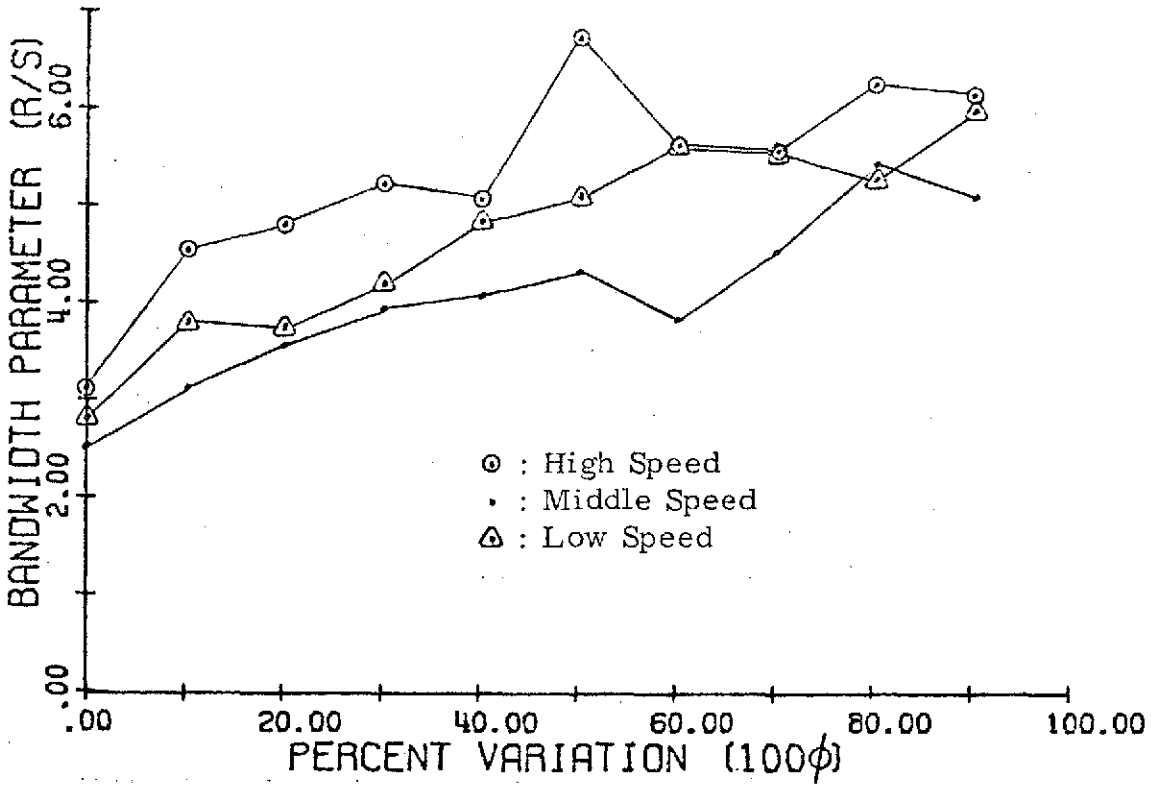

Figure 7.7 Bandwidth Parameter Averaged over Filter Frequency, Subject A

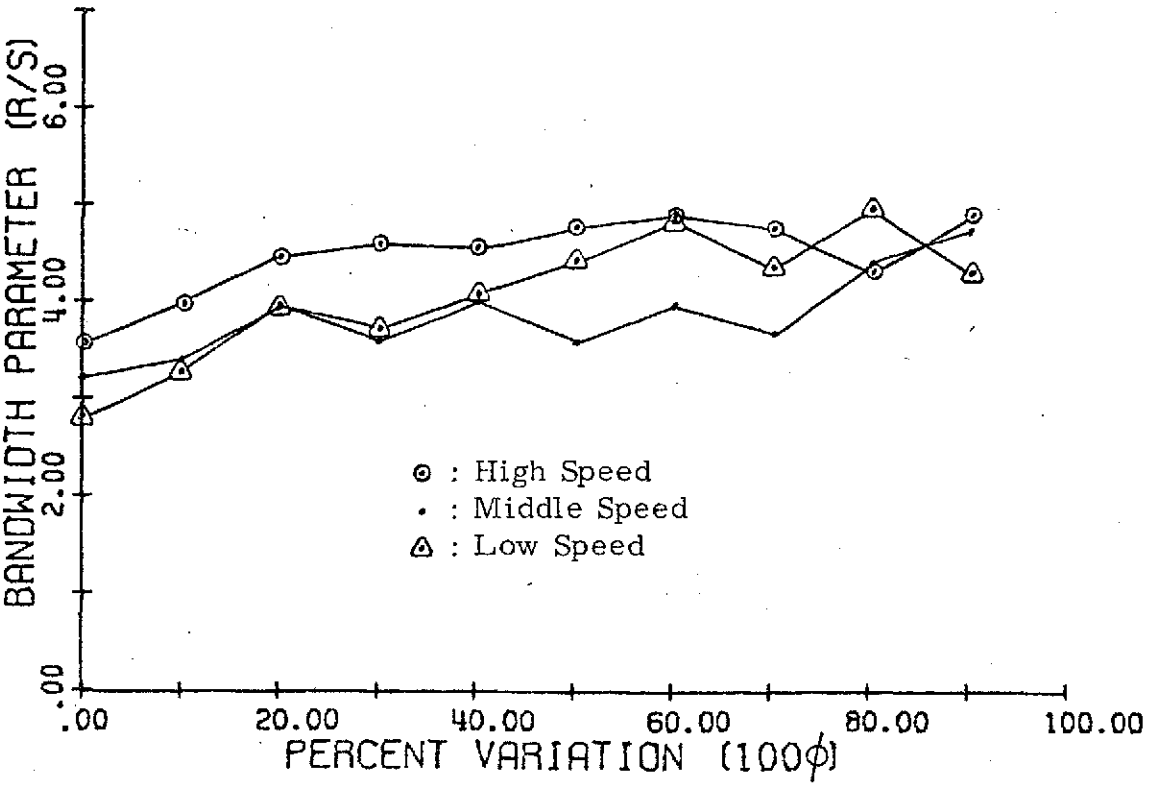

Figure 7.8 Bandwidth Parameter Averaged over Filter Frequency, Subject B

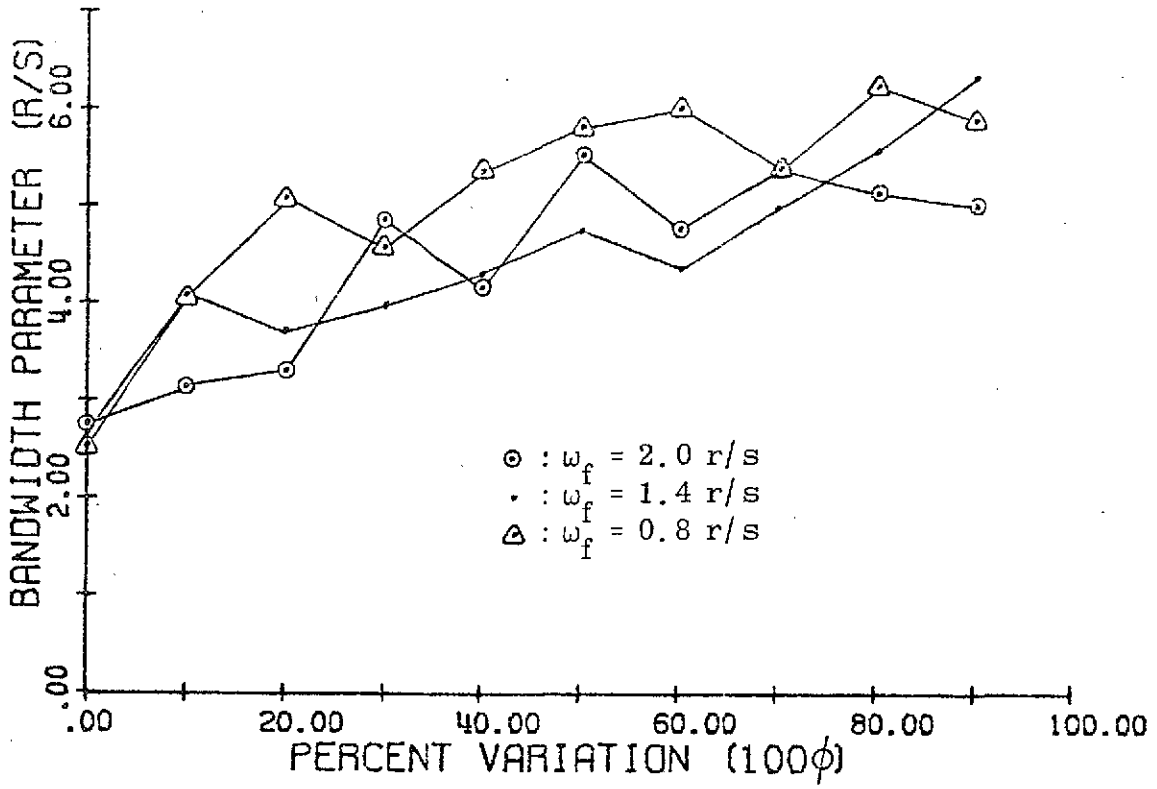

Figure 7.9 Bandwidth Parameter Averaged over Speed, Subject A

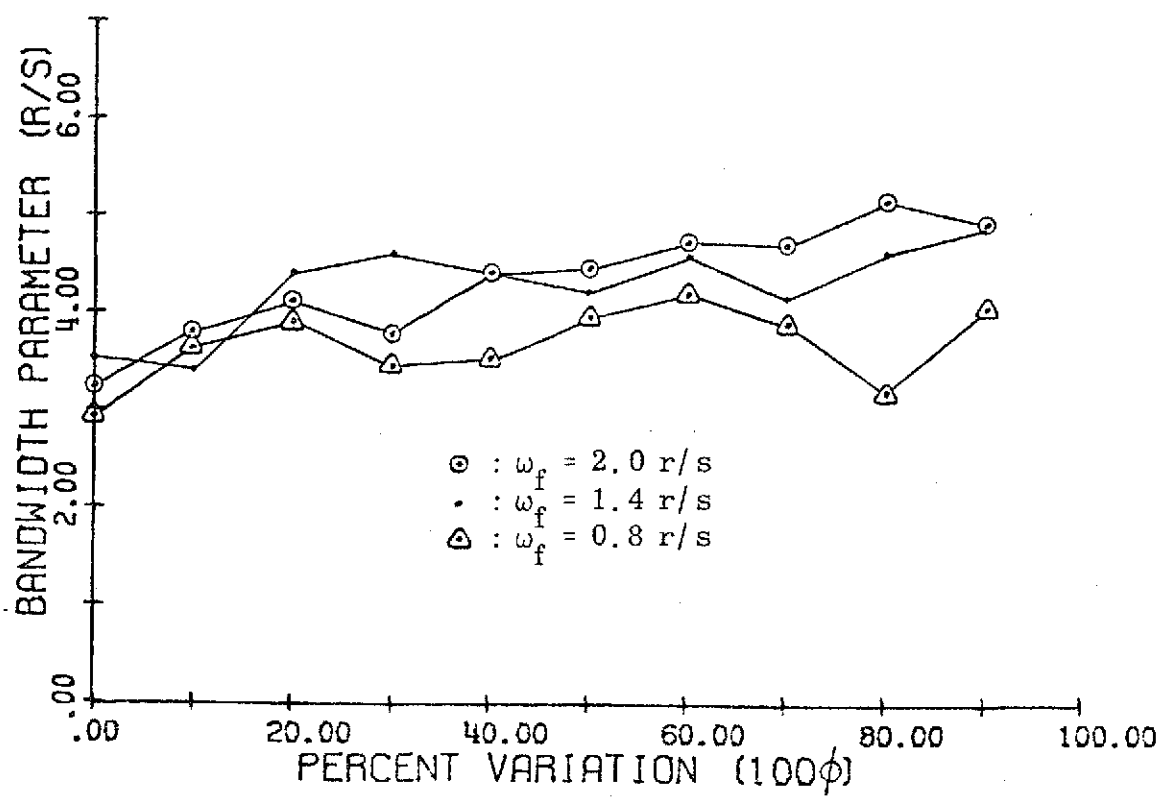

Figure 7.10 Bandwidth Parameter Averaged over Speed, Subject B

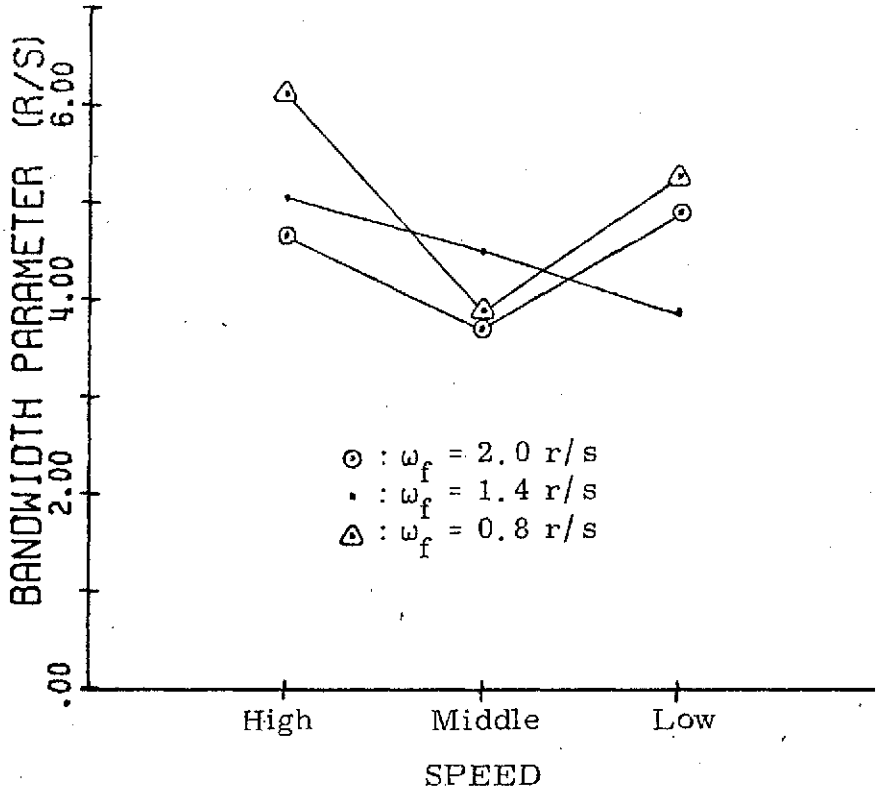

Figure 7.11 Bandwidth Parameter Averaged over Percent, Subject A

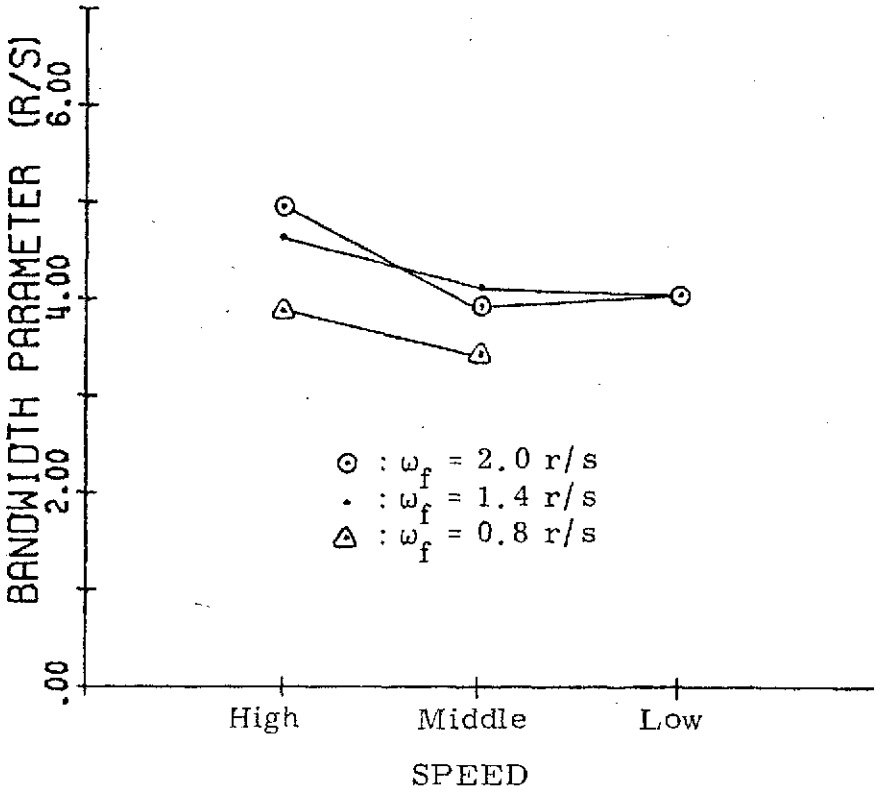

Figure 7.12 Bandwidth Parameter Averaged over Percent, Subject B

Analysis of Variance Data

Speed	Mean	Filter Frequency	Mean
High	5.27	0.8	5.04
Middle	4.03	1.4	4.47
Low	4.68	2.0	4.43

Speed Mean Test

	T_1 Middle	T_2 Low	T_3 High	r	$q_{.99}(r,36)\sqrt{MS_{error}/30}$
Middle	---	0.65***	1.24***	3	0.651
Low		---	0.59***	2	0.569

Filter Frequency Mean Test

	T_1 2.0	T_2 1.4	T_3 0.8	r	$q_{.99}(r,36)\sqrt{MS_{error}/30}$
2.0	---	0.1	0.66***	3	0.651
1.4		---	0.62***	2	0.569

***denotes significance @ $\underline{P} < .01$

Table 7.7 Newman-Keuls Test on Bandwidth Parameter Means, Subject A

per second condition. This latter phenomenon is also indicated in the Subject B data by the fact that without the 0.8 radian per second data, the Analysis of Variance show no significant effect due to the Filter Frequency filter. The factor does become significant when data from all three Filter Frequencies are present.

Stationary Point Analysis

As discussed in Chapter 3, Subject B was also asked to control a stationary plant with ϕ held constant at six different values. The input filter cutoff frequency was 1.4 radians per second for each run. Although a thorough analysis of this sort would require many replicates of each point, it was decided to make one run of four minutes in length for each value of ϕ. This would then serve to indicate whether or not the results from the stationary analysis were different enough from the time-varying data to warrant further investigation. As will be shown in subsequent paragraphs, the results of the stationary analysis were indeed similar enough to the time-varying data to preclude further investigation.

The time-averaged standard deviation of the error signal $\epsilon(t)$ for each value of ϕ, is shown in Figure 7.13. This quantitity was calculated in the usual "time series" manner, assuming stationarity of the signal. This same length of data was then broken into ten subsets and those subsets used as replicates to perform the ensemble standard deviation calculations. These results are also shown in Figure 7.13. The figure shows the two sets of static results superimposed upon the time-varying σ plot for Subject B, F14T75, which

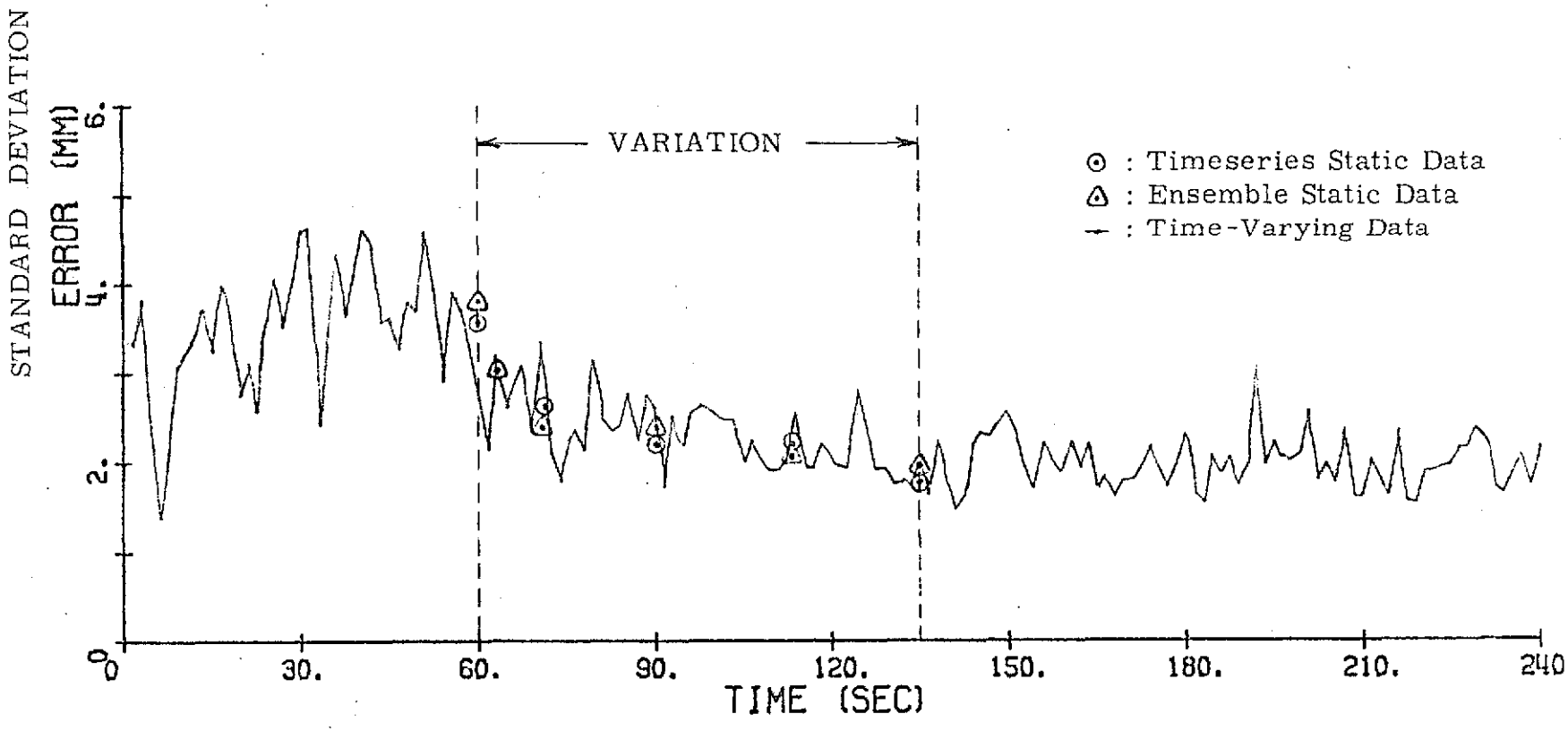

Figure 7.13 Comparison of Static and Time-Varying σ_ϵ Data for F14T75, Subject B

was obtained by ensemble averaging 10 replicates. Figure 7.13 shows that the time-varying standard deviation, and thus the power parameter, seems to be in good agreement with those values predicted by the stationary point analysis.

The power spectral density of the error signal for each value of ϕ in the set of static runs was determined using "MIDAS"(7). The bandwidth (-3db frequency) was computed for each case. The bandwidth was also computed using the bandwidth parameter approach, by breaking each run into 10 small replicates. The results of both methods are presented in Figure 7.14 along with the values of $\hat{\omega}_c$ obtained from the time varying replicates of F14T75, Subject B. When the points from the static set are compared to the large sets shown in Figures 7.7 through 7.12, it becomes apparent that the time-varying data and the data from the static analysis are in general agreement. This figure also gives further evidence of the validity of the bandwidth parameter $\hat{\omega}_c$.

Replicate Increase

The last set of verification experiments consisted of taking 40 replicates (instead of 10) of condition F14T75, Subject B. For these runs, the duration of the initial and final stationary portions of the runs were shortened to 40 and 45 seconds, respectively. The standard deviations of the stick deflection $x_p(t)$, the attack angle $\alpha(t)$, and the error signal $\epsilon(t)$ are shown in Figure 7.15. The plot can be compared to Figure 5.1 to see the reduced variance which results from the increase in replicates.

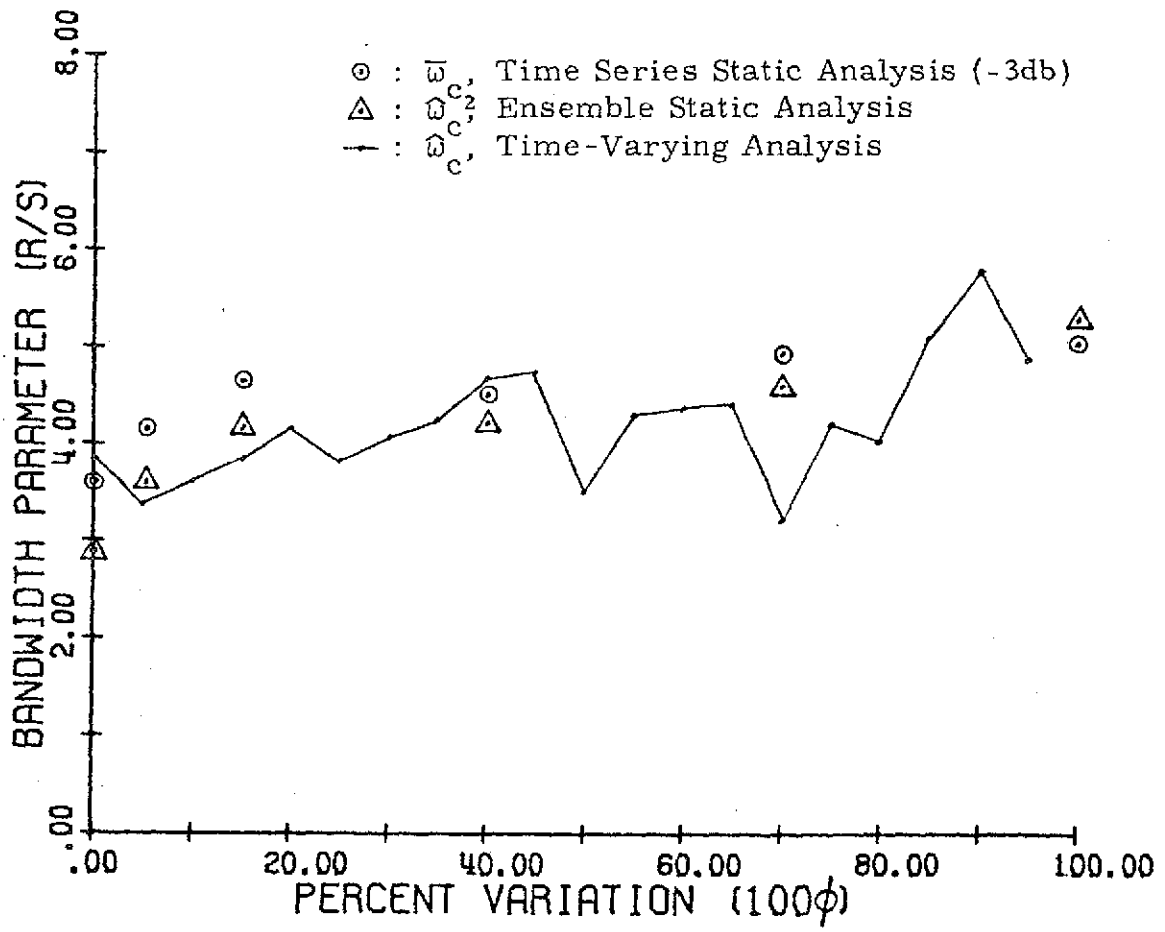

Figure 7.14 Comparison of Static and Time-Varying $\hat{\omega}_c$ Data for F14T75, Subject B

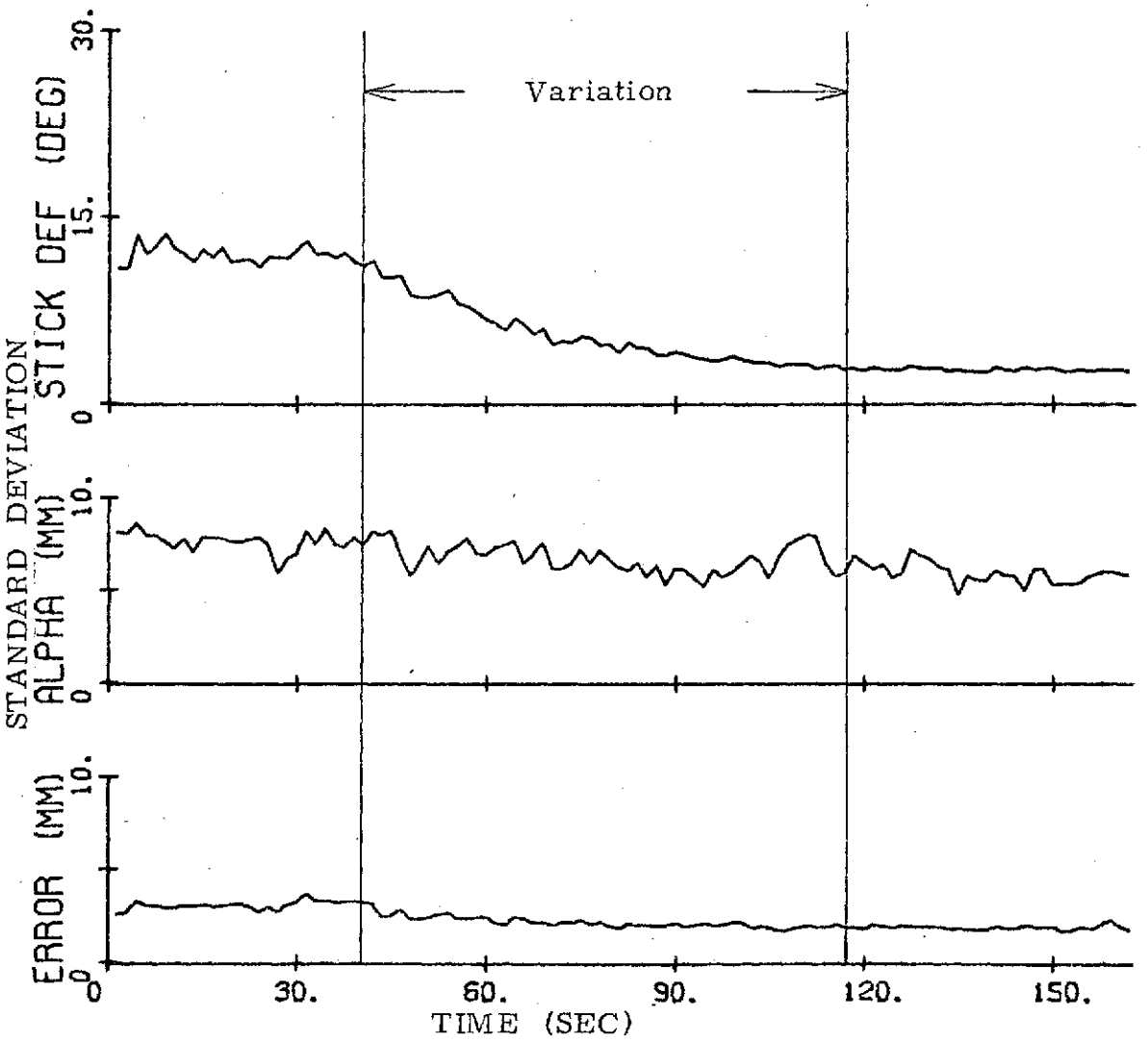

Figure 7.15 Standard Deviation of Recorded Data, F14T75, Subject B, 40 Replicates

Numerically, the standard deviation of the error signal, calculated over the initial time invariant portion of the ensemble, has a mean of 3.099 mm and sample standard deviation of 0.24 mm, resulting in 95% confidence interval of 3.003 to 3.195 mm, which is ± 3% of the mean value as compared with ± 6% of the mean value for the 10 replicate case. This is expected since the number of replicates has increased by a factor of four over the 10 replicate case. The corresponding accuracy of the power parameter is a 95% conficence interval of ± 6% of the mean value.

The value of bandwidth parameter $\hat{\omega}_c$ during the transition is shown on Figure 7.16. The data points for the 10 replicate ensemble of F14T75, Subject B are also shown to demonstrate the decrease in scatter due to increased replicates. The trends noted for 10 replicates seem to be supported by the increase in replicates.

It is necessary to note that there are two significant factors which affect the usefulness of this 40 replicate set of data. The first is that the session did not take place at the same relative time as the other sessions and because of the number of trials, the trials were not interspersed with trials for other variation speeds. The other factor to be noted is that the subject was no longer naive, that is to say, he had been exposed to much more information on the purpose of the experiment and on the analysis techniques than had been the case for the original set of conditions. Thus it seems reasonable to use the 40 replicate data as an indication of the effect of replicate number on the accuracy of numerical calculations and to discount somewhat

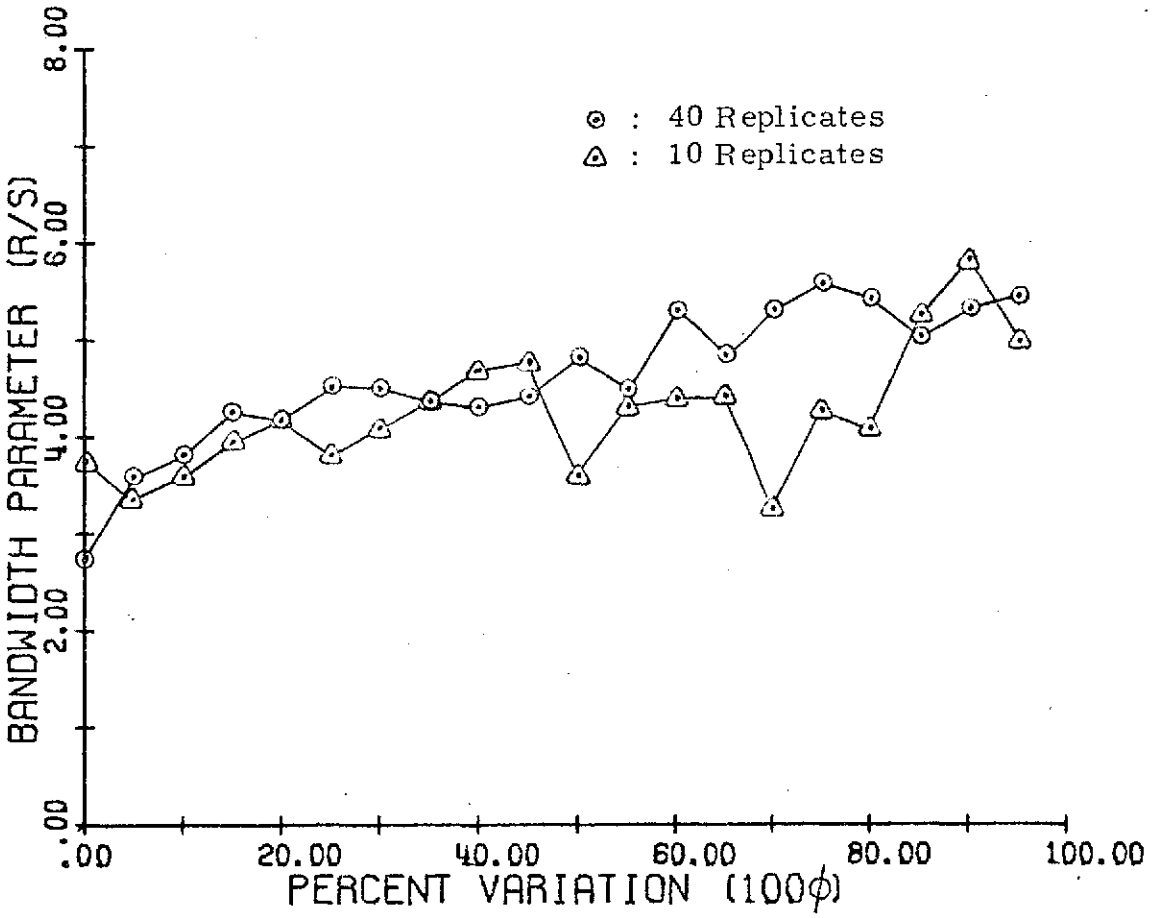

Figure 7.16 Comparison of Bandwidth Parameter for 40 Replicates and 10 Replicates, F14T75, Subject B

the significance of data trends that result from this particular set of 40 replicates.

Crossover Model Comparison

As was stated in the introduction, the regulation task is very closely related to the compensatory tracking task. In fact, the usual compensatory task block diagram is topologically equivalent to a portion of the block diagram for the regulator task, as shown in Figure 7.17. This diagram results from the simple block diagram manipulation being performed on the diagram of Figure 3.3. Since the regulator task includes the compensatory task as shown in Figure 7.17, it is reasonable to apply the Crossover Model (11) to the regulator task to see how the results of using an existing analytical model agree with the experimental results.

Model Specifics - The Crossover Model is a model which takes advantage of the pilot's ability to vary his own characteristics to complement those of the vehicle he is controlling. It is a combination of pilot and vehicle transfer functions which is relatively invariant for a large class of vehicles and a large class of inputs. Certain adjustment rules and refinements exist (11, 12) for the fundamental form, and the one chosen is shown below

$$Y_p Y_c = \frac{\omega_c e^{-j\omega \tau_e}}{j\omega} \qquad (7.1)$$

In accordance with McRuer, et al (11), the parameters τ_e and ω_c are adjusted as follows:

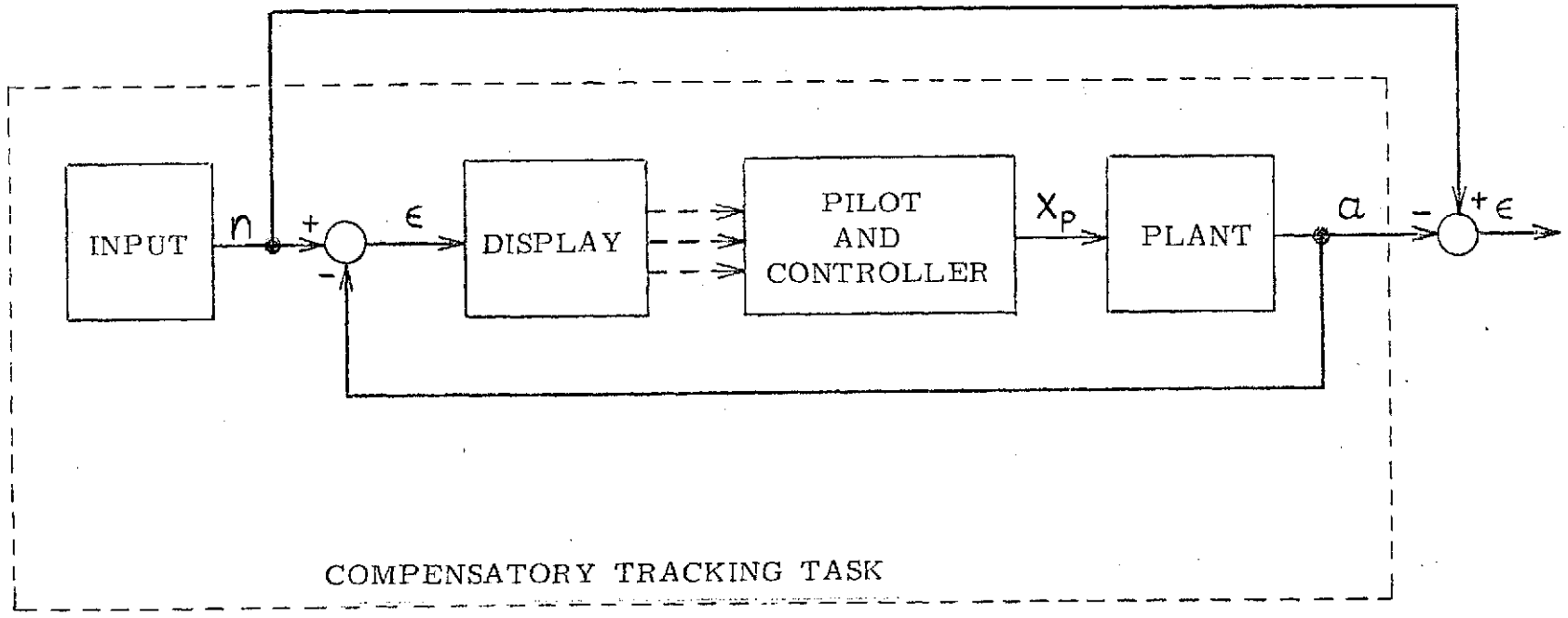

Figure 7.17 Block Diagram of Compensatory Tracking Task within Pilot-Vehicle-Regulator

$$\omega_c = \frac{\pi}{2\tau_o} + 0.18\,\omega_i \qquad (7.2)$$

$$\tau_e = \tau_o - 0.08\,\omega_i \qquad (7.3)$$

where τ_o is taken from Table 7.8 as presented in Reference 11, and ω_i is the input bandwidth.

$Y_c(j\omega)$	τ_o (sec)
k_c	0.33
$k_c/j\omega$	0.36
$k_c/(j\omega - \frac{1}{\tau})$	0.36
$k_c/(j\omega)^2$	0.51

Table 7.8 Crossover Model Parameters

Experiments (11) have shown that the system crossover frequency will generally lie between the values of 3 and 6 radians per second for most controlled elements. Within this frequency range, the 2nd order system representing the vehicle during the final phase of the experiment is equivalent to a pure double integrator with the proper gain constant. Thus, as far as the Crossover Model is concerned, the time-varying task is merely that of matching the effects of a changing gain constant on a pure double integrator. Unfortunately, the methodology associated with the basic form of the Crossover Model says that if this were the only criterion, there would be no change in the Crossover Model, and this would preclude getting trends of changing bandwidth and signal power which the experimental results

clearly show. It is, however, instructive to utilize the basic Crossover Model in this task to see that the experimental results do show some qualitative agreement with the analytical methods available.

For an input bandwidth of 1.4 rad/sec, with a pure double integrator plant, the Crossover Model would be given by

$$Y_p\, Y_c = \frac{3.25\, e^{-j0.43\omega}}{j\omega} \tag{7.4}$$

An analysis of the closed loop transfer function between input disturbance and output angle of attack yields the Bode magnitude plot of the square of the closed loop system gain shown in Figure 7.18. Also shown on this figure are the results of a spectral analysis on the input signal for one of the replicates of condition F14T0, Subject B. By subtracting the value of the input power at a particular frequency from the value of the output power at a particular frequency, one can obtain the experimental version of the Bode plot shown in Figure 7.18. This is done using the angle-of-attack signal from the same replicate as the input, and the result is the plot of Figure 7.19. This figure shows that the experimental results do indicate an increase in high frequency content as the signal passes thru the compensatory tracking task system.

A simple manipulation of the block diagram for the regulation task results in a system whose input is the disturbance, whose output is the error, and whose feedback path contains the Crossover Model.

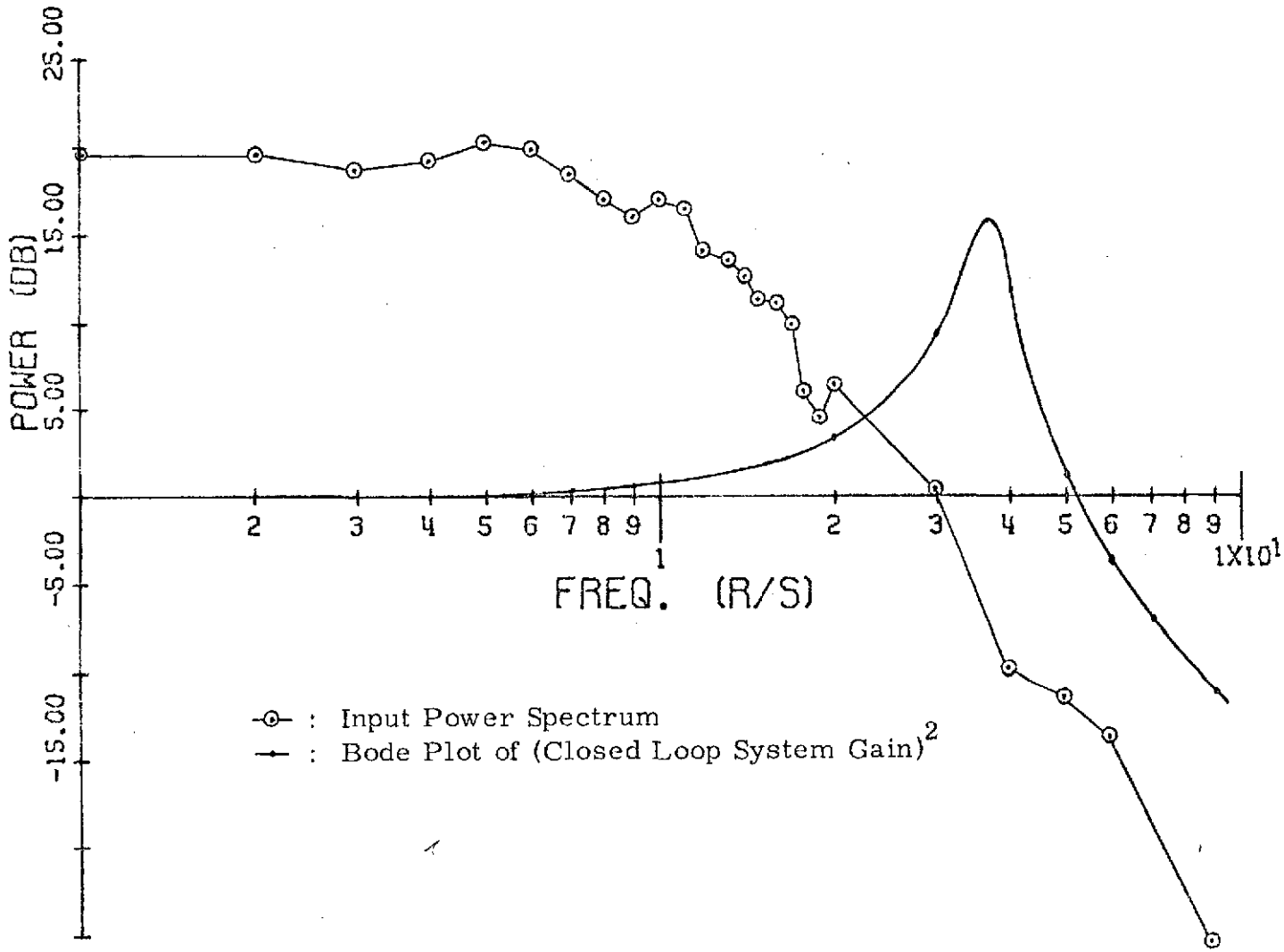

Figure 7.18 Crossover Model Bode Plot and Input Power Spectral Density

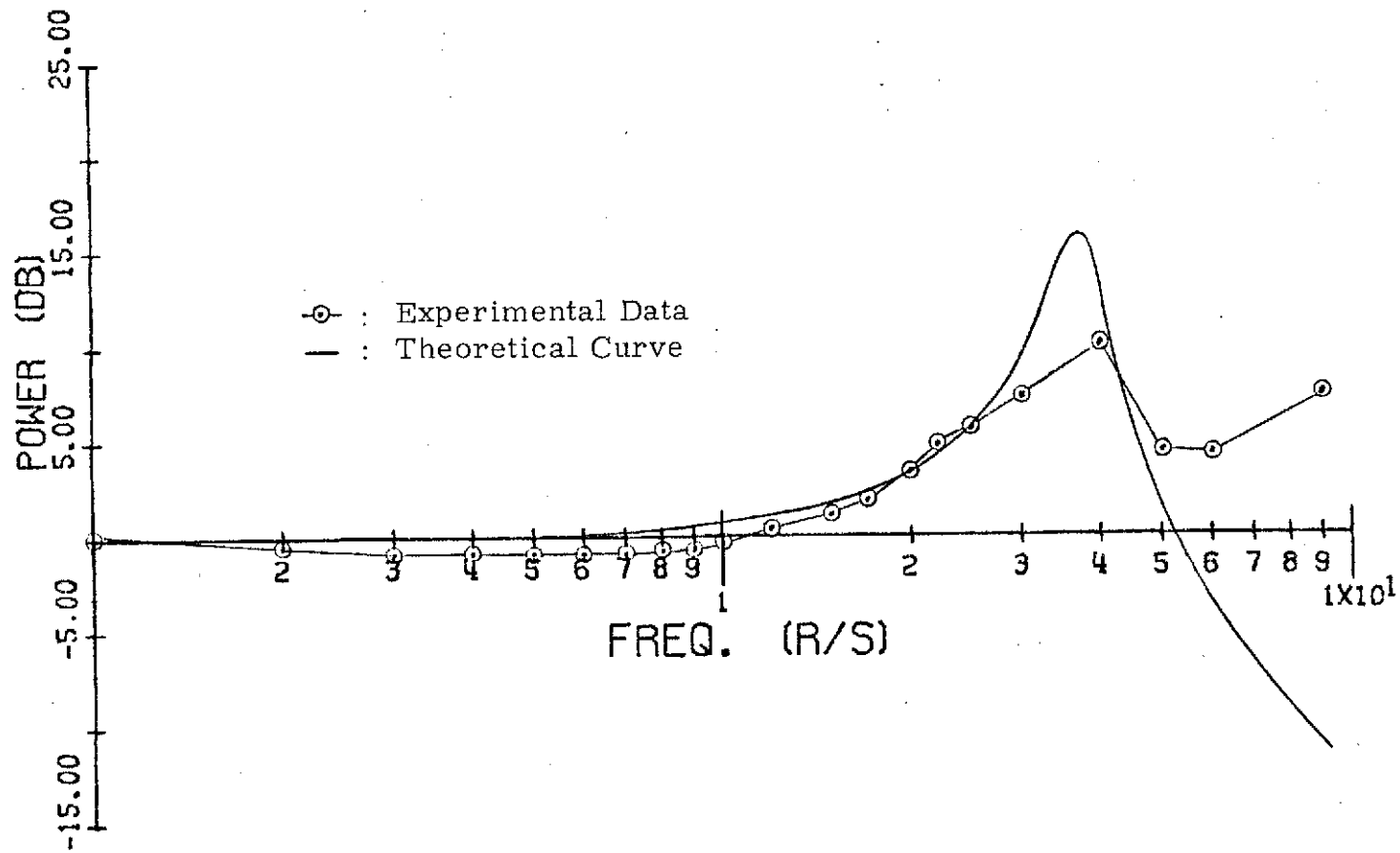

Figure 7.19 Comparison of Bode Plots of the Square of the Closed Loop System Gain from Theoretical Methods and Experimental Data

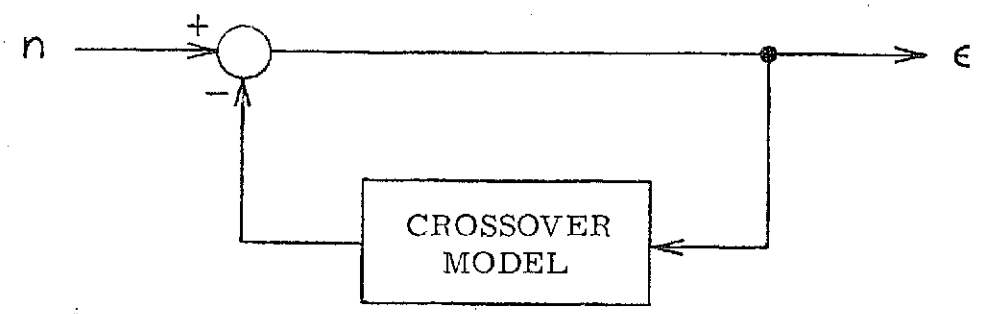

Figure 7.20 Crossover Model in the Regulator Task

The forward path is unity. The Bode magnitude plot on Figure 7.21 is the result of the closed loop analysis; that is, the plot of the square of the Pilot-Vehicle-Regulator System magnitude based on a Crossover Model. Superimposed on this figure is plot of the same function determined experimentally.

Crossover Summary - One deficiency of the Crossover Model as presented thus far in this report is its lack of ability to account for low frequency lag which is present in experimental data. However, a set of more sophisticated versions called "Extended Crossover Models" can be used to eliminate this inaccuracy, and thus the apparent low frequency inaccuracies shown in previous figures are explainable and could be accounted for it necessary. The more important region for the purposes of this report is, however, the region with $\omega \geq 1$ radian per second where crossover occurs and where the bandwidth parameter values lie.

The compensatory task data agree reasonably well with the Crossover Model prediction as shown by Figures 7.18 and 7.19. The model predicts somewhat higher spectral levels in the region from

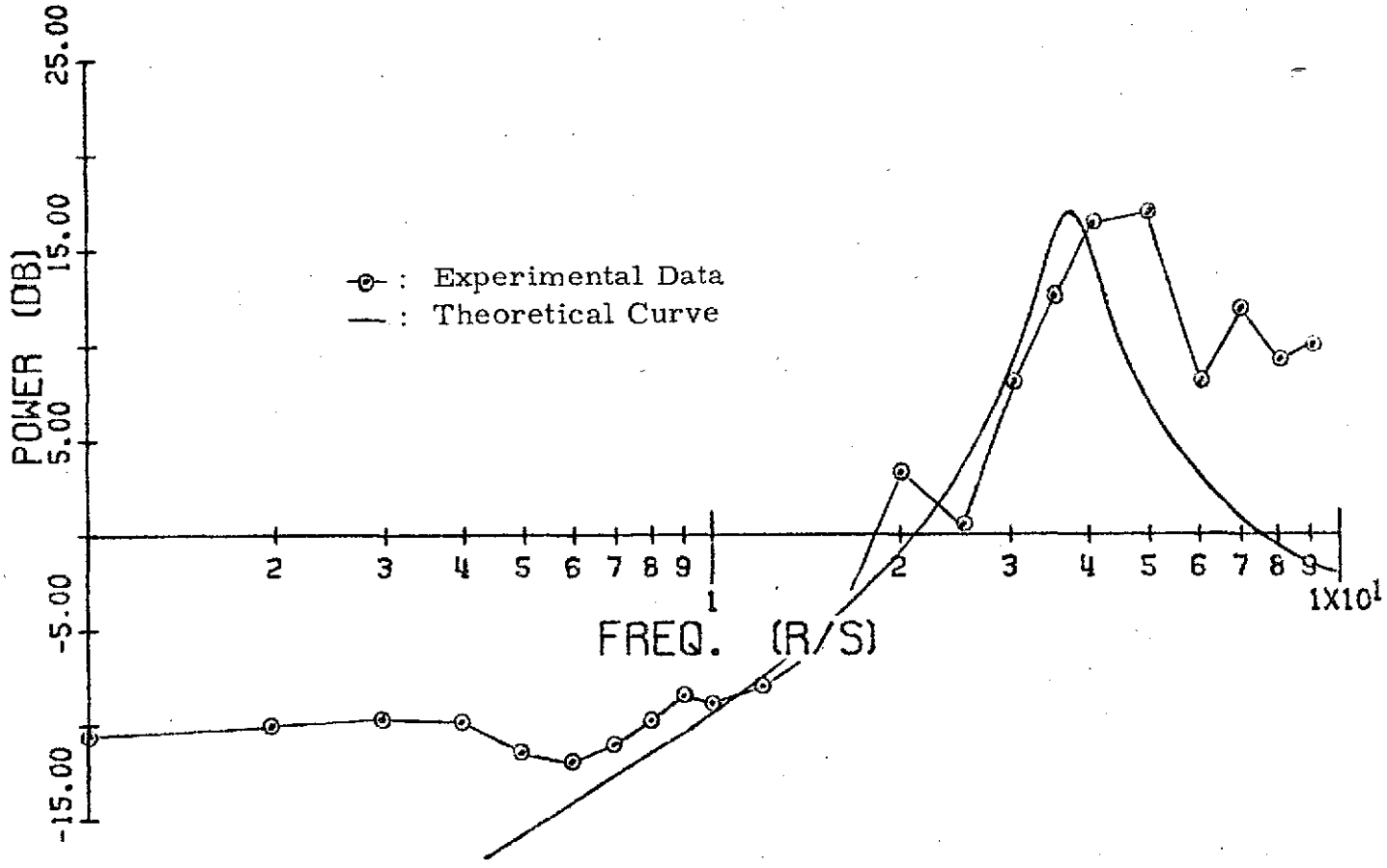

Figure 7.21 Comparison of Bode Plots of the Square of the Regulator System Gain from Theoretical Methods and Experimental Data

2 to 5 radians per second, than is visible in the output spectrum, but certainly there is qualitative agreement between the model predictions and the observed data.

In the regulator task, the agreement between the observed data and the Crossover Model predictions is even better. The Crossover Model predicts a significant increase in bandwidth of the output error signal over the input noise signal and this is indeed the case. Ignoring the low frequency inaccuracies it appears that for the data presented, the Crossover Model predictions agree both qualitatively and quantitatively with the experimental results.

Unfortunately, the agreement shown in the regulator task occurs when $\phi = 1.0$ in the vehicle transfer function and the Crossover Model really has no mechanism to change its form for the other observed values of ϕ. This would be desirable since for $\phi = 0.0$ in the same run, the half-power frequency of $\epsilon(t)$ is at about 3.5 radians per second as opposed to a half-power frequency at around 5 radians per second for $\phi = 1.0$ in the data shown on Figure 7.21.

The main results of this analysis are that (1) the Crossover Model qualitatively predicts the observed phenomena in the Pilot-Vehicle-Regulator data, when low frequency errors are ignored or eliminated by estension of the model and (2) the Crossover Model doesn't have enough fidelity to be directly usable in verifying bandwidth and power parameter changes that occur in the error signal as ϕ changes in value.

8. CONCLUSIONS AND RECOMMENDATIONS

There are four main areas into which conclusions and recommendations can be separated. They are General Methodology, Bandwidth Parameter, Pilot-Vehicle-Regulator and Models. Each will be treated separately in the following sections.

General Methodology

A significant result of this research effort is that the Ensemble Averaging approach to analysis and description of time-varying systems does yield meaningful information. Further, the level of difficulty of performing the experiments and collecting the data is not particularly high. The use of the concept of quasi-stationarity to decrease statistical variance by time averaging the ensemble-averaged quantities within regions of quasi-stationarity is more effective as the sampling rate gets higher, since more samples can be averaged. However, the correlation between two samples gets higher as the sampling rate increases so that as the sampling rate is increased, each increase is less effective and results in a smaller increase in precision than the previous one. One must also consider the effect of higher sampling rates upon the magnitude of the resulting data set to be processed, since this can be quite costly. Clearly, there is a tradeoff to be made between accuracy and cost which will result in specification of ensemble size and sampling frequency. Most time-varying situations could be analyzed by the proper choice of quasi-stationary region size and sampling frequency, at least in

terms of signal means and standard deviations which do reflect power content. The autocorrelation or autocovariance functions and the cross correlation or cross covariance functions can be generated and theoretically these provide descriptions of system characteristics. Just what practical insight can be obtained from these ensemble average descriptors depends somewhat upon a priori information about the system, i.e. how fast it can vary, what it is used for etc., and also upon what the description is to be used for.

Bandwidth Parameter

The bandwidth parameter $\hat{\omega}_c$ as developed and described in Chapter 6 is important in its own right as well as being critical to the goal of this research effort. Although it is relatively simple to use, its theoretical structure and justification are fairly complex.

The ability of this parameter to predict bandwidths of signals based upon very short records of data is critical, and although in Chapter 6 the performance of the parameter is addressed and documented, the analysis is by no means complete. Based upon the empirical methods used for the tests in this document, the accuracy is quite good, but obviously this question deserves more attention in the future.

The development of $\hat{\omega}_c$ in Chapter 6 is based upon a rectangular low-pass spectrum and the resulting position of the first relative minimum in the corresponding autocorrelation function. The choice of the rectangular low-pass spectrum yielded good results but obviously, other

spectral shapes whose autocorrelation function exhibits a relative minimum could be used. Indeed, power spectra that fall off continuously might be more representative of the spectral shapes usually found in manual control tasks. The change in the estimation results that would result from using other spectral shapes is not clear. Thus, a reasonable extension of the development of this parameter would appear to be the analytical study of various spectral shapes and the resulting first relative minima of the autocorrelation functions. When approached analytically, new insight into the bandwidth parameter could be gained.

Another area of interest is the actual determination of the first relative minimum. Obviously when working with digital data on computers capable of generating accurate and uniform plots, the method utilized in this study is relatively simple and easy to mechanize. On the other hand, if the capability were available, a better way to estimate the bandwidth of the unknown spectrum or pseudo-spectrum would be to directly analyze the first and second derivative of the autocovariance function. Here too, further effort could result in higher estimating precision.

The bandwidth parameter approach to generating the bandwidth of a signal has possible application to situations other than non-stationary analysis. The relative simplicity of the necessary calculations can result in significant savings in data reduction costs. For example, consider the use made in Chapter 6 where a recorded stationary signal was broken into ten subsections which were then used as

replicates for the ensemble calculations. If one is only interested in obtaining signal bandwidth, the bandwidth parameter technique may be quite useful since the length of the replicates doesn't influence the accuracy of the parameter; and the higher the bandwidth is, the shorter the replicates can be. The only requirement is that a first relative minimum is, in fact, observed in the autocovariance function.

Pilot-Vehicle-Regulator

The Pilot-Vehicle-Regulator analysis has been performed with the goal of describing the output signal $\epsilon(t)$ as the system varies with time. The two descriptors used are the power parameter $P_\epsilon(t)$ and the bandwidth parameter $\hat{\omega}_c(t)$, which together give insight into the character of the pseudo power spectral density of $\epsilon(t)$. One conclusion that can immediately be drawn from the results in Chapter 7 is that for the tasks encompassed by this experiment, the pilot's performance in controlling the time-varying system is essentially equivalent to his performance in controlling time-invariant systems which correspond to various points in the transition.

Power Parameter - In Chapter 7, it was shown that for transition times of 30 seconds or longer, $\sigma_\epsilon(t)$ was essentially independent of the speed of the vehicle transition. It was a function of both the bandwidth of the input disturbance (ω_f) and the value of ϕ by which the vehicle dynamics are characterized. The general relation is shown as

$$\sigma_\epsilon(t) = \sigma_\epsilon(\phi(t),\ \omega_f). \tag{8.1}$$

This is further supported by the agreement between the data from dynamic condition F14T75 and the static data shown in Figure 7.13. The significant interaction term indicates that the shape of the curve is different for different combinations of variable values. The plots in Figures 7.5 and 7.6 show that the interaction is manifested in the fact that the transition from the initial to the final level is slower for larger values of input filter frequency.

One way of mathematically formulating the observed relationships is shown below:

$$\sigma_\epsilon(t) = \omega_f \left[K_1 + K_2 \left\{1 - EXP\left[- K_3 \omega_f \phi(t)\right] \right\} \right] \qquad (8.2)$$

where K_1 determines the initial level, K_2 determines the final level, and K_3 influences the speed of the transition between the two levels. For this experimental data, the K's vary between subjects. The author does not intend to propose that equation 8.2 be used as anything more than a general way of interpreting the observed data, since the nature of the transitions in the data are still not clearly defined.

The average power $P_\epsilon(t)$ in the quasi-stationary error signal and hence the area under the curve pseudo power spectral density is

$$P_\epsilon(t) = 2\pi \sigma_y^2(t) \qquad (8.3)$$

Using Equation 8.4, results in

$$P_\epsilon(t) = \omega_f^2 \left[K_1 + K_2 \left\{1 - EXP\left[-K_3 \omega_f \phi(t)\right]\right\}\right] \qquad (8.4)$$

An obvious question which remains unanswered is: How does the artificial quantity ϕ affect the average power in the error signal? Clearly the answer must lie in the relationships between ϕ and the parameters of the controlled vehicle transfer function, and this area of research deserves further analysis.

Bandwidth Parameter - Chapter 7 presented the data on the bandwidth parameter along with the results of several statistical tests. It was felt that the tests did not in themselves produce clear insight into the relationships present, and thus their interpretation was largely left to this section where one can be more speculative.

The Analyses of Variance for Subject B showed that the shapes of all the curves were essentially the same. The interaction between Filter Frequency and Speed for Subject A appeared to be the result of the data for Filter Frequency = 1.4 radians per second where the 75 second variation seems to be causing the different in the curve shown on Figure 7.11. It is felt that this could very well be caused by subject non-stationarity since this data was produced during a session from which no other data points appear in the graphs. When the subject non-stationarity is considered, it becomes more justifiable to assume that the $\hat{\omega}_c$ curve shapes are essentially the same within subjects.

The main factors of Filter Frequency, Speed and Percent are all shown by the Analyses to be significant for the data. However, as is shown by the Newman-Keuls test in Table 7.7, the middle speed or

75 second transition data seems to be showing the effects of subject non-stationarity by having a mean well below the other two. In the same table, the Filter Frequency means show that only the mean for the low value of frequency ($\omega_f = 0.8$) is significantly different and this value has been mentioned previously as being the cause of frustration in the subjects. It is the opinion of the author that the significance of the Speed and Filter Frequency factors in the Analyses of Variance on $\hat{\omega}_c$ should not be weighted too heavily. There are clear possibilities of confounding effects present in the data. A further observation is that the significance of these two factors may well be there in a statistical sense, but whether the variance due to these factors is of practical importance to the results of the experiment has not been answered. The lack of interaction, and the significance of the Percent factor are certainly of prime importance.

A first approximation to a functional relationship for $\hat{\omega}_c$ is that the curve shapes are the same, and that only the Percent factor is significant. Thus,

$$\hat{\omega}_c(t) = \hat{\omega}_c\,(\phi(t)). \tag{8.5}$$

A functional relationship capable of exhibiting the same general data trends is

$$\hat{\omega}_c(t) = K_4 - K_5 \cdot \mathrm{EXP}\ [-K_6\,\phi(t)] \tag{8.6}$$

where $K_4 - K_5$ determines the initial value of $\hat{\omega}_c$, K_6 determines the shape of the curve, and K_4, K_5 and K_6 combine to determine the value of $\hat{\omega}_c$ for $\phi = 1.0$.

Useful future efforts in the description of the Pilot-Vehicle-Regulator or any time-varying pilot tracking task would be to increase the speed of variation until it could be determined that (1) the pilot was changing his mode as he does when the dynamics switch instantaneously or (2) time-varying analysis results are significantly different from those obtained from point by point stationary methods.

Models

A Descriptive Model. - The results of the analysis on the Pilot-Vehicle-Regulator output signal, as given in Chapter 7 and amplified in the previous section, constitute a rudimentary descriptive model for the system, in the sense that given the input and some information about how the aircraft within the system is changing, it is possible to describe the output of the system, $\epsilon(t)$, in terms of its standard deviation $\sigma(t)$ and its pseudo bandwidth $\hat{\omega}_c(t)$.

This descriptive model is defined only for that class of inputs whose bandwidths are between 0.4 and 1.4 rad/sec. The average input power was constant at $P_n = 245.4\ mm^2$; however, it was shown in Reference 8 and in other efforts that the pilot in a compensatory task and also the Pilot-Vehicle-Regulator are relatively insensitive to input gain variation within reasonable limits. Since the gain directly affects the input standard deviation and hence the average power P_n, it is reasonable to expect that the Pilot-Vehicle-Regulator descriptive model will be valid for different average power levels so long as they are not so high as to cause control limiting, or so low as to be

comparable to those of the pilot's remnant. Also, this descriptive model is only well defined for vehicle and transition speeds such that the resulting changing configurations can be essentially obtained from

$$\frac{K(0.0178\ \phi\ s + 1.15\ \phi + 0.25)}{s^2 + 0.805\ \phi\ s + 1.35\ \phi} \qquad (8.8)$$

with $\phi \in [0, 1]$ and $\frac{d\phi}{dt} \leq 0.033$ units/sec.

Crossover Model. - In Chapter 7, it was shown that when the Crossover Model and its parameter methodology was assumed, it did not contain the fidelity to match the observed changes in the Pilot-Vehicle-Regulator output as the vehicle varied. There is however another way to utilize the Crossover Model.

If the general form of the Crossover Model is assumed, i.e.

$$Y_p Y_c \approx \frac{\omega_c\ e^{-j\omega\tau_e}}{j\omega} \qquad (8.9)$$

Then, for a given input spectrum it should be possible to determine ω_c and τ_c so as to match the observed values of $\hat{\omega}_c$ and P_ϵ. This information would be useful in determining how the pilot is changing his characteristics to account for changes in the vehicle, under the assumption that the Pilot-Vehicle-Regulator output due to the pilot's remnant is not significant.

APPENDIX A

SIMULATION DETAILS

The experiment utilized the facilities of The University of Michigan Simulation Center. This appendix discusses the details of the simulation that was developed. Figure A. 1 shows the flow of control and data signals within the simulation. The single line paths represent the control of the given devices and the double line paths represent the flow of data between the units. Within the hybrid computer are six blocks representing the six different functions performed by that device. The experiment room contained two hardware units as well as the subject. There were four other devices utilized, and they are shown in their respective functional positions. The following sections and subsections describe each device and its function.

Digital Noise Generator

A 22-bit Pseudo-Random Binary Noise Generator was fabricated in order to produce the low-frequency noise required for this experiment. The generator developed has a variable clock frequency from 0 to 23 hz and thus can be used to generate analog signals of zero-mean, approximately-Gaussian, bandwith-limited white noise with bandwidth up to 7.2 radians per second. To do this, the logic output of the noise generator is passed through an analog filter with cutoff frequency = clock frequency/20. The length of the shift register can be set to 5, 6, 7, 9, 10, 11, 15, 17, 18, 20, 21, or 22 bits, thus allowing the experimenter to vary the repetition period of the noise signal.

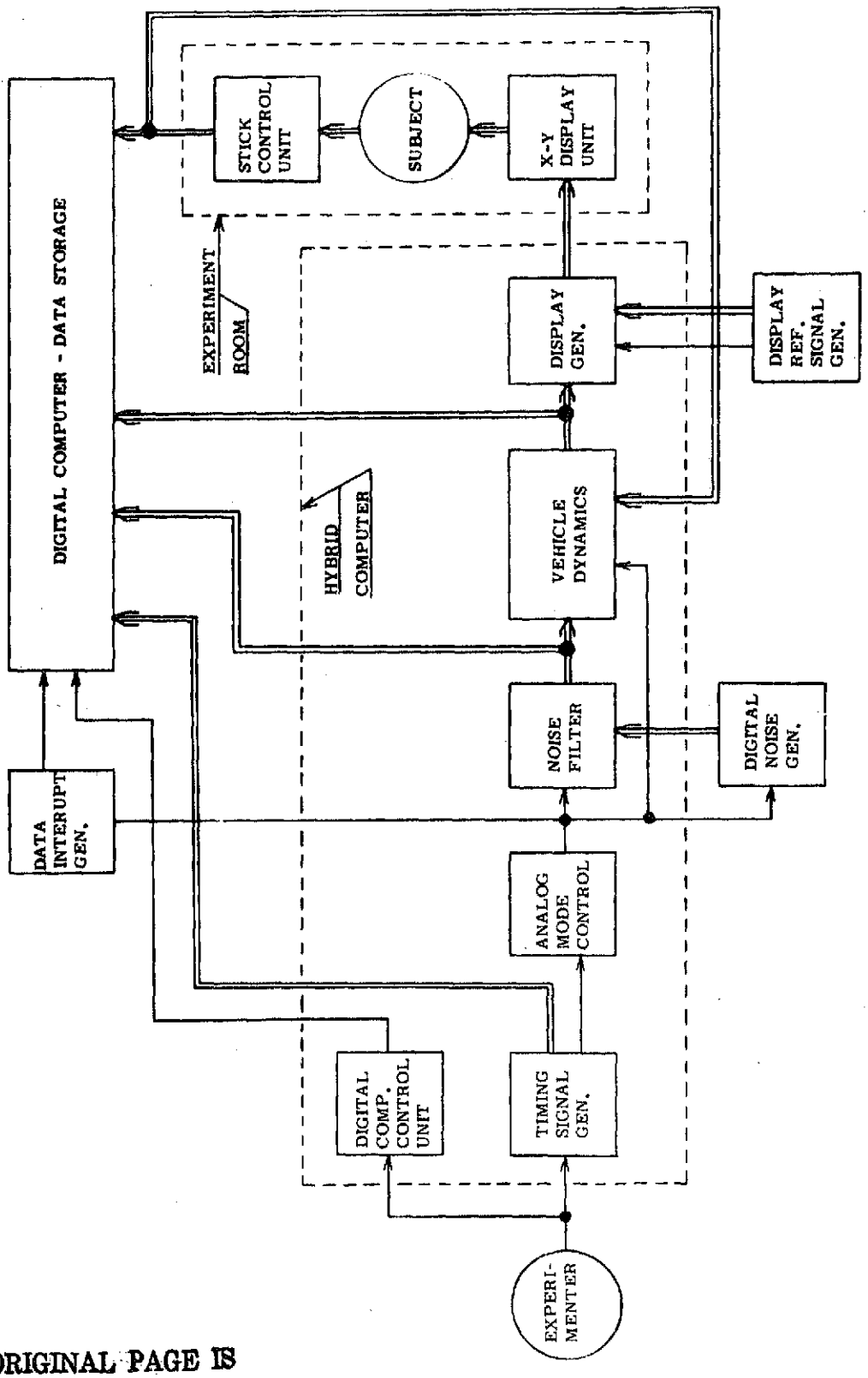

Figure A.1 Simulation Diagram

Data Interrupt Generator

A variable-frequency solid-state square-pulse-train generator was fabricated in order to provide an accurate timing signal compatible with both the hybrid computer and the digital computer. The interrupt signals were used to indicate the point in time at which the digital computer is to sample and record the data signals. Thus the need for accuracy in this device was crucial. The frequency range of the interrupt generator is from 0.2 hz to 200 khz.

Display Reference Generator

The display reference generator provided a 7 volt rms sinusoid at 150 hz. The device was a Test Oscillator, Model 650A, manufactured by Hewlett Packard, Inc. The signal from the display reference generator provided hybrid computer with a timing reference for switching as well as a time-varying voltage with which to draw the lines.

Experiment Room

As was stated in the body of this thesis, a small room in the Simulation Center was set up for conducting the experiment. The windows were shielded and doors blocked to isolate the experiment from peripheral disturbances. The room contained the display unit and the chair mounted stick control unit. Figure A.2 shows the position of the equipment in the experiment room.

Stick Control Unit - The control stick shown in Figure A.2 is 6 1/2 inches long, and full deflection is ± 40 degrees. The restoring spring constant is given by

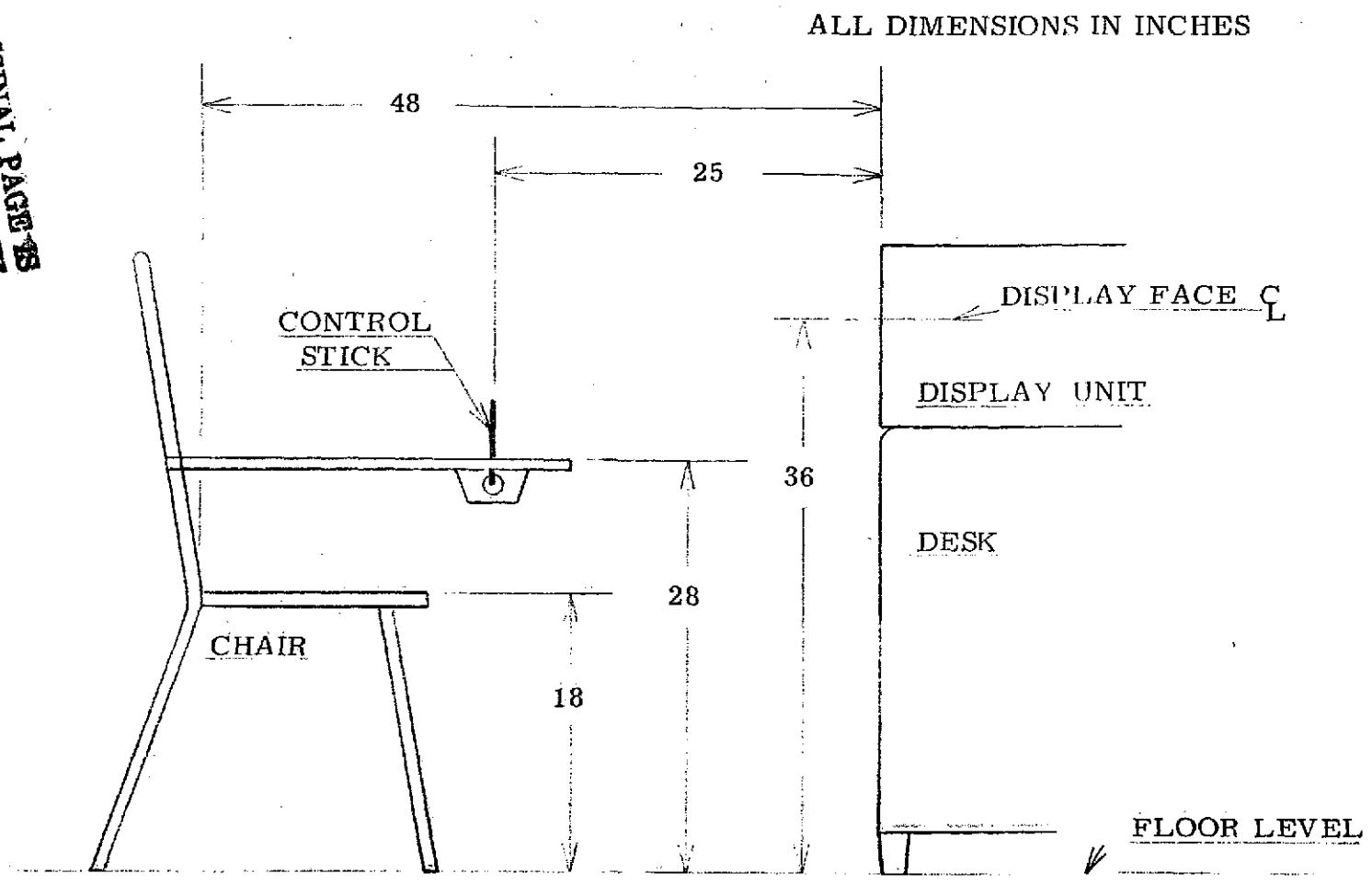

Figure A. 2 Experiment Room Equipment Positions

$$K_\theta = 0.34 \text{ ft-lbs/radian}, \tag{A.1}$$

and the coefficients in a damped second order system representation of the control stick are

$$\omega_n = 78.5 \text{ radians per second} \tag{A.2}$$

$$\zeta = 0.02 \tag{A.3}$$

X-Y Display Unit - The x-y display unit was a cathode ray tube storage display unit. The device was a Type 611 Storage Monitor, manufactured by Tektronics, Inc. The tube had a P1 phospor, and the unit was operated in the Non-Store mode.

Digital Computer

As discussed in the body of this thesis, data was stored on-line, in digital form by the CDC 160-A Digital Computer, which used a twelve bit data word. The technique was as follows: The 160-A is placed in the proper mode by the experimenter before initiating the trial. When the experimenter places the hybrid in operate, the hybrid sends a pulse train down the data interrupt trunk line to the 160-A until the end of the run, at which point the hybrid stops the pulses. Each time the 160-A receives a data interrupt pulse, it samples and records up to 8 channels of data. The maximum data rate is approximately 500 samples per second on each of 8 channels. The sample sets taken at each interrupt pulse are converted to binary numbers and are stored on magnetic tape (two 6-bit frames per number) in files that are identified by an arbitrary identification number, the file number on the tape, and the number of

channels recorded. This identification is in each record block on the tape itself and is automatically generated by the 160-A.

Since full-scale analog reference is 100 volts, the least significant bit of the 12-bit A-D converter corresponds to 0.05 volts. In theory one would therefore expect a converter accuracy of the order of 0.1 volt. In practice, the inaccuracies associated with the conversion process appear to be zero mean Gaussian with $\sigma = 0.4$ volts. The next stage in the data reduction consists of changing the 12 bit words to two 8-bit byte words to be compatible with the IBM 360 word form. An assembly-language digital computer program performs this conversion in an optimum manner. The output of this routine is also stored on magnetic tape thus making the data immediately available in a form compatible with the IBM 360 Computer.

In their original form the data tapes can be run through the 160-A in a D-A conversion routine so that the data can be displayed in analog form using a recording oscillograph.

Hybrid Computer

The following six functions are all performed within the Applied Dynamics 64-PB Hybrid Computer:

Digital Computer Control Unit - A control unit for the CDC 160-A was fabricated and installed in the control panel of the 64-PB hybrid computer to allow the experimenter to control both computers from the same console. This unit has the capability of giving both run and interrupt 10 signals to the digital unit.

Timing Signal Generator - The timing signals for each trial were a series of ramps that caused modes to be switched when the ramps reached certain preset levels. The ramps were generated by integrating controlled voltages that were obtained by using analog summers to attenuate the reference voltages. Two ramps were used: one to start the time variation and end the trial; and one to produce 100ϕ and end the time variation.

Analog Mode Control - The timing generator caused the mode control of various analog amplifiers to switch so as to start and stop the trial. The analog mode control also gated the output of the data interrupt generator. It controlled the output of the noise generator and was used to initialize all the data signals in the simulation.

Noise Filter - The binary output of the digital noise generator was first converted to ± 100 volt steps by electronic switches. These steps were then filtered by a third order filter of the form shown in Equation A.4,

$$\frac{1}{\left(\frac{j\omega}{\omega_f} + 1\right)^3} \qquad \text{(A.4)}$$

where the clock frequency was adjusted to be twenty times the value of ω_f.

Vehicle Dynamics - One section of the analog portion of the 64-PB was used to simulate the time-varying transfer function presented in Chapter 3 of the body of the thesis. The time-varying parameters

were created by using the 100 ϕ ramp as a multiplier on the appropriate signals.

Display Generator - The output of the display reference signal generator was compared against zero volts and this resulted in a logic signal pulse train. This train was fed into a series of two flip-flops which served as a frequency divider. The resulting logic signals were utilized in such a way that the display wrote the moving line for one cycle of the generator then blanked for one cycle. Next it wrote the non-moving line and then blanked again before beginning the process over again. The lines were actually the sinusoidal generator signal with two different values of gain. The switch from one line position to the other was accomplished during the blanked cycles.

Calibration

Prior to each session, the stick and display sensitivities were calibrated to insure their agreement with those values stated in Chapter 3. The step response of the vehicle for various values of ϕ was also determined in order to verify that the proper coefficients had been set in and that the analog components were functioning properly. Before and after each session, a set of calibration signals were generated and tested on the analog console, and then these signals were recorded on magnetic tape using the A-D conversion routine. The calibration signals consisted of $\pm$ 100 volt reference signals, $\pm$ 10 volt signals, and a sinusoidal signal of 22.35 RMS volts at a frequency of 3.14 radians per second.

APPENDIX B

SESSION DETAILS

This appendix presents the details of each formal session of the experiment. Each subject saw the same order of sessions. As mentioned in the body of the thesis, the last session was an exact duplicate of the first session. In the following sessions the transition speeds of the vehicle are defined by the time rate of change of ϕ as described in Chapter 3. The speeds are defined as follows:

Speed # 1: Instantaneous Switch, $\frac{d\phi}{dt} = \infty$

Speed # 2: 30 second variation, $\frac{d\phi}{dt} = 0.0333$ units/second

Speed # 3: 75 second variation, $\frac{d\phi}{dt} = 0.0133$ units/second

Speed # 4: 120 second variation, $\frac{d\phi}{dt} = 0.00833$ units/second.

The hyphens between groups of five trials in the sequence of trial speeds denote the 10 to 15 minute breaks discussed in Chapter 4.

Session 1 and Session 7

Input Disturbance Filter Frequency: 2.0 radians per second

Noise Generator Clock Frequency: 6.37 hz

Noise Generator Register Length: 15 bits

Noise Generator Repetition Period: 85 minutes

Sequence of Trial Speeds:

4, 2, 2, 2, 2, - 4, 4, 4, 2, 2 - 2, 2, 4, 4, 4 - 4, 2, 4, 4, 2

Session 2

Input Disturbance Filter Frequency: 2.0 radians per second

Noise Generator Clock Frequency: 6.37 hz

Noise Generator Register Length: 15 bits

Noise Generator Repetition Period: 85 minutes

Sequence of Trial Speeds:

3, 3, 1, 1, 3 - 1, 1, 1, 3, 3 - 1, 3, 1, 3, 3 - 1, 3, 1, 3, 1

Session 3

Input Disturbance Filter Frequency: 0.8 radians per second

Noise Generator Clock Frequency: 2.54 hz

Noise Generator Register Length: 10 bits

Noise Generator Repetition Period: 6.71 minutes

Sequence of Trial Speeds:

2, 4, 4, 4, 2 - 4, 4, 2, 2, 4 - 2, 2, 4, 2, 4 - 2, 4, 2, 4, 2

Session 4

Input Disturbance Filter Frequency: 0.8 radians per second

Noise Generator Clock Frequency: 2.54 hz

Noise Generator Register Length: 10 bits

Noise Generator Repetition Period: 6.71 minutes

Sequence of Trial Speeds:

1, 1, 1, 3, 1 - 1, 3, 1, 3, 3 - 1, 3, 3, 1, 1 - 1, 3, 3, 3, 3

Session 5

Input Disturbance Filter Frequency: 1.4 radians per second

Noise Generator Clock Frequency: 4.45 hz

Noise Generator Register Length: 11 bits

Noise Generator Repetition Period: 7.6 minutes

Sequence of Trial Speeds:

2, 4, 4, 4, 2 - 2, 2, 2, 4, 4 - 4, 4, 2, 2, 2 - 4, 4, 2, 2, 4

Session 6

Input Disturbance Filter Frequency: 1.4 radians per second

Noise Generator Clock Frequency: 4.45 hz

Noise Generator Register Length: 11 bits

Noise Generator Repetition Period: 7.6 minutes

Sequence of Trial Speeds:

1, 1, 1, 3, 3 - 3, 3, 3, 3, 1 - 3, 1, 3, 1, 1 - 1, 1, 3, 1, 3

APPENDIX C

SUBJECT DATA

Subject A

Age: 32 years

Height: 71 inches

Occupation: USAF Officer-Pilot

Experience: 1700 hours in jet fighter aircraft

Subject B

Age: 32 years

Height: 73 inches

Occupation: USAF Officer-Pilot

Experience: 2200 hours in jet fighter aircraft

Instructor Pilot

Flight Examiner

APPENDIX D

ADDITIONAL DATA PLOTS

This appendix contains the plots of signal standard deviation for stick deflection, angle of attack, and error, all versus time. The six figures represent all twelve experimental conditions for both subjects.

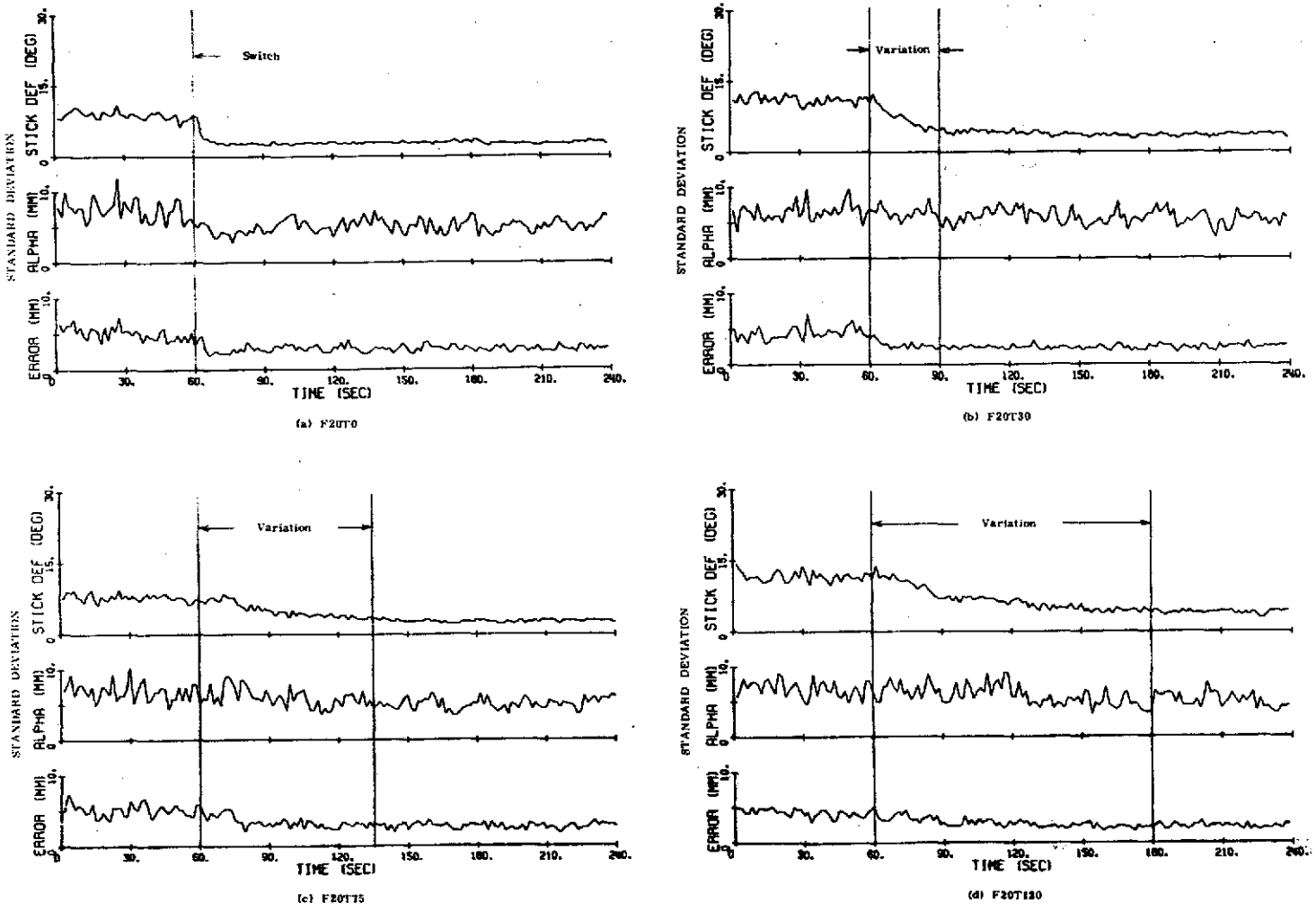

Figure D.1 Standard Deviation of Recorded Data, Subject A, Conditions as Indicated

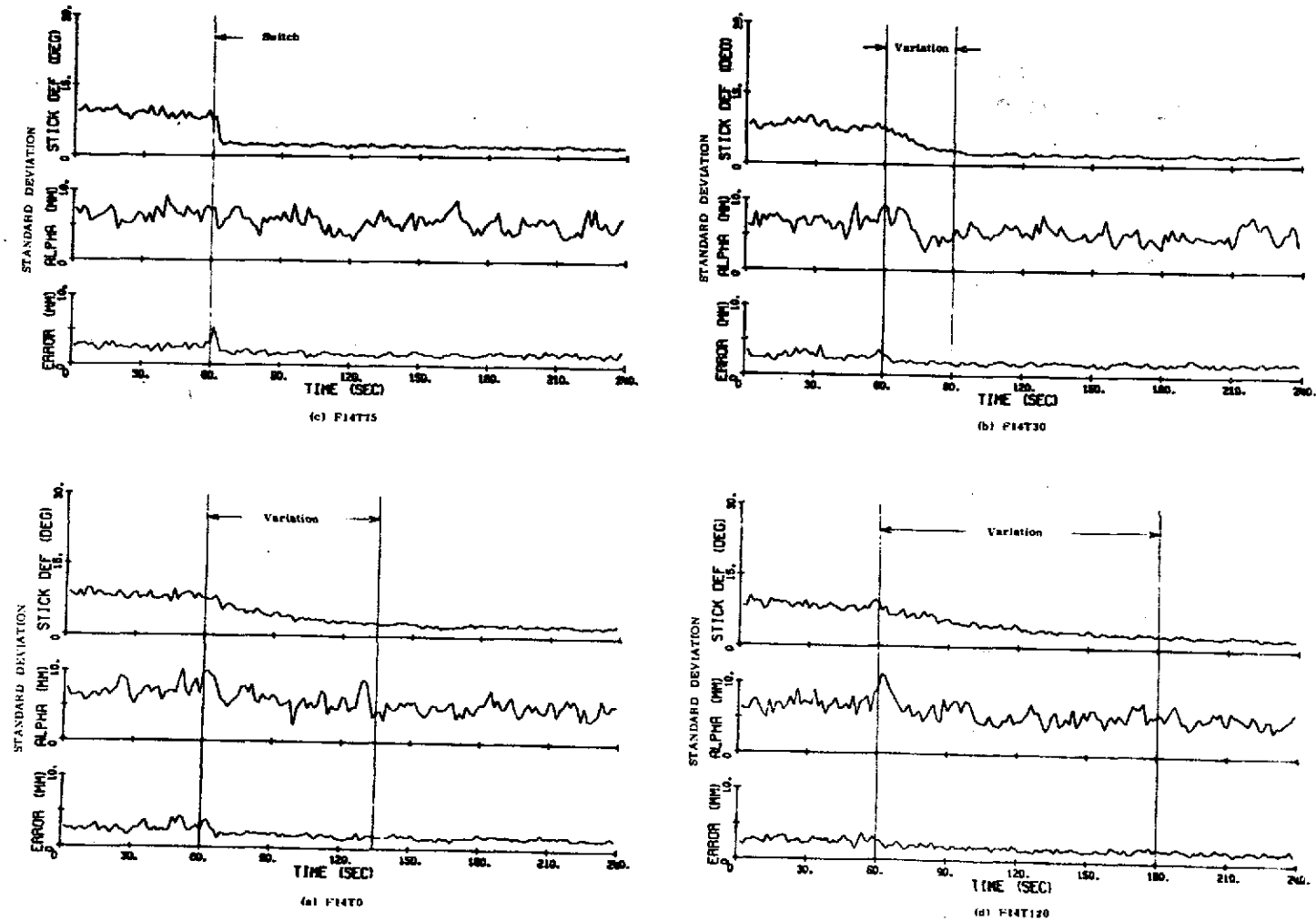

Figure D.2 Standard Deviation of Recorded Data, Subject A, Conditions as Indicated

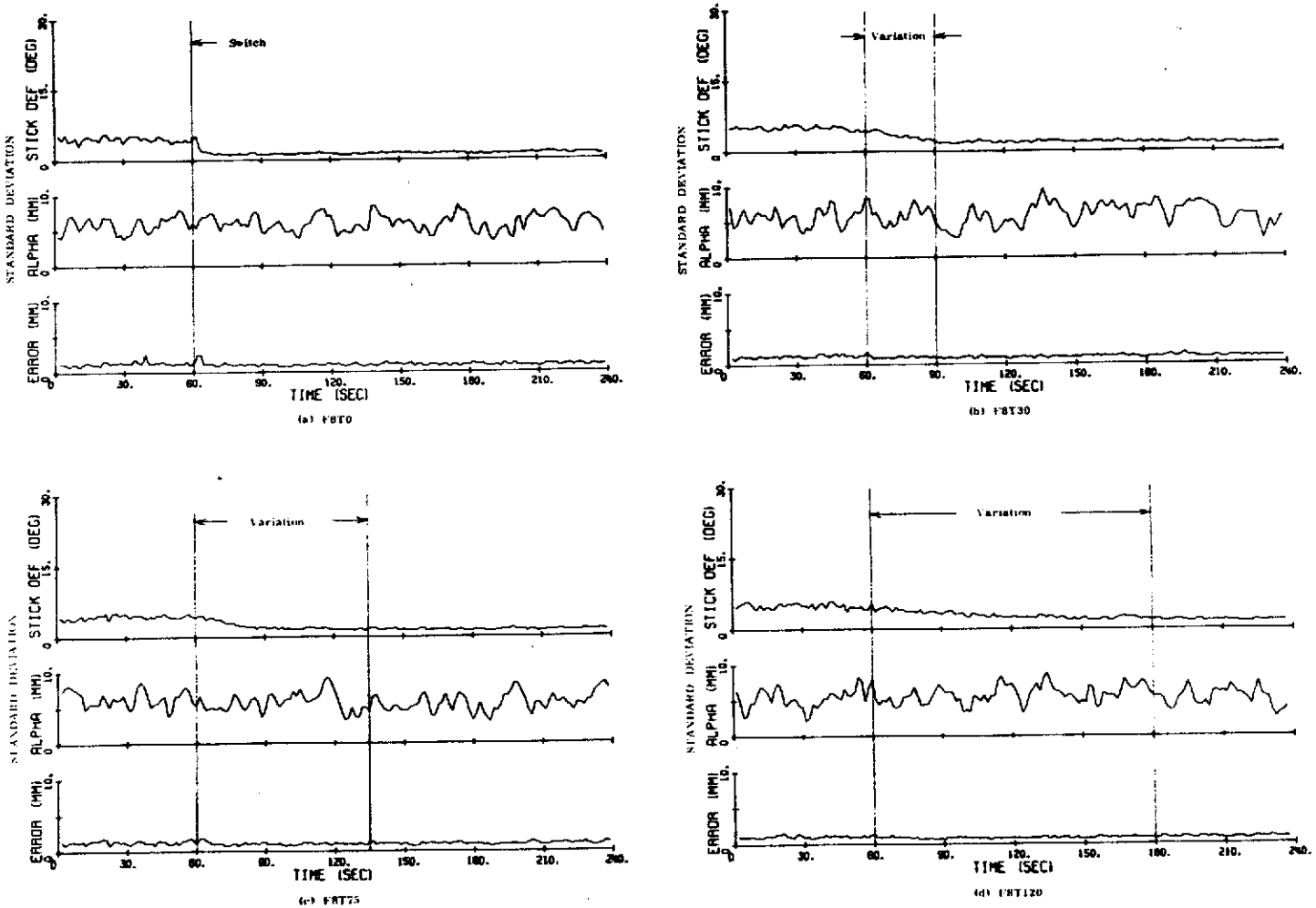

Figure D.3 Standard Deviation of Recorded Data, Subject A, Conditions as Indicated

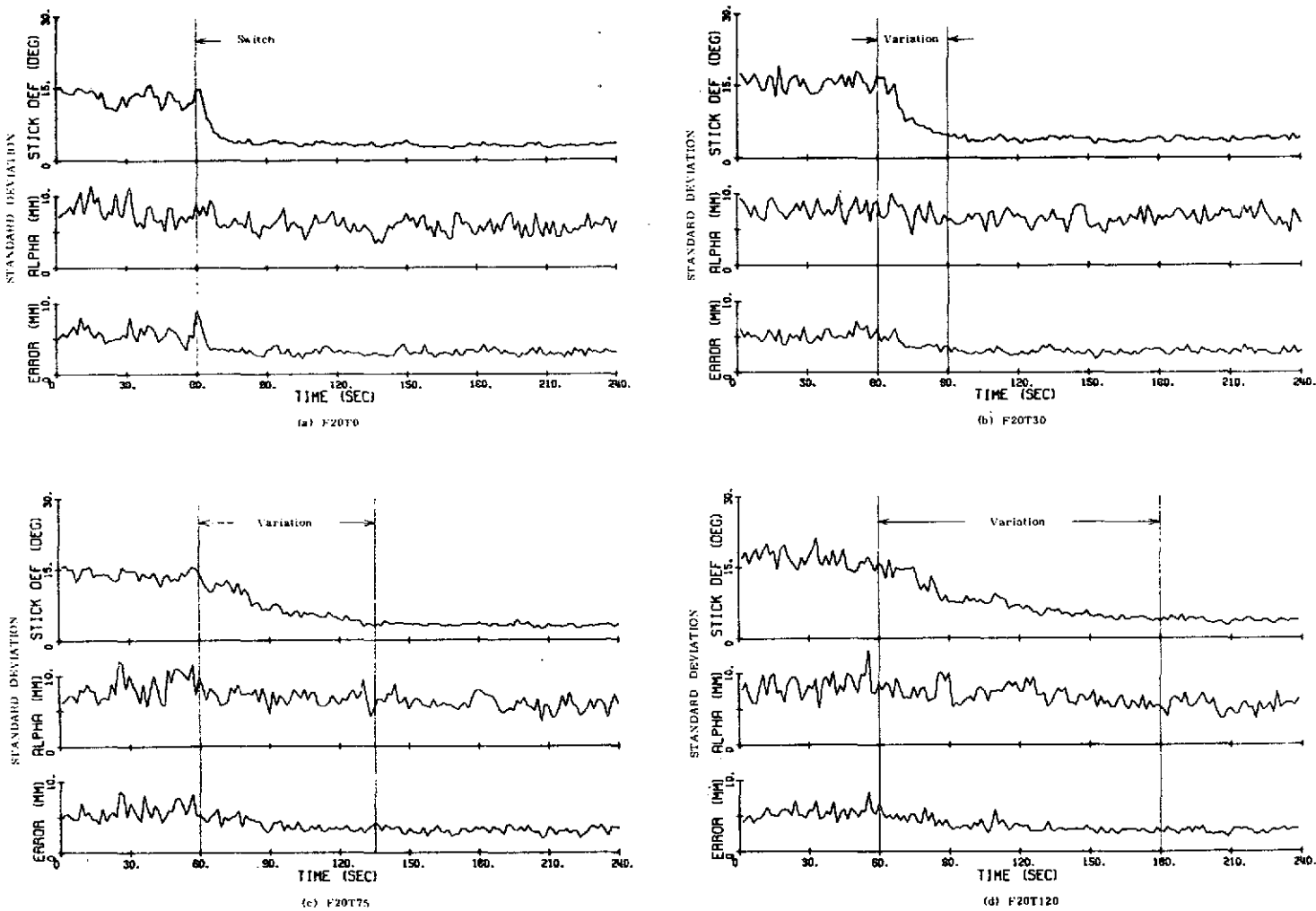

Figure D.4 Standard Deviation of Recorded Data, Subject B, Conditions as Indicated

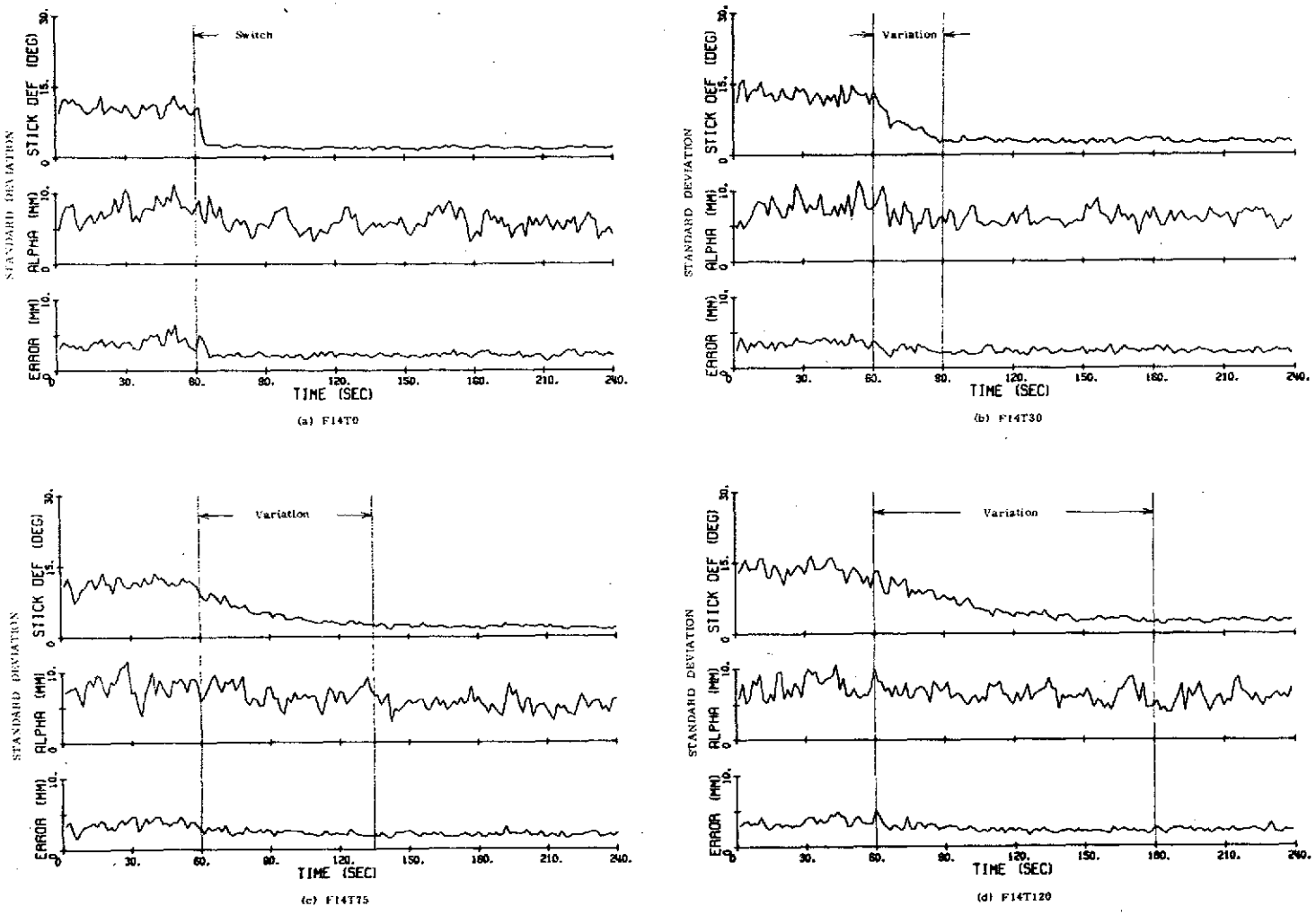

Figure D.5 Standard Deviation of Recorded Data, Subject B, Conditions as Indicated

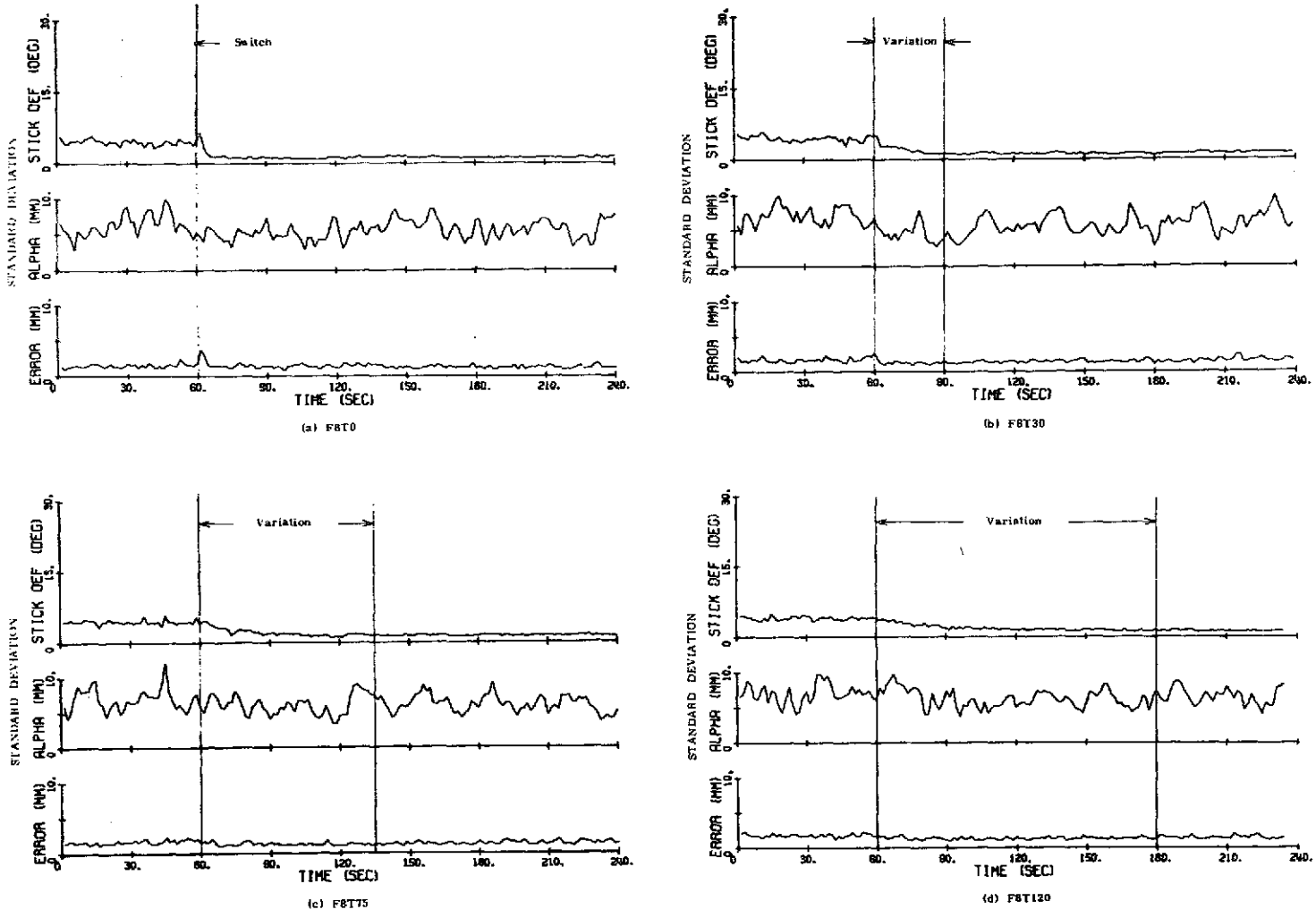

Figure D.6 Standard Deviation of Recorded Data, Subject B, Conditions as Indicated

BIBLIOGRAPHY

1. Baron, S., et al, "Application of Optimal Control Theory to the Prediction of Human Performance in a Complex Task," Air Force Flight Dynamics Laboratory, AFFDL-TR-69-81, March 1970.

2. Blackman, R. B. and Tukey, J. W., The Measurement of Power Spectra, New York, Dover, 1959.

3. Blakelock, J. H., Automatic Control of Aircraft and Missiles, New York, Wiley, 1965.

4. Bracewell, R., The Fourier Transform and Its Applications, New York, McGraw-Hill, 1965.

5. Brownlee, K. A., Statistical Theory and Methodology in Science and Engineering, New York, Wiley, 1960.

6. Elkind, J. I., and Miller, D. C., "The Process of Adaption by the Human Controller," Second Annual NASA University Conference on Manual Control, NASA-SP-128, 1966, pp. 47-63.

7. Fox, D., and Guire, K., Documentation for MIDAS, Statistical Research Laboratory, University of Michigan, 1972.

8. Howe, R. M., and Pew, R. W., "Manual Control Systems Research," Proposal to NASA, University of Michigan, October 1972.

9. Ince, F., and Williges, R. C., "Detecting Slow Changes in System Dynamics," Aviation Research Laboratory, Institute of Aviation, University of Illinois, Technical Report ARL-72-4/AFOSR-72-2, April 1972.

10. McRuer, D. T. and Krendel, E. S., "Dynamic Response of Human Operators," Wright Air Development Center, WADC-TR-56-524, October 1957.

11. McRuer, D. T., et al, "Human Pilot Dynamics in Compensatory Systems," Air Force Flight Dynamics Laboratory, AFFDL-TR-65-15, July 1965.

12. McRuer, D. T., et al, "New Approaches to Human-Pilot/Vehicle Dynamic Analysis," Air Force Flight Dynamics Laboratory, AFFDL-TR-67-150, February 1968.

13. Papoulis, A., The Fourier Integral and Its Applications, New York, McGraw-Hill, 1962.

14. Papoulis, A., Probability, Random Variables and Stochastic Processes, New York, McGraw-Hill, 1965.

15. Rice, S. O., "Mathematical Analysis of Random Noise," Bell System Technical Journal, Vol. 23, 1944, pp. 282-332, also Vol. 24, 1945, pp. 46-156.

16. Root, W. L., "On the Structure of a Class of System Identification Problems," Automatica, Vol. 7, 1971, pp. 219-231.

17. Wierwille, W. W. and Gagne, G. A., "Nonlinear and Time-Varying Dynamical Models of Human Operators in Manual Control Systems," Human Factors, April 1966, pp. 97-120.

18. Winer, B. J., Statistical Principles in Experimental Design, 2nd Ed., New York, McGraw-Hill, 1971.

19. Young, L. R., Green, R. M., Elkind, J. I. and Kelly, J. A., Adaptive Dynamic Response Characteristics of the Human Operator in Simple Manual Control," Transactions on Human Factors in Electronics, Vol. HFE 5, No. 1, September 1964, pp. 6-13.

20. Young, L. R., "On Adaptive Manual Control," Ergonomics, Vol. 12, No. 4, July 1969, pp. 635-674.